University of Alberta

The Tumor Promoting Role of BAD in Breast Cancer Cells

by

Timothy William Buckland

A thesis submitted to the Faculty of Graduate Studies and Research

in partial fulfillment of the requirements for the degree of

Master of Science

Department of Biochemistry

Spring 2012

Edmonton, Alberta

Abstract

In Canada, approximately 40% of the population will be diagnosed with cancer and 25% will die of this disease. In order to treat cancer more effectively, new prognostic and therapeutic targets need to be discovered. In breast cancer, the BH3 only protein BAD has been shown to correlate with response to treatment. However, the role of BAD in cancer is unclear. Although BAD is well characterized as a pro-apoptotic protein, alternative roles exist that may influence cancer progression. In this study, we determine that BAD over-expression promotes proliferation and tumor growth of MDA-MB-231 breast cancer cells. These roles are regulated by serine phosphorylation, specifically serine 118. Finally, enforced phosphorylation of BAD at serine 118 promotes apoptotic resistance. This study suggests that in order to use BAD as a prognostic or therapeutic target, the phospho-status of BAD must also be examined.

Acknowledgements

As an undergraduate student, I always had an interest for cancer. This is partly due to my scientific curiosity and my interaction with the disease. I am a two time survivor and as a cancer survivor, I have been blessed with a different perspective than most. My dream was to work on the disease that had shaped my life, to understand it and fight against it.

Luckily as I was finishing my undergraduate degree, I ended up taking Biochem 401. This course not only gave me laboratory building blocks but was also located close to Dr. Ing Swie Goping's laboratory. I was blessed to do a summer studentship and Biochem 498 here and continued working as a laboratory assistant and ended up doing my Master's degree here. Dr. Ing Swie Goping has sacrificed laboratory funds and her own time to make my experience the success that it was. Her guidance within and outside of the lab has taken me places I would never have dreamed without it. For this I sincerely thank her, as she is one of the main reasons I have gone this far.

I would also like to thank the lab members, past and present for the guidance and friendship. Matt Czernick and Richard Veldhoen, who initially trained me quickly moved educators to companions. Without their individual expertise and friendship, I would not be where I am today. Alison Craik who joined the laboratory at nearly the same time I did has become a respected colleague and friend that I am truly grateful to have. Shanna Banman who is the newest member of our laboratory quickly became a friend and respected colleague.

I would like to thank the Department of Biochemistry for allowing me the opportunity to be a complete my degree here. I would like to thank Drs. Adrienne Wright, Jo Parrish and Rachel Milner for going above and beyond the duty of an educator; crossing over onto a friendship level. Administrators within this department; Shannon Swan, Sue Smith and Kim Arndt, have worked tirelessly to get me where I am and for this I am indebted.

My committee members, Dr. Shairaz Baksh and Dr. Roseline Godbout have provided endless scientific guidance. I would like to thank Dr. Baksh for technical support with the xenograft model and for taking time out of an incredibly busy schedule to teach me this technique. His patience and companionship have been an asset to my project. I would also like to thank Dr. Roseline Godbout who has provided enormous support for this project. She has provided supplies, expertise and protocols; for this I am grateful. I would also like to specifically thank a member of her lab, Dr. Lei

Li for collaboration with 2-dimensional western blot experiments. Without his expertise these experiments would not have been completed to the caliber that they were.

Members of both Biochemistry and Cell Biology departments have proved essential to my experience, specificially:

Dr. Fahlman for accepting the invitation to join my examining committee.

Dr. Simmen's laboratory, for being a great source of companionship and scientific knowledge. Specifically: Emily Lynes, Mike Bui, Arun Raturi, Matt Benson, Carolina Ortiz and Thomas Simmen have been great friends and neighbors.

Dr. Bleackley's laboratory, specifically Marcelo Marcet-Palacios, Katia Carmine-Simmen, Brenda Duggan, Nancy Ehrman, Tracy Geskes, Diane Marganski and Chris Bleackley have provided our lab with endless technical support.

I would not be where I am today without the love and support of my family. They have sacrificed more for me than I would like to admit. I cannot begin to express the appreciation I have for what they have done. They have been one my greatest assets in dealing with the daily hardships of graduate life.

I would finally like to thank my wife Savanna; whose love and support carried me through this degree. She has been there for me, through the exceptionally tough times and ecstatically good. Without her constant support, I know I would not have made it this far.

Table of Contents

List of Abbreviations

A1	BCL-2A1
AIPC	Androgen independent prostate cancer
ALV	Avian myelocytomatosis virus
Amp	Ampicillin
ASO	Antisense oligonucleotides
BAD -/-	BAD null cells
$BAD^{3SA/3SA}$	serine 75,99 and 118 alainine mutant
BADD119G	BAD mutated at aspartic acid 119 to glycine
BAK	BCL-2-homologous antagonist/killer
BAX	BCL-2 associated x protein
BCL-2	B-cell leukemia/lymphoma-2
BH	BCL-2 homology
BrdU	Bromodeoxyuridine
BSA	Bovine Serum Albumin
CCRF	Cytochrome C release factor (BID)
cDNA	Complementary DNA
ChIP	Chromatin immunoprecipitation
complete media	RPMI 1640 + 10% FBS
DAPI	4',6-diamidino-2-phenylindole
DFS	Disease free survival
dPBS	Dulbecco's Phosphate Buffered Saline
Eμ	Enhancer μ
EGF	Epidermal Growth Factor
EMSA	Electrophoretic mobility shift assay
EMT	Epithelial mesenchymal transition
FBS	Fetal Bovine Serum
GFP	Green fluorescent protein
GM-CSF	Granulocyte-macrophage colony stimulating factor
Go	Cell cycle quiescence
GST-HMK	Glutathione-S-transferase conjugated heart muscle kinase
hBAD	Human BAD
HPLC	High Performance Liquid Chromatography
IDT	Integrative DNA Technologies
IGF-1	Insulin like growth factor-1
IHC	Immunohistochemistry

IL-3	Interleukin-3
IP	Immunoprecipitation
IVTT	*In vitro* transcription and translation
JNK	c-Jun N-terminal kinase
Kan	Kanamycin
kDa	Kilodalton
LB	Lysogeny Broth
LBD	Lipid binding domain
mBAD	Murine (or Mouse) BAD
MEF	murine embryonic fibroblasts
c-MYC	Cellular MYC
MycER	Myc estrogen receptor fusion
v-*MYC*	Viral Myc
NEB	New England Biolabs
PCR	Polymerase Chain Reaction
PEST domain	Proline-glutamate-serine-threonine domain
PI	Propidium iodide
PI3K	Phosphinositide 3 kinase
PKA	Protein Kinase A
PKG	Protein Kinase G
PMT	Photomultiplier Tube
PP1	Protein phosphatase 1
PP2A	Protein phosphatase 2A
PRMT	Proline methyl arginine transferase
RSK1	Ribosomal S6 Kinase1
RSK-2	pp90 ribosomal 6 kinase-2
RT-PCR	Reverse Transcriptase Polymerase Chain Reaction
RXSpSXP or RXY/FXpSXP	14-3-3 binding consensus sites
S118A#	serine 118 to alanine mutation clone #
S118D#	serine 118 to aspartic acid mutation clone #
SAHB	Stabilized α-helix of BCL-2 (hydrocarbon stapled peptide)
v-*SRC*	Viral sarcoma
SDS-PAGE	Sodium dodecyl sulfate polyacrylamide gel electrophoresis
siRNA	Small interfering ribonucleic acid
t(14;18)	Translocation of chromosome 18 to chromosome 14
t(8;14)	Translocation of chromosome 8 to chromosome 14
tBID	Caspase cleaved or truncated BID
TLC	Thin layer chromatography
TMRE	Tetramethylrhodamine ester

TNFα	Tumor necrosis factor-α
TPA	12-O-tetradecanoylphorbol-13-acetate
TRE	Transcription response element
UV	Ultraviolet
UVC	Ultraviolet-C
V#	Vector control clone #
VEGF	Vascular endothelial growth factor
WAVE-1	Wiskott-Aldrich family member

List of Figures

List of Tables

Chapter 1: Introduction

1.1 Cancer

Cancer is a set of diseases characterized by the deregulated proliferation and invasiveness of cells. In Canada, approximately 45% of males and 40% of females will be diagnosed with cancer within their lifetime. Due to the high prevalence and lack of effective treatments, 1 in 4 Canadians will end up dying of these diseases (Canadian Cancer Society's Steering Committee on Cancer Statistics, 2011). As a means of increasing patient survival, extensive research is aimed at increasing treatment efficacy.

Due to the similarities between cancer cells and surrounding normal tissue, understanding differences between them can be used for developing treatments. In 2000, Hanahan and Weinberg published a review article which characterized six "Hallmarks of Cancer" (Hanahan and Weinberg, 2000). Hallmarks of cancer are biological capabilities that lead to evasion of anti-cancer defense mechanisms and is sometimes described as transformation. These hallmarks are: resisting cell death, sustaining proliferative signaling, evading growth suppressors, activating invasion and metastasis, enabling replicative immortality and inducing angiogenesis. Recently, two new hallmarks have been added: avoiding immune destruction and deregulation of cellular energetics (Hanahan and Weinberg, 2011). Although these hallmarks enable a greater insight of tumor development, alone they have limited therapeutic use. Understanding the pathways that lead to these hallmarks is critical for therapy development.

Two hallmarks essential for tumor growth are proliferative signaling and resistance to cell death (Scott, 1970; Skaff *et al.*, 2005). In order for cancer treatment to be successful, both of these hallmarks must be averted. Studies have been conducted on the cellular pathways associated with these hallmarks in an aim to discover new therapeutic targets.

As the net effect of deregulation of these hallmarks leads to increased cell number, researchers have looked for overlapping targets. Specifically, research has focused on gene products (proto-oncogenes) that are mutated or deregulated in uncontrolled cell proliferation. Proto-oncogenes are tightly regulated in healthy cells but mutations or chromosomal abnormalities provide deregulated expression.

1.2 Proto-oncogenes

One of the most commonly mutated proto-oncogenes is c-MYC. This gene was initially discovered by DNA analysis of the avian myelocytomatosis virus (ALV) strain MC-29 which transformed chicken bone marrow cells (Todorov and Yakimov, 1967). Similar to a previously discovered retrovirus (Rous sarcoma virus) which contained a transforming gene product (v-*SRC*), MC-29 contained v-*MYC* (Hayward *et al.*, 1981; Murphy and Rous, 1912; Rous, 1911; Vennstrom *et al.*, 1982). Using a v-*MYC* DNA probe, chicken embryo DNA was screened (Radke and Martin, 1979; Swanstrom *et al.*, 1983; Vennstrom *et al.*, 1982). c-*MYC* was detected and was later characterized as a transcription factor that promoted cell cycle progression. In rat fibroblasts, c-*MYC* null cells or the addition of c-*MYC* antibodies inhibited S-phase progression (Mateyak *et al.*, 1997; Mateyak *et al.*, 1999). In quail embryo fibroblasts, infection with MC-29 led to

increased proliferation but did not enhance xenograft growth in BALB/c nude mice (Palmieri *et al.*, 1983). Surprisingly, 13 of 15 transgenic mice containing deregulated Eμ-*MYC* developed lymphoma and died between 6 and 15 weeks of age (Adams *et al.*, 1985). Based on this evidence, c-*MYC* was classified as a pro-proliferative proto-oncogene although it was unclear of its role in transformation.

While the cellular role of c-*MYC* was being elucidated, the clinical relevance of c-*MYC* deregulation remained unknown. To trace on which chromosome c-*MYC* was located, rat-human somatic cell hybrids containing specific human chromosomes were sequentially mapped. Comparing c-*MYC* DNA probe hybridization via southern blot analysis to human chromosome numbers, it was deduced that c-*MYC* was present on human chromosome 8 (Dalla-Favera *et al.*, 1982). Prior to this study, a chromosome 8 translocation was correlated to Burkitt's lymphoma progression. This translocation involved the q branch of chromosome 8 to the q branch of chromosome 14 (Kakati *et al.*, 1979; Zech *et al.*, 1976). Using restriction enzyme mapping of Burkitt's lymphoma cell lines containing the t(8;14), c-*MYC* was shown to be attached to the immunoglobulin heavy chain locus (Taub *et al.*, 1982). Depending on the translocation break point, c-*MYC* is located in cis with the regulatory region and/or immunoglobulin heavy chain enhancer region (Eμ). Regardless, translocation to this chromosome was sufficient for increased expression of c-*MYC* (Erikson *et al.*, 1983; Yan *et al.*, 2007). Chromosomal translocation of c-*MYC* was shown to induce transcriptional deregulation, cellular proliferation and promote tumorigenesis.

Analysis of other blood cancers showed a different translocation being correlated with leukemia and lymphoma. Lymph node biopsies of follicular lymphoma patients were

analyzed using high resolution chromosome analysis. Of the 19 patients analyzed, 16 contained a translocation of chromosome 18 to chromosome 14 (t(14;18)) (Yunis *et al.*, 1982). *In vitro*, karyologic analysis of an acute lymphoblastic leukemia line (380 cell line) revealed that the q21-qter section of chromosome 18 was translocated to the q branch of chromosome 14 (t(14;18)) (Billen *et al.*, 2008; Pegoraro *et al.*, 1984; Tsujimoto *et al.*, 1984). In both the 380 leukemia and LN128 follicular lymphoma cell lines, a DNA probe specific for chromosome 18 was detected on chromosome 14. This probe recognized DNA located at human chromosome 18, band q21 and was identified as B cell lymphoma/leukemia-2 (BCL-2) (Tsujimoto *et al.*, 1984). Analysis of this translocation showed that the 5' region of the BCL-2 gene locus was inserted downstream of the immunoglobulin heavy chain enhancer Eμ (Cleary *et al.*, 1986; Graninger *et al.*, 1987; Yunis *et al.*, 1982). Similar to the c-MYC translocation results, increased expression of the *BCL-2* transcript was observed (Graninger *et al.*, 1987). A *BCL-2* specific probe was used to compare BCL-2 RNA levels in cells that contained the t(14;18) versus cells without this translocation. *BCL-2* mRNA levels were found to be elevated in t(14;18) cell lines (Graninger *et al.*, 1987). This data showed that *BCL-2* gene expression was correlated to B cell lymphoma and leukemia carcinogenesis.

Although BCL-2 transcripts were elevated as a result of the t(14;18) translocation, the role *BCL-2* had in tumorigenesis was unclear. Studying the protein product of *BCL-2* enabled analysis of the functional role of this gene. *In vitro* transcription and translation (IVTT) of the *BCL-2*α open reading frame (ORF) produced proteins ranging from 28 and 30 kilodaltons (kDa) (Tsujimoto and Croce, 1986). Transfection of FDC-P1 cells, a murine non-transformed bone marrow progenitor cell

line, was used to examine the transforming potential of BCL-2 (Vaux *et al.*, 1988). In the presence of factor (IL-3), *BCL-2* transfected stable cells had a similar propidium iodide (PI) profile to mock infected control. When factor was removed, mock and c-MYC infected cells died. However, *BCL-2* stably transfected cells survived, although they were mainly quiescent. *BCL-2* was capable of rescuing c-*MYC* as cells expressing both constructs survived IL-3 withdrawal. Furthermore, Eμ-*MYC* expressing bone marrow cells that were cultured with *BCL-2* producing fibroblasts survived non-adherent growth. Bone marrow cells that were not cultured with fibroblasts did not survive (Vaux *et al.*, 1988). These data suggested that BCL-2 was able to prevent cell death in a non-adherent environment. Based on this data, BCL-2 was the first proto-oncogene described to not contain a proliferative function.

1.3 Anti-apoptotic family members

As a result of the discovery of BCL-2, a novel anti-apoptotic proto-oncogene, the scientific community began looking for other members of this family. In ML-1 myeloid leukemia cells, 12-O-tetradecanoylphorbol-13-acetate (TPA) promoted expression of a novel early-induction gene, *MCL-1*. Protein prediction software was used to model the structure of *MCL-1* reverse transcribed cDNA (complementary DNA) sequences. Based on the predicted amino acid sequence, MCL-1 had a strong C-terminal amino acid identity (35%) and similarity (59%) to BCL-2 (Kozopas *et al.*, 1993). As had been shown previously with *BCL-2*, the *MCL-1* gene was also disrupted in a number of neoplastic and preneoplastic cells. The chromosome location of *MCL-1* (chromosome 1) was determined by the use of somatic cell hybrids (human/rodent).

This in combination with in situ hybridization of genomic *MCL-1* overlayed with a G-banded image was used for intra-chromosomal localization (1q21) (Craig *et al.*, 1994). Clinically, a number of neoplastic diseases had been mapped to this region; e.g., myeloproliferative disorders encompassing trisomy of 1q21-25 and q25-32 (Rowley, 1975; Rowley, 1977) as well as diffuse lymphoma patients having decreased remission and survival length with breaks at 1q21-23 (Offit *et al.*, 1991). Furthermore, long arm rearrangements of chromosome 1 had been reported in acute monocytic leukemia (Hawkins *et al.*, 1992).

Functionally, MCL-1 and BCL-2 are similar. In FDC-P1 cells, stable transfection of human *MCL-1* inhibited death caused by Etoposoide (Zhou *et al.*, 1997) which is consistent with BCL-2 over-expression in the murine mast cell line NSF/N1.H7 cells (Ito *et al.*, 1997). However, functional redundancy is dependent on the cell type. For example, human myeloma cell lines (U266, OPM-2 and L363), electroporated with antisense oligonucleotides (ASO) specific for BCL-2, BCL-XL and MCL-1 had significant differences in apoptotic sensitivity (Derenne *et al.*, 2002). Surprisingly, only the ASO specific for MCL-1 showed decreased cell viability (as measured by eosin exclusion), and increased APO2.7 binding (specific for 7A6 epitope on outer mitochondrial membrane indicative of apoptotic induction). These results indicate that although BCL-2 and MCL-1 have similar functions, MCL-1 is critical for myeloma cell survival.

Sequence comparisons to BCL-2 resulted in the identification of three other members of the anti-apoptotic BCL-2 family members: BCL2A1 (A1), BCL-w and BCL-XL. Similar to MCL-1, A1 was initially discovered as an early-response gene to a differentiation factor for hematopoietic cells (granulocyte-macrophage colony

stimulating factor (GM-CSF)) (Lin *et al.*, 1993). The predicted peptide sequence of A1 has 80 amino acids in common with MCL-1 and BCL-2 (Lin *et al.*, 1993) and have similar anti-apoptotic outcomes. IL-3 withdrawal of 32D C13 murine progenitor cells was equally protected by A1 or BCL-2 transfection (Lin *et al.*, 1996).

BCL-w also has a prominent role in anti-apoptosis although more restricted than other BCL-2 members (Gibson *et al.*, 1996; Print *et al.*, 1998). Although BCL-w transcripts are found in a number of mouse tissue (moderate in brain, colon and salivary gland; low in testis, liver, heart, skeletal muscle and placenta) BCL-w -/- mice are viable with most tissues unaffected (Print *et al.*, 1998). The main dysfunction is in testicular development near sexual maturity, leading to incomplete spermatogenesis. In situ hybridization and western blot analysis of BCL-w +/+ testicular cell lines determined that BCL-w was elevated in germ cells (sperm producing) and Sertoli cells (sperm maturation) but not Leydig cells (hormone production). Based on this, BCL-w is essential for mouse spermatogenesis but seems to have a redundant role in other tissues.

BCL-XL has the strongest sequence similarity to BCL-2 (44% identity between mBCL-XL and mBCL-2) and was detected using a BCL-2 cDNA probe (Boise *et al.*, 1993; Gonzalez-Garcia *et al.*, 1994). This probe detected a novel expressed sequence that codes for two splice variant cDNAs in murine brain tissue, BCL-XL and BCL-XS (Boise *et al.*, 1993). The anti-apoptotic variant, BCL-XL, is the predominant cDNA produced in murine post-natal cells (Gonzalez-Garcia *et al.*, 1994). This was determined using a quantitative S1 nuclease assay probed with BCL-X and BCL-2 probes. Results showed increased expression of BCL-XL compared to BCL-XS in brain, kidney, heart, lymph

nodes, spleen and liver. Also, in 15.5d whole embryo and 15.5d embryonic tissue, BCL-XL was elevated. BCL-XL has a similar function to BCL-2. BCL-XL transfected FL 5.12 cells were equally resistant to IL-3 withdrawal as BCL-2 transfected cells (Boise *et al.*, 1993).

Due to sequence and functional similarities of the anti-apoptotic family members, parallels can be drawn between them. The "traditional" anti-apoptotic BCL-2 family members (BCL-2, BCL-XL and BCL-w) have five similar regions of sequence homology. They contain four BCL-2 homology domains (BH1-4) and a C-terminal hydrophobic segment. The two outliers of this structure are MCL-1 which is missing the BH4 domain (Kozopas *et al.*, 1993) and A1 which depending on the report is missing both BH3, 4 and the transmembrane domain or just the transmembrane domain (Lanave *et al.*, 2004; Lin *et al.*, 1993; Vogler, 2011). The N-terminus of MCL-1 is not conserved between anti-apoptotic BCL-2 members and includes a proline-glutamate-serine-threonine (PEST) domain. This domain is characteristic of proteins with short half-lives (Rogers *et al.*, 1986). Unlike traditional BCL-2 anti-apoptotic family members, MCL-1 and A1 are regulated by degradation (Herold *et al.*, 2006; Yang *et al.*, 1996). Ultraviolet treatment (UV) of HeLa cells caused a rapid degradation of MCL-1 from both cytosolic and mitochondrial fractions (Nijhawan *et al.*, 2003). This was shown to be ubiquitin-proteosome dependent by the addition of MG132 (proteosomal inhibitor) which increased MCL-1 protein levels.

Another sequence similarity of anti-apoptotic family members is the presence of a C-terminal hydrophobic segment. This sequence encodes a C-terminal transmembrane domain which causes binding to intracellular membranes (Nguyen *et*

al., 1993). Through to this domain, BCL-2, BCL-XL, BCL-w and MCL-1 bind the mitochondrial membrane (Wilson-Annan *et al.*, 2003; Yang *et al.*, 1995; Yang *et al.*, 1996). For BCL-w, the C-terminal transmembrane domain occupies the hydrophobic binding pocket prior to activation; therefore, BCL-w is only loosely associated with the mitochondria until an apoptotic stimuli is applied. In FDC-P1 cells, apoptotic stimuli such as staurosporine, IL-3 withdrawal and γ-irradiation induce strong mitochondrial membrane binding (Wilson-Annan *et al.*, 2003). For A1, it likely does not have a transmembrane domain although mitochondrial localization is achieved in HMEC (human mammary epithelial) cells after TNFα stimulation (Duriez *et al.*, 2000). This localization was determined by immunoelectron microscopy of A1. The protective role of A1 at this location is transient as prolonged stimulation of tumor necrosis factor-α (TNFα) decreased viability after 72 hours.

For BCL-2, *in vitro* mitochondrial membrane insertion is dependent on the transmembrane domain (Nguyen *et al.*, 1993). This domain was also shown to be necessary for BCL-2 anti-apoptotic function in KB cells (human oral epidermoid carcinoma) treated with E1B-defective adenovirus (Nguyen *et al.*, 1994). Based on these studies, the C-terminal effects of targeting are necessary for function of anti-apoptotic BCL-2 family members.

Localization of BCL-XL is similar to BCL-2 due to the hydrophobic sequence associated with membrane insertion (Chen-Levy and Cleary, 1990); (Hockenbery *et al.*, 1990). However, both BCL-XL and BCL-2 can homodimerize. BCL-XL has been shown to form homo-dimeric structures in the cytosol of transfected HeLa cells while BCL-2 homodimerizes in HEK 293T cells (Huang *et al.*, 1998; Jeong *et al.*, 2004). BCL-XL

cytosolic homodimerization was shown by transfecting HeLa cells with mBCL-XL, immunoprecipitating hBCL-XL from the soluble (S100) fraction and blotting for mBCL-XL. This study also demonstrated through C-terminal truncation mutants that the C-terminal hydrophobic tail of BCL-XL is necessary for homodimer formation.

In summary, anti-apoptotic BCL-2 members are critical in protecting cells from apoptotic stimuli. These members are mainly found at the mitochondria due to membrane insertion of their transmembrane domains.

1.4 Multi-domain pro-apoptotic BCL-2 members

Protein interaction studies were carried out with the goal of understanding how BCL-2 prevents apoptosis. Co-immunoprecipitations of BCL-2 in ^{35}S methionine labeled RL-7 cells revealed a 21 kiloDalton (kDa) protein defined as BCL-2 associated x protein (BAX) which binds BCL-2 (Oltvai *et al.*, 1993). This result was recapitulated in FL5.12 cells (murine pro-B lymphoid cell line) in the presence of IL-3 and the interaction was diminished when IL-3 was depleted. Sequence comparison of BAX to BCL-2 revealed 20.8% identity and 43.2% similarity. Although the sequence of BAX is similar to BCL-2, the apoptotic role is not. FL5.12-BAX stable clones were less viable upon IL-3 withdrawal than FL5.12-BCL-2 and FL5.12-vector (Oltvai *et al.*, 1993). Furthermore, the apoptotic function of BAX was dependent on BCL-2 concentrations. Increased amounts of BCL-2 inhibited BAX homodimer formation and apoptotic induction. Immunoprecipitation of over-expressed HA-BAX yielded mainly endogenous BAX with small amounts of BCL-2 binding. Increasing amounts of BCL-2 enhanced BCL-

2/BAX heterodimer formation and inhibited BAX homodimer formation (Oltvai *et al.*, 1993).

Another multi-domain pro-apoptotic protein, the BCL-2-homologous antagonist/killer (BAK), was detected using a binding assay of two domain probes specific for BCL-2 (Kiefer *et al.*, 1995). BAK, like BAX, was shown to induce cell death upon IL-3 withdrawal (Kiefer *et al.*, 1995). Multi-domain pro-apoptotic proteins are crucial for development as BAX/BAK double knock-out (DKO) mice have significant developmental defects and are often embryonic lethal (Lindsten *et al.*, 2000; Wei *et al.*, 2001). These defects include interdigital webbing, unresponsiveness to auditory stimuli, increased neuronal accumulation and increased number of lymphoid and myeloid cells (Lindsten *et al.*, 2000). BAX/BAK DKO thymocytes were also resistant to UV irradiation and Etoposide yet responded normally to cross-linked Fas receptor. This suggests that DNA damage induced cell death through a BAX/BAK dependent pathway while Fas did not (Lindsten *et al.*, 2000). Other stimuli known to induce apoptosis through the intrinsic mitochondrial pathway were also tested (Wei *et al.*, 2001). BAX/BAK DKO murine embryonic fibroblasts (MEF) were more resistant to ultraviolet-C (UVC), staurosporine, Thapsigargin, Tunicamycin. Based on these studies, the multi-domain pro-apoptotic BCL-2 family members are critical for mitochondrial dependent apoptosis and development.

1.5 BH3 only BCL-2 proteins

Protein interaction studies with anti-apoptotic proteins also yielded a novel set of proteins with limited sequence homology to BCL-2 (Boyd *et al.*, 1995). This BH3 only

family is characterized by the minimal death domain (BH3). Further classification separates these proteins based on their binding partners and BH3 domains (Letai *et al.*, 2002). Direct activator BH3 only proteins (BID, BIM and PUMA), induce apoptosis through direct activation of BAX and BAK as well as by inhibiting anti-apoptotic BCL-2 members (Kim *et al.*, 2009). Sensitizer BH3 only proteins (eg. BAD, BIK, NOXA and HRK) are only able to bind anti-apoptotic BCL-2 family members and inhibit their function. Due to the vast number of apoptotic BH3 only proteins, I will focus on one direct activator and one sensitizer to demonstrate binding interactions and regulation.

1.5.1 Direct Activator BH3 Only Protein - BID

BID is a direct activator BH3 only protein. BID was discovered in a binding assay using glutathione-S-transferase conjugated to heart muscle kinase (GST-HMK)-BCL-2 and GST-HMK-BAX (Wang *et al.*, 1996). These two proteins were used to screen an expression library constructed from the murine hybridoma line, 2B4. BID bound both of these proteins and through sequence analysis was determined to contain a BH3 domain. Unlike multi-domain pro-apoptotic and anti-apoptotic BCL-2 proteins, the sequence and structure of BID do not contain a hydrophobic C-terminal domain (McDonnell *et al.*, 1999). In basal growth conditions, this restricts the localization of BID mainly to the cytosol (Li *et al.*, 1998; Luo *et al.*, 1998) and to a lesser extent nucleus (Gajkowska *et al.*, 2004). When an apoptotic stimulus is presented, BID translocates to the mitochondria to induce apoptosis. *In vitro*, this was determined through purification of a caspase-8 dependent cytochrome c releasing factor (CCRF or BID) (Luo *et al.*, 1998). Addition of BID to purified caspase-8 produces an 11 kDa and a 15 kDa

cleavage product of BID. This result was recapitulated in Jurkat T-cells where Fas activation, a potent inducer of caspase-8, caused cleavage of BID into two fragments. Furthermore, cell-free analysis showed that caspase-8 induced the C-terminal fragment of BID (tBID) to localize to mitochondria and induce cytochrome c release. Mitochondria enriched pellets of HL-60 cells (human promyelocytic leukemia cells) over-expressing BCL-2 showed a reduction in cleaved tBID induced cytochrome c-release. This data demonstrated that BID was cleaved by caspase-8 in Fas induced cell death and that the C-terminal cleavage product translocated to the mitochondria and induced cytochrome c release (Luo *et al.*, 1998).

1.5.2 Sensitizer BH3 only protein - BAD

BAD is a sensitizer BH3 only member of the BCL-2 family (Yang *et al.*, 1995). Murine BAD (mBAD) was initially discovered in both yeast two-hybrid screening and λ expression cloning where it bound to BCL-2 and BCL-XL (Yang *et al.*, 1995). *In cellulo* confirmation in FL5.12 murine prolymphocytic cells was done using HA (Haemagglutinin) tagged BAD. Immunoprecipitation (IP) of HA and BCL-2 showed binding to BCL-2 and BAD, respectively. HA-BAD also bound BCL-XL using a similar method and was determined to be a stronger interaction based on release of BAX from BCL-XL but not BCL-2. This result complemented cell viability results of BAD transfected cells as release of BAX was correlated to increased sensitivity to IL-3 withdrawal. BAD over-expressing cells were more sensitive to IL-3 withdrawal than control vector. Based on this initial characterization of BAD, it was shown to interact

with BCL-2 and BCL-XL which caused a decrease of BAX:BCL-XL heterodimers (Yang *et al.*, 1995).

1.6 BAD sequence and structure

As BAD was first isolated from mouse brain and thymus libraries, initial studies focused on mBAD (del Peso *et al.*, 1997; Yang *et al.*, 1995; Zha *et al.*, 1996). After sequencing the human isoform it was determined that the structure of mBAD is not identical to hBAD although it has a similar pro-apoptotic function (Ottilie *et al.*, 1997) (Figure 1). mBAD has a 43 amino acid N-terminal addition that has been shown to act as a regulatory domain of apoptotic function (Figure 1) (Condorelli *et al.*, 2001; Seo *et al.*, 2004). Upon apoptotic stimulation, mBAD can be cleaved at two aspartate residues (Asp 56 and 61) by caspase-3 (Condorelli *et al.*, 2001). hBAD lacks one of these sites (mBAD Asp 61, equivalent to hBAD Glu 19) and although one group reported hBAD could be cleaved which induces a pro-apoptotic protein (Condorelli *et al.*, 2001) a similar study determined that this cleavage is likely inconsequential (Seo *et al.*, 2004).

Although the N-terminus of BAD is not evolutionarily conserved there are similarities in post-translational modification sites. Three conserved serines (human numbering 75, 99 and 118, Figure 1) are recognized phosphorylation sites (Zha *et al.*, 1996); (Lizcano *et al.*, 2000; Virdee *et al.*, 2000; Zhou *et al.*, 2000).

Structurally, little is known about BAD which is classified as an innately unstructured protein (IUP) with a random coil conformation (Hinds *et al.*, 2007). The

most stable portion of BAD is the BH3 domain which becomes structured upon binding to anti-apoptotic BCL-2 proteins (Hinds *et al.*, 2007). Unlike the multi-domain pro-apoptotic protein BAK which requires 16 amino acids of the BH3 domain to bind BCL-XL, BAD requires a 25-mer. This domain (residues 140-164 of mBAD) does not form a stronger binding affinity compared to the 16-mer but rather increases the stability of the α-helix (Petros *et al.*, 2000). Intriguingly, the BH3 domain consists of residues 151-163 [murine numbering, hBAD 103-123 (Ottilie *et al.*, 1997)] which suggests that this domain is functionally critical yet not sufficient for the interaction of BAD and BCL-XL. Unlike anti-apoptotic BCL-2 proteins, BAD lacks a transmembrane domain therefore promoting cytosolic localization. However, BAD can localize to membrane sites such as the mitochondria through direct binding to BCL-2 and BCL-XL (Ottilie *et al.*, 1997; Zha *et al.*, 1996).

Alternatively, it has been reported that BAD contains two C-terminal lipid binding domains (LBD1 and 2) which promote binding to negatively charged lipids (Hekman *et al.*, 2006; Polzien *et al.*, 2009). These domains have been shown *in vitro* to promote BAD interactions with mitochondria although this has not been demonstrated in intact cells (Hekman *et al.*, 2006). Furthermore, this same group showed that hBAD phosphorylated at serine 134 was capable of forming pores within

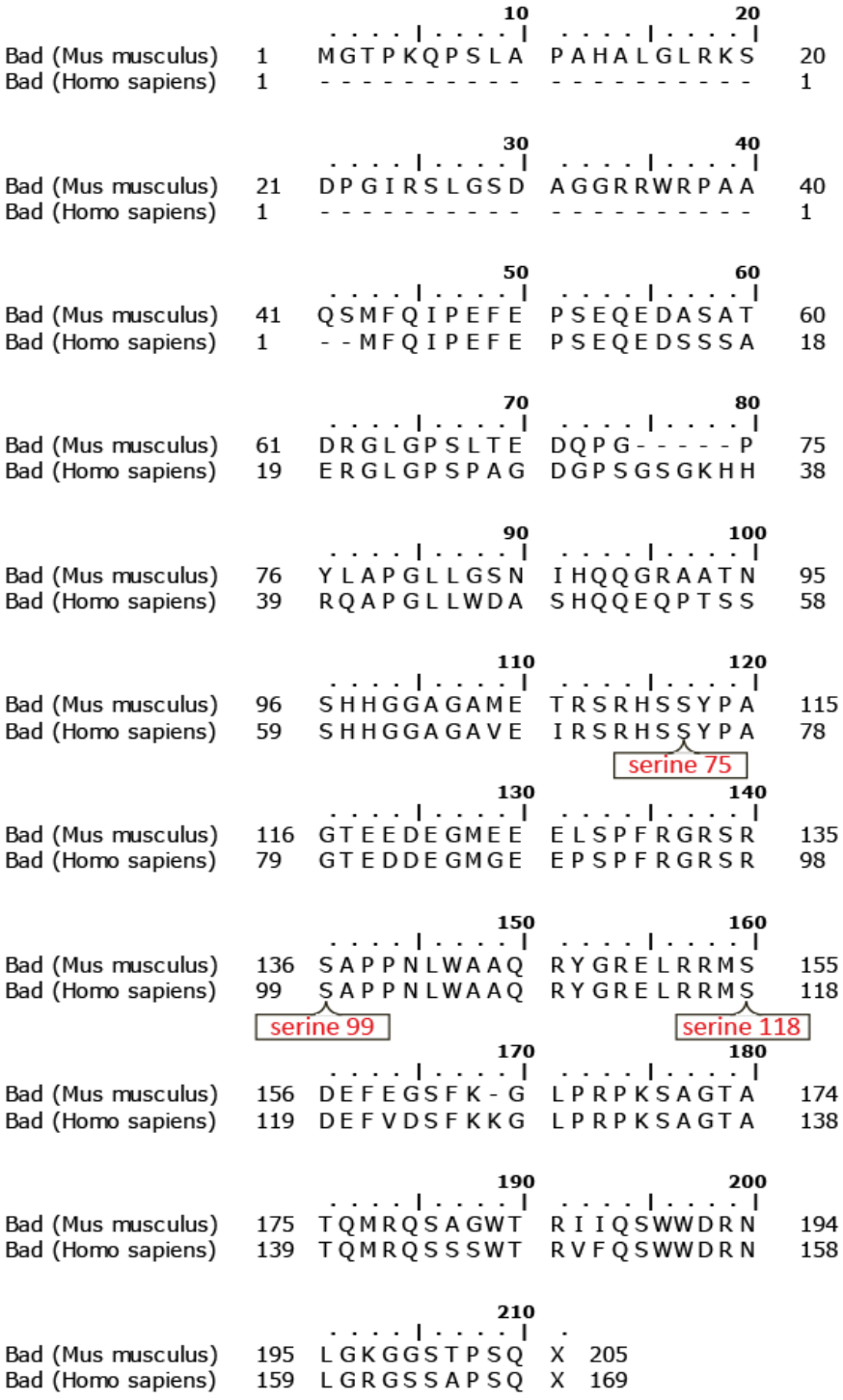

Figure 1: Sequence alignment of mouse and human BAD

Coding sequences (CDS) were acquired from NCBI database and aligned using Bioedit software (Ibis Biosciences). Three well established human serine phosphorylation sites are indicated in red and surrounded by black boxes.

synthetic membranes (Polzien *et al.*, 2009). Based on these data, BAD can form membrane interactions *in vitro* although this is yet to be confirmed in cells.

1.7 BCL-2 family member interactions

Although BAD and BID have dramatically different modes of regulation, one shared characteristic is translocation upon apoptotic induction. Both proteins translocate to the mitochondria to induce apoptosis. For BAD, mitochondrial localization is dependent on binding BCL-2 or BCL-XL (Yang *et al.*, 1995). Solving the BCL-XL structure provided evidence for domains of the anti-apoptotic proteins to bind apoptotic members such as BAD (Muchmore *et al.*, 1996). A hydrophobic cleft, formed by BH1, 2 and 3, was proposed to be a major binding site for pro-apoptotic BH3 domains. Single mutations to BH1 (G145A) and BH2 (W188A) of BCL-2 (and homologous mutations in BCL-XL) prevent interactions with multi-domain pro-apoptotic BAX (Cheng *et al.*, 1996; Yin *et al.*, 1994). Inability of BCL-2/BCL-XL to bind BAX abrogates the anti-apoptotic effect of this interaction in IL-3 deprived FL5.12 cells (Sedlak *et al.*, 1995; Yin *et al.*, 1994).

BAX activation is a stepwise process that leads to mitochondria localization and apoptotic induction. Upon apoptotic activation, BAX translocates from the cytosol to the mitochondrial membrane. Immunofluorescence shows that GFP-BAX has a diffuse cytosolic localization in L929 fibroscarcoma cells (Wolter *et al.*, 1997). Addition of staurosporine caused green fluorescent protein (GFP)-BAX to shift from the cytosol to the mitochondria. Upon apoptotic stimulation, BAX undergoes a conformational change that allows mitochondrial localization. In FL5.12 cells, IL-3 withdrawal caused

translocation of BAX from the cytosol to mitochondrial membranes. This translocation promoted protection from alkali induced membrane dissociation therefore suggesting that BAX localization involves membrane insertion (Goping *et al.*, 1998). Solving the monomeric BAX crystal structure showed a similar conformation to BCL-w, where the transmembrane domain is hidden within its hydrophobic cleft (Mizushima, 1968). The transmembrane domain is exposed upon direct activator BH3 protein binding. Through the use of BIM-SAHB (stabilized α-helix of BCL-2) BH3 peptide, NMR results showed that this peptide bound BAX at α-helices 1 and 2 (Suzuki *et al.*, 2000). This interaction was outside the usual hydrophobic cleft and functionally activated BAX *in vitro* and in MEFs to induce cytochrome c release. Further NMR data demonstrated that α-helix 9 (transmembrane domain) was dislodged upon BIM-SAHB binding. The transmembrane domain is released so is the BH3 domain (Gavathiotis *et al.*, 2008). With the BH3 domain exposed, BAX can form homodimers and heterodimers with BAK and BCL-2/BCL-XL at the mitochondria (Gavathiotis *et al.*, 2010). Using atomic force microscopy, BAX homodimers have been shown to insert into planar membranes and through channel studies, form pores (Kim *et al.*, 2009).

Once BAX is localized to mitochondrial membranes, anti-apoptotic BCL-2 family members are then able to interact and inhibit its function. BCL-XL interacts with BAX and tBID at the mitochondrial membrane to inhibit membrane permeabilization (Epand *et al.*, 2002). Immunoprecipitation of purified mouse liver mitochondria showed that BCL-XL binds to both BAX and tBID. Therefore, BCL-XL inhibits BAX

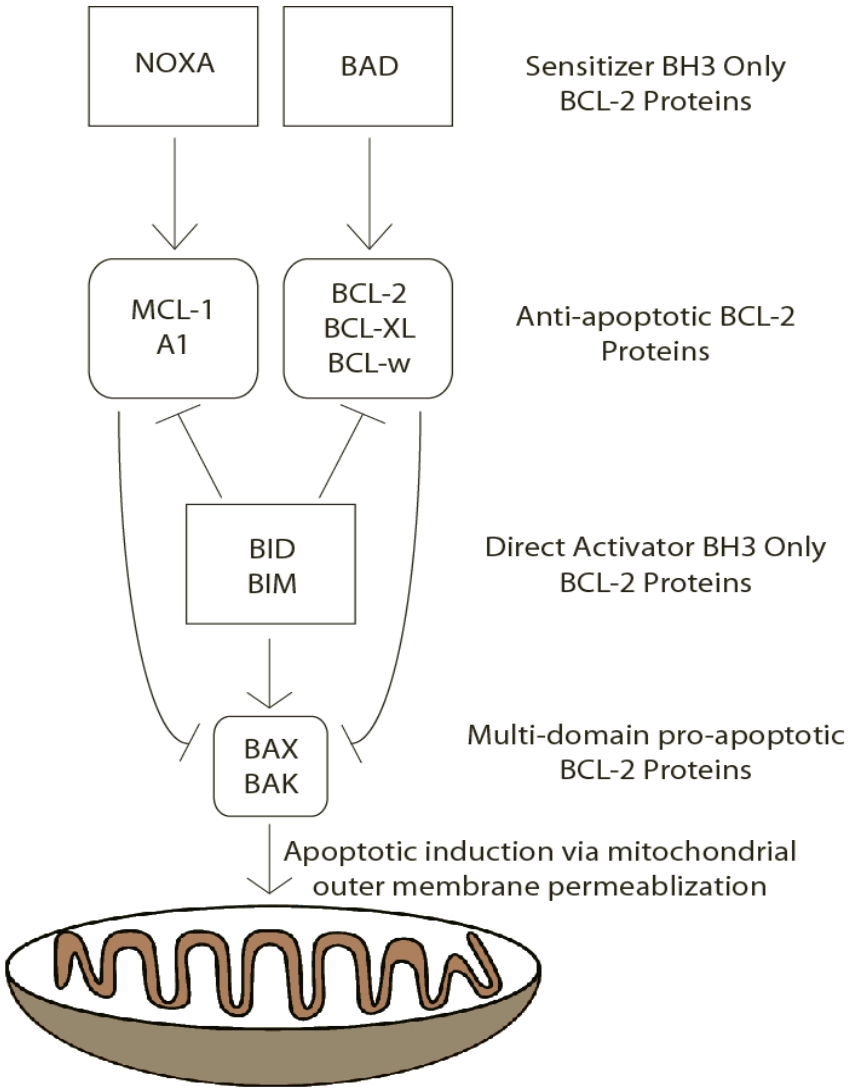

Figure 2: Hierarchical structure of BCL-2 family

Multi-domain pro-apoptotic BCL-2 proteins promote apoptosis through pore formation of the outer mitochondrial membrane. Anti-apoptotic members prevent this from occurring by directly binding BAX and BAK to prevent pore formation. Direct activator BH3 only proteins bind multi-domain pro-apoptotic proteins and induce an activating conformational change. They also bind anti-apoptotic proteins and inhibit their interactions with BAX and BAK. Sensitizer BH3 only proteins bind to anti-apoptotic members to promote release of multi-domain pro-apoptotic members. Sensitizer BH3 only proteins are activated by extracellular and intracellular signals that induce translocation to the mitochondria. [Image modified from (Billen *et al.*, 2008)].

activation two-fold, first by preventing oligomerization of BAX at the mitochondria and second by removing the activating signal, tBid (Figure 2).

The role of sensitizer BH3 only proteins is well known when apoptosis is activated. However, their role when not bound to anti-apoptotic BCL-2 proteins is poorly understood. For BAD, apoptotic induction promotes translocation from the cytosol to the mitochondrial membrane (Labi *et al.*, 2008). BAD interacts with 14-3-3 proteins in the cytosol, thus providing a cytosolic mechanism of apoptotic regulation (Wang *et al.*, 1999).

1.8 14-3-3 interactions with BAD

14-3-3 is a family of ubiquitiously expressed proteins which have a wide range of functions. Initial nomenclature of this family is derived from the position on DEAE (Diethylaminoethyl) - cellulose chromatography in combination with migration in gel electrophoresis (Zha *et al.*, 1996). This family of proteins is composed of 7 different isoforms (β, ε, γ, η, σ, τ and ζ) which were initially separated by reverse phase HPLC (High Performance Liquid Chromatography) (Fu *et al.*, 2000; Moore and Perez, 1967). Two other species α and δ, are phosphorylated forms of β and ζ, respectively. Although 14-3-3 proteins are expressed in every cell, different isoforms are cell type specific.

All human isoforms of 14-3-3 structure have been solved showing that each monomer contains 9 α-helices and forms a dimeric complex (Ichimura *et al.*, 1988; Martin *et al.*, 1993). Each 14-3-3 monomer contains an amphipathic groove (initially

determined in 14-3-3ζ) which is responsible for protein binding (Gardino *et al.*, 2006). Additionally, due to each monomeric unit containing this domain, 14-3-3 proteins contain the ability to bind two substrates simultaneously (Liu *et al.*, 1995). This dual binding ability suggests a signal transduction role for 14-3-3 proteins by allowing a scaffold structure for proteins to interact.

Generally, the role of 14-3-3 proteins is in binding serine phosphorylated proteins. There are two consensus sequences for this interaction, RXSpSXP (where X can be any amino acid and pS is the phosphorylated serine) and RXY/FXpSXP (where Y is an aromatic residue, F is a basic residue, X is any amino acid and pS is the phosphorylated serine) which were deduced from binding interactions from peptide libraries (Petosa *et al.*, 1998). Intriguingly, it has also been shown that 14-3-3 proteins can interact with unphosphorylated proteins. An example of this is 5-phosphatase which contains a RSESEE motif (Yaffe *et al.*, 1997). This motif is thought to act in a similar fashion to phosphorylated serines due to the negative charge produced by the respective glutamic acids.

Through the use of a cell free IVTT and yeast two hybrid binding system, BAD was shown to bind all seven isoforms of 14-3-3 (Campbell *et al.*, 1997). Interactions with 14-3-3 proteins inhibit the pro-apoptotic role of BAD (Subramanian *et al.*, 2001). In serum deprived HeLa (human cervical cancer) cells, BAD induced apoptosis was inhibited slightly more by σ, γ and η than the other isoforms. In COS 7 cells, 14-3-3β was the only isoform that resulted in a strong reduction in viability upon BAD induced cell death (Zha *et al.*, 1996). Structurally, BAD binds 14-3-3 proteins within the amphipathic groove as conserved residues within this groove are necessary for

BAD:14-3-3ζ interactions (Subramanian *et al.*, 2001). BAD binding 14-3-3ζ is also necessary for AKT induced cell protection in COS-7 cells. Mutation of a lysine residue (K49E) within the hydrophobic groove prevented AKT induced survival. Although BAD binding 14-3-3 is a pro-survival mechanism, whether this interaction induces downstream signaling is unknown.

1.9 Regulation of BAD

BAD was shown to interact with BCL-2/BCL-XL although it was unknown how this interaction was regulated. Using IL-3 dependent FL5.12 cells over-expressing BAD, the function of IL-3 on BAD induced apoptosis was tested. λ expression cloning and HA-BAD immunoprecipitations showed that BAD interacted with 14-3-3τ (Yang *et al.*, 2001). Intriguingly, BAD migrated as a doublet which collapsed to a single band when potato acid phosphatase (PAP) was added. BAD was immunoprecipitated from cells incubated with ^{32}P as a means of looking for specific phosphorylation sites. Tryptic peptides of BAD were applied to a thin layer chromatography (TLC) plate and separated by charge in the first dimension and hydrophobicity in the second dimension. Through Edman degradation and direct TLC comparison to peptides where serines were replaced with phosphoserines; serine 112 (S112) and serine 136 (S136) were deduced as BAD phosphorylation sites. By mutating S112, S136 or both sites to alanine, it was shown that either phosphorylation site was sufficient for 14-3-3β/γ binding (Zha *et al.*, 1996).

Consistent with many other BCL-2 family members, the apoptotic role of BAD is regulated mainly by its intracellular location (Zha *et al.*, 1996). The BH3 domain of

BAD interacting with BCL-XL is critical for BAD localization to the mitochondria. Deletion mutants of BAD in BL21 (competent *E.coli*) cells showed that mBAD 141-172 is necessary and sufficient for BCL-2/BCL-XL binding (Puthalakath and Strasser, 2002). These residues contain the BH3 α-helix of BAD (mBAD 143-153) thus providing evidence of the importance of this domain. In fact, a single point mutation, L151A (L114A in human) is enough to disrupt the interaction with BCL-XL by greater than 90%. This interaction was determined *in vitro* using co-immunoprecipiation of BCL-XL combined with IVTT-generated BAD and BADL151A as well as in cells using FL5.12-BCL-XL cells transfected with BAD constructs. In FL5.12 cells, BADL151A did not induce apoptosis upon IL-3 withdrawal.

Although this assay used an artificial approach in manipulating the BH3 domain, one post-translational modification site, serine 118 (hBAD numbering), is within the BH3 domain (Zha *et al.*, 1997). In the presence epidermal growth factor (EGF), BAD is phosphorylated at this site (Lizcano *et al.*, 2000; Tan *et al.*, 2000; Virdee *et al.*, 2000). This phosphorylation site is within the hydrophobic face of the amphipathic α-helix and directly disrupts the binding of BAD to BCL-XL (Zhou *et al.*, 2000). At this time, serine 118 is the only site of post-translational modification within the BH3 domain although it has been shown that other mutations (eg. L114A and D119G) lead to an inability of BAD to bind anti-apoptotic BCL-2 members (Tan *et al.*, 2000; Virdee *et al.*, 2000; Zhou *et al.*, 2010).

In order for serine 118 to become phosphorylated, multiple growth promoting or anti-apoptotic kinases are necessary. The phosphorylation of serine 118 is a cell type and stimulus dependent event. *In vitro* and in HEK 293 (Human Embryonic

Kidney) cells, PKA (Protein Kinase A) and RSK1 (Ribosomal S6 Kinase1) are potent kinases for serine 155 (mouse numbering, serine 118 in human) (Adachi *et al.*, 2003). In HEK 293T cells, it was shown that Chk1 phosphorylates mBAD at serine 155 *in vitro* and was detected via immunoprecipitation to bind with mBAD in HEK 293T cells (Zhou *et al.*, 2000). In N1E-115 cells (mouse neuroblastoma line), serine 155 phosphorylation was induced by PKG (Protein Kinase G) (Han *et al.*, 2004). Other known kinases for serine 118 include the Pim kinases (Pim-1,2 and 3) which phosphorylate this site with differing specificities in HEK 293 cells (Johlfs and Fiscus, 2010). Due to this cell type specific kinase activation, identifying upstream pro-survival signaling pathways is crucial in understanding the role of BAD in different cells.

Kinases that phosphorylate serine 75 and 99 are also stimuli and cell type dependent. Initial discovery of these sites demonstrated that extracellular factors (eg. IL-3) were capable of inducing phosphorylation at both sites (Macdonald *et al.*, 2006). In primary neurons, IGF-1 (insulin like growth factor-1) stimulation induces specific activation of phosphatidylinositol 3 kinase (PI3K) and elicits a pro-survival response (Zha *et al.*, 1996). Activation of PI3K induces a downstream cascade of other kinase activations including AKT. Transfection of active AKT into granule neuronal cells induces a pro-survival effect through phosphorylation of mBAD at serine 136 (serine 99 in human). By mutating mBAD at serine 136 to alanine, this protective effect of IGF-1 was ablated (Dudek *et al.*, 1997).

On the other hand, addition of IL-3 induces phosphorylation of mBAD serine 112 (hBAD 75). *In vitro* immunoprecipitation analysis of FL5.12 lysates determined that in the presence of IL-3, BAD binds PKA (Datta *et al.*, 1997). Addition of a PKA

specific inhibitor (H89) prevented serine 112 phosphorylation. Another kinase responsible for mBAD serine 112 phosphorylation is pp90 ribosomal 6 kinase-2 (RSK-2). Activated RSK2 immunoprecipitates with BAD in HEK 293T lysates and induces BADS112 phosphorylation (Bonni *et al.*, 1999). In cerebral granular neurons grown in serum free media, co-transfection of RSK-2 and wild-type BAD prevented cell death. Transfection of BAD S112A or dominant negative RSK-2 still promoted apoptosis (Bonni *et al.*, 1999).

Unlike the three major phosphorylation sites, serine 91 (mBAD serine 128) has an opposing role. Through *in vitro* kinase assays and *in vivo* pathways stimulation, c-Jun N-terminal kinase (JNK) was shown to phosphorylate this site (Bonni *et al.*, 1999). Phosphorylation of mBAD serine 128 promoted cell death in granule neurons that were insulin deprived. Furthermore, an ischemic brain injury model in mice promoted increased mBAD serine 128 phosphorylation through JNK activation (Donovan *et al.*, 2002). Although serine 128 phosphorylation promoted cell death, this site was dependent on AKT activation and serine 136 phosphorylation.

Similar in function to mBAD serine 128 phosphorylation, a recent report has demonstrated that BAD can be methylated on two arginine residues (Wang *et al.*, 2007). Intriguingly, the AKT consensus sequence (RxRxxS) also contains two Rx motifs which are consensus sites for protein methyl arginine transferase (PRMT) (Sakamaki *et al.*, 2011). Through the use of point mutants in HEK 293T cells, arginine 94 and 96 were shown to be methylated by PRMT1 (Wooderchak *et al.*, 2008). Methylation of these sites inhibits phosphorylation of serine 99 by AKT1. Furthermore, BAD

immunoprecipitations from HEK 293T lysates determined that arginine methylation promoted binding to BCL-XL and inhibited binding to 14-3-3β (Sakamaki *et al.*, 2011).

The phosphatases that dephosphorylate serine 75, 99 and 118 are also site specific and stimulus sensitive. For example, hBAD serine 75 is dephosphorylated by protein phosphatase 2A (PP2A) and is thought to be a gatekeeper to the other phosphorylation sites (Sakamaki *et al.*, 2011). This was shown in FL5.12 cells stably expressing BAD and BCL-XL. Upon IL-3 withdrawal, cell lysates were prepared at different time points and were immunoblotted for phosphorylation of mBADS112 and mBADS136. Based on these data, serine 112 was dephosphorylated prior to serine 136 (Chiang *et al.*, 2003).

The role of phosphatase activation is important for the function of BAD. For instance, in HEK 293 cells calcineurin induces BAD translocation to the mitochondria (Chiang *et al.*, 2003). This was shown by transiently transfecting HEK 293 cells with catalytically active calcineurin, FLAG-BAD and BCL-XL. By immunoprecipitating FLAG-BAD, it was determined that calcineurin increased the binding affinity of BAD with BCL-XL. Subsequent immunofluorescence experiments showed that increasing cytosolic calcium [through addition of thapsigargin; known inducer of calcineurin (Wang *et al.*, 1999)] promoted BAD localization to the mitochondria (Tombal *et al.*, 2000). Later, it was determined that calcineurin dephosphorylated mBAD at mainly serine 155 (hBADS118) (Wang *et al.*, 1999). This was determined using phospho-specific serine 155 antibodies in the presence of calcineurin inhibitors cyclosporine A and FK506. However, based on the experiments conducted other sites cannot be ruled out.

In summary, serines 75, 99 and 118 phosphorylation prevents the apoptotic function of hBAD. Alternatively, serine 91 (mBAD 128) and methylation of arginine 94 and 96 act in an opposing manner by inducing apoptosis. Although these mechanisms are critical for the apoptotic role of BAD, their function in non-canonical pathways is poorly understood.

1.10 Cell cycle effects of BCL-2 family – The role of BAD in cell cycle

BCL-2 family members are critical in regulating apoptosis; however, non-canonical cell cycle roles have emerged. BCL-2 and BCL-XL have been shown to have direct effects on cell cycle progression. T-cells in transgenic mice expressing the lck-*BCL-2* transgene exhibited delayed S-phase entry following T-cell activation (Yang *et al.*, 2004). Consistent with this, IL-3 withdrawal in FDC-P1 cells expressing BCL-2 generated mainly quiescent cells (Linette *et al.*, 1996; O'Reilly *et al.*, 1996). Intriguingly, the apoptotic and cell cycle functions of BCL-2 were separated by mutating a conserved N-terminal tyrosine (Y28, within the BH4 domain). In FDC-P1 cells, IL-3 withdrawal induced equivalent cell death of Y28 mutants as BCL-2 control. However, after IL-3 re-addition wild-type BCL-2 cells took approximately 6 days to transition into S-phase while cells transfected with BCL-2 mutated at Y28 began cycling after 2 days (Vaux *et al.*, 1988). Consistent with this result, in the WAP-Tag-BCL-2 breast tumor progression mouse, BCL-2 retained anti-apoptotic function and lost anti-mitotic function (Huang *et al.*, 1997). Alternatively, in Rat1MycER (fibroblasts expressing a Myc-estrogen receptor fusion) cells, the role of BclxL/BCL-2 in apoptosis was completely linked to the cell cycle role and could not be separated by the Y28 mutation (Furth *et al.*, 1999). Due to the

contradictory nature of these studies, further analysis of Y28 and the BH4 domain is needed to address their functions.

Further investigation into the cell cycle role of BCL-2 showed that the effect of BCL-2/BCL-XL expression led to an inhibition of G_o/G1 progression (Janumyan *et al.*, 2003). The rationale as to how an anti-apoptotic protein can inhibit cell cycle progression is based on the binding partners BCL-2 and BCL-XL share. In BAX/BAK DKO MEF cells, over-expression of that BCL-2 and BCL-XL had no effect on cell cycle progression thus implicating BAX and BAK as mediators of the cell cycle effects. In these same cells, p27 levels were elevated as was an activating phosphorylation (serine 10). Re-expression of BAX and BAK caused depletion of p27 levels, decreased the kinase responsible for serine 10 phosphorylation (Mirk) and as a result decreased the phosphorylation of p27. Based on these data, the authors concluded that BCL-2 and BCL-XL interrupted cell cycle progression due to their interactions with BAX and BAK (Chattopadhyay *et al.*, 2001; Janumyan *et al.*, 2003).

BAD has been shown to inhibit this cell cycle effect by directly binding BCL-XL. Rat1 fibroblast cells stably over-expressing BAD and BCL-XL showed increased cell cycle progression in 0.1% serum and increased contact conditions compared to BCL-XL over-expressing cells (Janumyan *et al.*, 2008). Furthermore, Rat1 fibroblasts over-expressing wild-type BAD or mutant BAD unable to bind BCL-XL (BADL151A), demonstrated the importance of BAD binding to BCL-XL for progression to S-phase in 0.05% serum conditions (Chattopadhyay *et al.*, 2001).

Consistent with these results, a report from our group determined a similar role for BAD in MCF-7 and SK-BR-3 breast cancer cells. In MCF-7 cells, siRNA to BAD inhibited progression to the G2/M phase of the cell cycle (Chattopadhyay *et al.*, 2001). Furthermore, siRNA to BAD resulted in decreased overall cell numbers after 48 and 96 hours of growth for MCF-7 and SK-BR-3 cells, respectively.

Alternatively, BAD has also been shown to inhibit cell cycle by a novel DNA binding mechanism. In MCF-7 breast cancer cells, BAD over-expression caused a decrease in cyclin D1 protein (Craik *et al.*, 2010). Through electrophoretic mobility shift assay (EMSA) and chromatin immunoprecipitation (ChIP) BAD was shown to bind c-Jun at the transcription response element (TRE) for cyclin D1. Furthermore, BAD was shown using a luciferase reporter assay of the cyclin D1 TRE to inhibit transcription of cyclin D1 which was serine 75 and 99 dependent.

Due to the conflicting nature of these results, further analysis is needed to understand the role of BAD in the cell cycle. Importantly, BAD regulation between apoptosis and cell cycle progression could be used as a therapeutic target.

1.11 Clinical implications of BAD expression

Although removal of BAD has a minor role in mouse tumor promotion, clinically, increased BAD expression can positively correlate with patient outcome. For breast cancer patients, BAD expression was correlated with Docetaxel response (Fernando *et al.*, 2007). Patient samples were scored as either having high or low BAD expression by immunohistochemistry (IHC). Patients whose tumors had high BAD

levels also had increased disease free survival (DFS) and overall survival (Craik *et al.*, 2010). Furthermore, in estrogen receptor positive breast cancer, BAD is associated with response to tamoxifen (Craik *et al.*, 2010). Patients whose tumors expressed high levels of BAD had an increased disease free survival after tamoxifen treatment.

Independent of treatment type, BAD expression has been linked to patient outcome. In androgen independent prostate cancer (AIPC), BAD expression has been correlated to increased time prior to relapse and overall survival (Cannings *et al.*, 2007). Consistent with this result, non-small cell lung cancer patients whose tumors had low BAD expression had significantly shorter survival times (Teo *et al.*, 2007). However, in gastric cancer patients from Brazil, BAD has no prognostic significance for overall outcome (Huang *et al.*, 2011). Based on these results, the role of BAD in cancer is variable. Using BAD as a prognostic marker or therapeutic target may need to be addressed on a cancer type or even cell type basis.

Based on the regulatory role the BH3 domain plays in BAD function; it could be expected that these regions would be susceptible to mutation. Intriguingly, in six different cancer types: non-small cell lung cancer (Barrezueta *et al.*, 2010), B-cell lymphoma (Huang *et al.*, 2011), gastric cancer (Schmitz *et al.*, 2006), ovarian serous and muscinous tumors (Barrezueta *et al.*, 2010; Jeong *et al.*, 2007) and hepatocellular tumors (Kim *et al.*, 2006) there were no detectable mutations in the BAD gene. However in human colon cancer samples, 2 mutations were detected in 47 patient samples. Intriguingly, these mutations were shown *in vitro* to inactivate BAD and BCL-XL interactions (hBAD E113K and L114F) (Yoo *et al.*, 2006). Based on these data, BAD

mutations are unlikely to cause tumor induction although disruption of BCL-XL binding may increase susceptibility for tumor formation.

1.13 Non-canonical roles of BAD

The apoptotic role of BAD is well established while non-canonical roles are gradually emerging. In BAD knock-out mice (*BAD -/-*) there are two major phenotypes that arise.

First, BAD -/- mice display abnormal glucose homeostasis (Lee *et al.*, 2004). Liver mitochondria extracted from BAD -/- mice were less efficient than wild-type mice at using glucose as measured by glucokinase production of glucose-6-phophate. BAD promotes this phenotype by binding proteins outside the BCL-2 family. BAD formed a holoenzyme complex containing protein phosphatase 1 (PP1), Wiskott-Aldrich family member (WAVE-1), PKA and glucokinase. Using 3-dimensional western blot analysis (first dimension – gel filtration of mitochondrial proteins, second dimension – non-denaturing gel electrophoresis, third dimension – denaturing SDS-PAGE) the complex was resolved. In BAD -/- hepatocytes, the complex did not form thus providing evidence of the necessity of BAD in this complex. Intriguingly, complex formation was independent of mBAD phosphorylation status (determined by genomic knock-in of serine mBAD serine 112, 136 and 155 alanine mutant, $BAD^{3SA/3SA}$ mice) while mBAD phosphorylation was necessary for glucokinase activity (Danial *et al.*, 2003). Based on this result, BAD has a critical role in glucose homeostasis of mouse liver hepatocytes.

In mouse pancreatic β cells, a similar role for BAD emerges. In BAD -/- mice, glucose stimulation via hyperglycemic clamp studies resulted in depressed insulin secretion from β cells compared to BAD +/+ mice. BAD -/- mice could be rescued by transfection of GFP-BAD in which insulin release was restored. Mutation of the BH3 domain of BAD prevented this function (mBAD L151A) as did the non-phosphorylable mutant (BAD3SA) (Danial *et al.*, 2003). By probing the phosphorylation site responsible for BCL-XL binding (mouse BAD serine 155) it was determined that this site was critical for glucokinase activity in this complex (Danial *et al.*, 2008). Based on these data, BAD has a bifunctional role in regulating metabolic and apoptotic functions which is regulated by its BH3 domain.

Second, mice lacking BAD develop diffuse large B cell lymphoma after approximately 15 months (Danial, 2008). In comparison, *p53 -/-* mice develop tumors at an accelerated rate (approximately 6 months) (Ranger *et al.*, 2003). This relatively slow progression of tumor development supports the idea that BAD is not critical for apoptotic induction but sensitizes cells to extrinsic stimuli. Based on this, BAD does not have a direct transforming role as other gene mutations are potentially necessary for tumor progression.

Intriguingly, although BAD -/- mice develop tumors, BAD over-expressing cancer cells also develop tumors. C4 (prostate cancer) cells over-expressing luciferase tagged BAD had increased tumor growth in a xenograft model compared to control (Finlay, 1992). Consistent with this, these cells also proliferated at an accelerated rate *in vitro*. Alternatively, A549 (lung cancer) cells over-expressing BAD had decreased proliferation and tumor growth in a xenograft model.

The tumor promoting role of BAD is poorly understood. Based on these reports, BAD can act either by inhibiting or promoting tumor growth. In order to use BAD in a prognostic or a therapeutic setting, deciphering what causes these polar phenotypes is necessary.

1.14 Purpose of study

The primary aim of this study is to decipher the role of BAD in breast cancer cell proliferation and tumor growth. This study shows that BAD promotes cell survival which is regulated through phosphorylation. As well, this study shows that BAD promotes tumor growth and suggests a regulatory mechanism where serine 118 phosphorylation regulates apoptotic and tumor growth functions.

1.15 References - Introduction

Adachi M, Zhang YB, Imai K. (2003). Mutation of BAD within the BH3 domain impairs its phosphorylation-mediated regulation. *FEBS Lett* **551:** 147-152.

Adams JM, Harris AW, Pinkert CA, Corcoran LM, Alexander WS, Cory S *et al*. (1985). The c-myc oncogene driven by immunoglobulin enhancers induces lymphoid malignancy in transgenic mice. *Nature* **318:** 533-538.

Barrezueta LF, Oshima CT, Lima FO, De Oliveira Costa H, Gomes TS, Neto RA *et al*. (2010). The intrinsic apoptotic signaling pathway in gastric adenocarcinomas of brazilian patients: Immunoexpression of the bcl-2 family (bcl-2, bcl-x, bak, bax, bad) determined by tissue microarray analysis. *Mol Med Report* **3:** 261-267.

Billen LP, Kokoski CL, Lovell JF, Leber B, Andrews DW. (2008). Bcl-XL inhibits membrane permeabilization by competing with bax. *PLoS Biol* **6:** e147.

Boise LH, Gonzalez-Garcia M, Postema CE, Ding L, Lindsten T, Turka LA *et al*. (1993). Bcl-X, a bcl-2-related gene that functions as a dominant regulator of apoptotic cell death. *Cell* **74:** 597-608.

Bonni A, Brunet A, West AE, Datta SR, Takasu MA, Greenberg ME. (1999). Cell survival promoted by the ras-MAPK signaling pathway by transcription-dependent and -independent mechanisms. *Science* **286:** 1358-1362.

Boyd JM, Gallo GJ, Elangovan B, Houghton AB, Malstrom S, Avery BJ *et al*. (1995). Bik, a novel death-inducing protein shares a distinct sequence motif with bcl-2 family proteins and interacts with viral and cellular survival-promoting proteins. *Oncogene* **11:** 1921-1928.

Campbell JK, Gurung R, Romero S, Speed CJ, Andrews RK, Berndt MC *et al*. (1997). Activation of the 43 kDa inositol polyphosphate 5-phosphatase by 14-3-3zeta. *Biochemistry* **36:** 15363-15370.

Canadian Cancer Society's Steering Committee on Cancer Statistics. (2011). Canadian cancer statistics 2011.

Cannings E, Kirkegaard T, Tovey SM, Dunne B, Cooke TG, Bartlett JM. (2007). Bad expression predicts outcome in patients treated with tamoxifen. *Breast Cancer Res Treat* **102:** 173-179.

Chattopadhyay A, Chiang CW, Yang E. (2001). BAD/BCL-[X(L)] heterodimerization leads to bypass of G0/G1 arrest. *Oncogene* **20:** 4507-4518.

Cheng EH, Levine B, Boise LH, Thompson CB, Hardwick JM. (1996). Bax-independent inhibition of apoptosis by bcl-XL. *Nature* **379:** 554-556.

Chen-Levy Z, Cleary ML. (1990). Membrane topology of the bcl-2 proto-oncogenic protein demonstrated in vitro. *J Biol Chem* **265:** 4929-4933.

Chiang CW, Kanies C, Kim KW, Fang WB, Parkhurst C, Xie M *et al*. (2003). Protein phosphatase 2A dephosphorylation of phosphoserine 112 plays the gatekeeper role for BAD-mediated apoptosis. *Mol Cell Biol* **23:** 6350-6362.

Cleary ML, Smith SD, Sklar J. (1986). Cloning and structural analysis of cDNAs for bcl-2 and a hybrid bcl-2/immunoglobulin transcript resulting from the t(14;18) translocation. *Cell* **47:** 19-28.

Condorelli F, Salomoni P, Cotteret S, Cesi V, Srinivasula SM, Alnemri ES *et al*. (2001). Caspase cleavage enhances the apoptosis-inducing effects of BAD. *Mol Cell Biol* **21:** 3025-3036.

Craig RW, Jabs EW, Zhou P, Kozopas KM, Hawkins AL, Rochelle JM *et al*. (1994). Human and mouse chromosomal mapping of the myeloid cell leukemia-1 gene: MCL1 maps to human chromosome 1q21, a region that is frequently altered in preneoplastic and neoplastic disease. *Genomics* **23:** 457-463.

Craik AC, Veldhoen RA, Czernick M, Buckland TW, Kyselytzia K, Ghosh S *et al*. (2010). The BH3-only protein bad confers breast cancer taxane sensitivity through a nonapoptotic mechanism. *Oncogene* .

Dalla-Favera R, Bregni M, Erikson J, Patterson D, Gallo RC, Croce CM. (1982). Human c-myc onc gene is located on the region of chromosome 8 that is translocated in burkitt lymphoma cells. *Proc Natl Acad Sci U S A* **79:** 7824-7827.

Danial NN. (2008). BAD: Undertaker by night, candyman by day. *Oncogene* **27 Suppl 1:** S53-70.

Danial NN, Gramm CF, Scorrano L, Zhang CY, Krauss S, Ranger AM *et al*. (2003). BAD and glucokinase reside in a mitochondrial complex that integrates glycolysis and apoptosis. *Nature* **424:** 952-956.

Danial NN, Walensky LD, Zhang CY, Choi CS, Fisher JK, Molina AJ *et al*. (2008). Dual role of proapoptotic BAD in insulin secretion and beta cell survival. *Nat Med* **14:** 144-153.

Datta SR, Dudek H, Tao X, Masters S, Fu H, Gotoh Y *et al*. (1997). Akt phosphorylation of BAD couples survival signals to the cell-intrinsic death machinery. *Cell* **91:** 231-241.

del Peso L, Gonzalez-Garcia M, Page C, Herrera R, Nunez G. (1997). Interleukin-3-induced phosphorylation of BAD through the protein kinase akt. *Science* **278:** 687-689.

Derenne S, Monia B, Dean NM, Taylor JK, Rapp MJ, Harousseau JL *et al*. (2002). Antisense strategy shows that mcl-1 rather than bcl-2 or bcl-x(L) is an essential survival protein of human myeloma cells. *Blood* **100:** 194-199.

Donovan N, Becker EB, Konishi Y, Bonni A. (2002). JNK phosphorylation and activation of BAD couples the stress-activated signaling pathway to the cell death machinery. *J Biol Chem* **277:** 40944-40949.

Dudek H, Datta SR, Franke TF, Birnbaum MJ, Yao R, Cooper GM *et al*. (1997). Regulation of neuronal survival by the serine-threonine protein kinase akt. *Science* **275:** 661-665.

Duriez PJ, Wong F, Dorovini-Zis K, Shahidi R, Karsan A. (2000). A1 functions at the mitochondria to delay endothelial apoptosis in response to tumor necrosis factor. *J Biol Chem* **275:** 18099-18107.

Epand RF, Martinou JC, Montessuit S, Epand RM, Yip CM. (2002). Direct evidence for membrane pore formation by the apoptotic protein bax. *Biochem Biophys Res Commun* **298:** 744-749.

Erikson J, ar-Rushdi A, Drwinga HL, Nowell PC, Croce CM. (1983). Transcriptional activation of the translocated c-myc oncogene in burkitt lymphoma. *Proc Natl Acad Sci U S A* **80:** 820-824.

Fernando R, Foster JS, Bible A, Strom A, Pestell RG, Rao M *et al*. (2007). Breast cancer cell proliferation is inhibited by BAD: Regulation of cyclin D1. *J Biol Chem* **282:** 28864-28873.

Finlay CA. (1992). P53 loss of function: Implications for the processes of immortalization and tumorigenesis. *Bioessays* **14:** 557-560.

Fu H, Subramanian RR, Masters SC. (2000). 14-3-3 proteins: Structure, function, and regulation. *Annu Rev Pharmacol Toxicol* **40:** 617-647.

Furth PA, Bar-Peled U, Li M, Lewis A, Laucirica R, Jager R *et al*. (1999). Loss of anti-mitotic effects of bcl-2 with retention of anti-apoptotic activity during tumor progression in a mouse model. *Oncogene* **18:** 6589-6596.

Gajkowska B, Wojewodzka U, Gajda J. (2004). Translocation of bax and bid to mitochondria, endoplasmic reticulum and nuclear envelope: Possible control points in apoptosis. *J Mol Histol* **35:** 11-19.

Gardino AK, Smerdon SJ, Yaffe MB. (2006). Structural determinants of 14-3-3 binding specificities and regulation of subcellular localization of 14-3-3-ligand complexes: A comparison of the X-ray crystal structures of all human 14-3-3 isoforms. *Semin Cancer Biol* **16:** 173-182.

Gavathiotis E, Reyna DE, Davis ML, Bird GH, Walensky LD. (2010). BH3-triggered structural reorganization drives the activation of proapoptotic BAX. *Mol Cell* **40:** 481-492.

Gavathiotis E, Suzuki M, Davis ML, Pitter K, Bird GH, Katz SG *et al*. (2008). BAX activation is initiated at a novel interaction site. *Nature* **455:** 1076-1081.

Gibson L, Holmgreen SP, Huang DC, Bernard O, Copeland NG, Jenkins NA *et al*. (1996). Bcl-W, a novel member of the bcl-2 family, promotes cell survival. *Oncogene* **13:** 665-675.

Gonzalez-Garcia M, Perez-Ballestero R, Ding L, Duan L, Boise LH, Thompson CB *et al*. (1994). Bcl-XL is the major bcl-x mRNA form expressed during murine development and its product localizes to mitochondria. *Development* **120:** 3033-3042.

Goping IS, Gross A, Lavoie JN, Nguyen M, Jemmerson R, Roth K *et al*. (1998). Regulated targeting of BAX to mitochondria. *J Cell Biol* **143:** 207-215.

Graninger WB, Seto M, Boutain B, Goldman P, Korsmeyer SJ. (1987). Expression of bcl-2 and bcl-2-ig fusion transcripts in normal and neoplastic cells. *J Clin Invest* **80:** 1512-1515.

Han EK, Butler C, Zhang H, Severin JM, Qin W, Holzman TF *et al*. (2004). Chkl binds and phosphorylates BAD protein. *Anticancer Res* **24:** 3907-3910.

Hanahan D, Weinberg RA. (2011). Hallmarks of cancer: The next generation. *Cell* **144:** 646-674.

Hanahan D, Weinberg RA. (2000). The hallmarks of cancer. *Cell* **100:** 57-70.

Hawkins JM, Wood M, Wright F, Secker-Walker LM. (1992). Isochromosome 1q in acute monocytic leukemia: A new nonrandom association. *Genes Chromosomes Cancer* **5:** 181-183.

Hayward WS, Neel BG, Astrin SM. (1981). Activation of a cellular onc gene by promoter insertion in ALV-induced lymphoid leukosis. *Nature* **290:** 475-480.

Hekman M, Albert S, Galmiche A, Rennefahrt UE, Fueller J, Fischer A *et al*. (2006). Reversible membrane interaction of BAD requires two C-terminal lipid binding domains in conjunction with 14-3-3 protein binding. *J Biol Chem* **281:** 17321-17336.

Herold MJ, Zeitz J, Pelzer C, Kraus C, Peters A, Wohlleben G *et al*. (2006). The stability and anti-apoptotic function of A1 are controlled by its C terminus. *J Biol Chem* **281:** 13663-13671.

Hinds MG, Smits C, Fredericks-Short R, Risk JM, Bailey M, Huang DC *et al*. (2007). Bim, bad and bmf: Intrinsically unstructured BH3-only proteins that undergo a localized conformational change upon binding to prosurvival bcl-2 targets. *Cell Death Differ* **14:** 128-136.

Hockenbery D, Nunez G, Milliman C, Schreiber RD, Korsmeyer SJ. (1990). Bcl-2 is an inner mitochondrial membrane protein that blocks programmed cell death. *Nature* **348:** 334-336.

Huang DC, Adams JM, Cory S. (1998). The conserved N-terminal BH4 domain of bcl-2 homologues is essential for inhibition of apoptosis and interaction with CED-4. *EMBO J* **17:** 1029-1039.

Huang DC, O'Reilly LA, Strasser A, Cory S. (1997). The anti-apoptosis function of bcl-2 can be genetically separated from its inhibitory effect on cell cycle entry. *EMBO J* **16:** 4628-4638.

Huang Y, Liu D, Chen B, Zeng J, Wang L, Zhang S *et al*. (2011). Loss of bad expression confers poor prognosis in non-small cell lung cancer. *Med Oncol* .

Ichimura T, Isobe T, Okuyama T, Takahashi N, Araki K, Kuwano R *et al*. (1988). Molecular cloning of cDNA coding for brain-specific 14-3-3 protein, a protein kinase-dependent activator of tyrosine and tryptophan hydroxylases. *Proc Natl Acad Sci U S A* **85:** 7084-7088.

Ito T, Deng X, Carr B, May WS. (1997). Bcl-2 phosphorylation required for anti-apoptosis function. *J Biol Chem* **272:** 11671-11673.

Janumyan Y, Cui Q, Yan L, Sansam CG, Valentin M, Yang E. (2008). G0 function of BCL2 and BCL-xL requires BAX, BAK, and p27 phosphorylation by mirk, revealing a novel role of BAX and BAK in quiescence regulation. *J Biol Chem* **283:** 34108-34120.

Janumyan YM, Sansam CG, Chattopadhyay A, Cheng N, Soucie EL, Penn LZ *et al*. (2003). Bcl-xL/Bcl-2 coordinately regulates apoptosis, cell cycle arrest and cell cycle entry. *EMBO J* **22:** 5459-5470.

Jeong EG, Lee SH, Kim SS, Ahn CH, Yoo NJ, Lee SH. (2007). Immunohistochemical analysis of phospho-BAD protein and mutational analysis of BAD gene in gastric carcinomas. *APMIS* **115:** 976-981.

Jeong SY, Gaume B, Lee YJ, Hsu YT, Ryu SW, Yoon SH *et al*. (2004). Bcl-x(L) sequesters its C-terminal membrane anchor in soluble, cytosolic homodimers. *EMBO J* **23:** 2146-2155.

Johlfs MG, Fiscus RR. (2010). Protein kinase G type-ialpha phosphorylates the apoptosis-regulating protein bad at serine 155 and protects against apoptosis in N1E-115 cells. *Neurochem Int* **56:** 546-553.

Kakati S, Barcos M, Sandberg AA. (1979). Chromosomes and causation of human cancer and leukemia: XXXVI. the 14q+ anomaly in an american burkitt lymphoma and its value in the definition of lymphoproliferative disorders. *Med Pediatr Oncol* **6:** 121-129.

Kiefer MC, Brauer MJ, Powers VC, Wu JJ, Umansky SR, Tomei LD *et al*. (1995). Modulation of apoptosis by the widely distributed bcl-2 homologue bak. *Nature* **374:** 736-739.

Kim H, Tu HC, Ren D, Takeuchi O, Jeffers JR, Zambetti GP *et al*. (2009). Stepwise activation of BAX and BAK by tBID, BIM, and PUMA initiates mitochondrial apoptosis. *Mol Cell* **36:** 487-499.

Kim MR, Jeong EG, Lee JW, Lee SH. (2006). Absence of the BH3 domain mutation of proapoptotic bcl-2 family gene BAD in serous and mucinous tumors of ovary. *Gynecol Oncol* **102:** 412-413.

Kozopas KM, Yang T, Buchan HL, Zhou P, Craig RW. (1993). MCL1, a gene expressed in programmed myeloid cell differentiation, has sequence similarity to BCL2. *Proc Natl Acad Sci U S A* **90:** 3516-3520.

Labi V, Grespi F, Baumgartner F, Villunger A. (2008). Targeting the bcl-2-regulated apoptosis pathway by BH3 mimetics: A breakthrough in anticancer therapy? *Cell Death Differ* **15:** 977-987.

Lanave C, Santamaria M, Saccone C. (2004). Comparative genomics: The evolutionary history of the bcl-2 family. *Gene* **333:** 71-79.

Lee JW, Soung YH, Kim SY, Nam SW, Kim CJ, Cho YG *et al*. (2004). Inactivating mutations of proapoptotic bad gene in human colon cancers. *Carcinogenesis* **25:** 1371-1376.

Letai A, Bassik MC, Walensky LD, Sorcinelli MD, Weiler S, Korsmeyer SJ. (2002). Distinct BH3 domains either sensitize or activate mitochondrial apoptosis, serving as prototype cancer therapeutics. *Cancer Cell* **2:** 183-192.

Li H, Zhu H, Xu CJ, Yuan J. (1998). Cleavage of BID by caspase 8 mediates the mitochondrial damage in the fas pathway of apoptosis. *Cell* **94:** 491-501.

Lin EY, Orlofsky A, Berger MS, Prystowsky MB. (1993). Characterization of A1, a novel hemopoietic-specific early-response gene with sequence similarity to bcl-2. *J Immunol* **151:** 1979-1988.

Lin EY, Orlofsky A, Wang HG, Reed JC, Prystowsky MB. (1996). A1, a bcl-2 family member, prolongs cell survival and permits myeloid differentiation. *Blood* **87:** 983-992.

Lindsten T, Ross AJ, King A, Zong WX, Rathmell JC, Shiels HA *et al*. (2000). The combined functions of proapoptotic bcl-2 family members bak and bax are essential for normal development of multiple tissues. *Mol Cell* **6:** 1389-1399.

Linette GP, Li Y, Roth K, Korsmeyer SJ. (1996). Cross talk between cell death and cell cycle progression: BCL-2 regulates NFAT-mediated activation. *Proc Natl Acad Sci U S A* **93:** 9545-9552.

Liu D, Bienkowska J, Petosa C, Collier RJ, Fu H, Liddington R. (1995). Crystal structure of the zeta isoform of the 14-3-3 protein. *Nature* **376:** 191-194.

Lizcano JM, Morrice N, Cohen P. (2000). Regulation of BAD by cAMP-dependent protein kinase is mediated via phosphorylation of a novel site, Ser155. *Biochem J* **349:** 547-557.

Luo X, Budihardjo I, Zou H, Slaughter C, Wang X. (1998). Bid, a Bcl2 interacting protein, mediates cytochrome c release from mitochondria in response to activation of cell surface death receptors. *Cell* **94:** 481-490.

Macdonald A, Campbell DG, Toth R, McLauchlan H, Hastie CJ, Arthur JS. (2006). Pim kinases phosphorylate multiple sites on bad and promote 14-3-3 binding and dissociation from bcl-XL. *BMC Cell Biol* **7:** 1.

Martin H, Patel Y, Jones D, Howell S, Robinson K, Aitken A. (1993). Antibodies against the major brain isoforms of 14-3-3 protein: An antibody specific for the N-acetylated amino-terminus of a protein. *FEBS Lett* **336:** 189.

Mateyak MK, Obaya AJ, Adachi S, Sedivy JM. (1997). Phenotypes of c-myc-deficient rat fibroblasts isolated by targeted homologous recombination. *Cell Growth Differ* **8:** 1039-1048.

Mateyak MK, Obaya AJ, Sedivy JM. (1999). c-myc regulates cyclin D-Cdk4 and -Cdk6 activity but affects cell cycle progression at multiple independent points. *Mol Cell Biol* **19:** 4672-4683.

McDonnell JM, Fushman D, Milliman CL, Korsmeyer SJ, Cowburn D. (1999). Solution structure of the proapoptotic molecule BID: A structural basis for apoptotic agonists and antagonists. *Cell* **96:** 625-634.

Mizushima S. (1968). Purification and properties of membrane bound NADH2 dehydrogenase in bacillus megaterium. *J Biochem* **63:** 317-323.

Moore BW, Perez VJ. (1967). Specific acidic proteins of the nervous system. *Physiological and biochemical aspects of nervous integration* pp. 343-59.

Muchmore SW, Sattler M, Liang H, Meadows RP, Harlan JE, Yoon HS *et al*. (1996). X-ray and NMR structure of human bcl-xL, an inhibitor of programmed cell death. *Nature* **381:** 335-341.

Murphy JB, Rous P. (1912). The behavior of chicken sarcoma implanted in the developing embryo. *J Exp Med* **15:** 119-132.

Nguyen M, Branton PE, Walton PA, Oltvai ZN, Korsmeyer SJ, Shore GC. (1994). Role of membrane anchor domain of bcl-2 in suppression of apoptosis caused by E1B-defective adenovirus. *J Biol Chem* **269:** 16521-16524.

Nguyen M, Millar DG, Yong VW, Korsmeyer SJ, Shore GC. (1993). Targeting of bcl-2 to the mitochondrial outer membrane by a COOH-terminal signal anchor sequence. *J Biol Chem* **268:** 25265-25268.

Nijhawan D, Fang M, Traer E, Zhong Q, Gao W, Du F *et al*. (2003). Elimination of mcl-1 is required for the initiation of apoptosis following ultraviolet irradiation. *Genes Dev* **17:** 1475-1486.

Offit K, Wong G, Filippa DA, Tao Y, Chaganti RS. (1991). Cytogenetic analysis of 434 consecutively ascertained specimens of non-hodgkin's lymphoma: Clinical correlations. *Blood* **77:** 1508-1515.

Oltvai ZN, Milliman CL, Korsmeyer SJ. (1993). Bcl-2 heterodimerizes in vivo with a conserved homolog, bax, that accelerates programmed cell death. *Cell* **74:** 609-619.

O'Reilly LA, Huang DC, Strasser A. (1996). The cell death inhibitor bcl-2 and its homologues influence control of cell cycle entry. *EMBO J* **15:** 6979-6990.

Ottilie S, Diaz JL, Horne W, Chang J, Wang Y, Wilson G *et al*. (1997). Dimerization properties of human BAD. identification of a BH-3 domain and analysis of its binding to mutant BCL-2 and BCL-XL proteins. *J Biol Chem* **272:** 30866-30872.

Palmieri S, Kahn P, Graf T. (1983). Quail embryo fibroblasts transformed by four v-myc-containing virus isolates show enhanced proliferation but are non tumorigenic. *EMBO J* **2:** 2385-2389.

Pegoraro L, Palumbo A, Erikson J, Falda M, Giovanazzo B, Emanuel BS *et al*. (1984). A 14;18 and an 8;14 chromosome translocation in a cell line derived from an acute B-cell leukemia. *Proc Natl Acad Sci U S A* **81:** 7166-7170.

Petosa C, Masters SC, Bankston LA, Pohl J, Wang B, Fu H *et al*. (1998). 14-3-3zeta binds a phosphorylated raf peptide and an unphosphorylated peptide via its conserved amphipathic groove. *J Biol Chem* **273:** 16305-16310.

Petros AM, Nettesheim DG, Wang Y, Olejniczak ET, Meadows RP, Mack J *et al*. (2000). Rationale for bcl-xL/Bad peptide complex formation from structure, mutagenesis, and biophysical studies. *Protein Sci* **9:** 2528-2534.

Polzien L, Baljuls A, Rennefahrt UE, Fischer A, Schmitz W, Zahedi RP *et al*. (2009). Identification of novel in vivo phosphorylation sites of the human proapoptotic protein BAD: Pore-forming activity of BAD is regulated by phosphorylation. *J Biol Chem* **284:** 28004-28020.

Print CG, Loveland KL, Gibson L, Meehan T, Stylianou A, Wreford N *et al*. (1998). Apoptosis regulator bcl-w is essential for spermatogenesis but appears otherwise redundant. *Proc Natl Acad Sci U S A* **95:** 12424-12431.

Puthalakath H, Strasser A. (2002). Keeping killers on a tight leash: Transcriptional and post-translational control of the pro-apoptotic activity of BH3-only proteins. *Cell Death Differ* **9:** 505-512.

Radke K, Martin GS. (1979). Transformation by rous sarcoma virus: Effects of src gene expression on the synthesis and phosphorylation of cellular polypeptides. *Proc Natl Acad Sci U S A* **76:** 5212-5216.

Ranger AM, Zha J, Harada H, Datta SR, Danial NN, Gilmore AP *et al*. (2003). Bad-deficient mice develop diffuse large B cell lymphoma. *Proc Natl Acad Sci U S A* **100:** 9324-9329.

Rogers S, Wells R, Rechsteiner M. (1986). Amino acid sequences common to rapidly degraded proteins: The PEST hypothesis. *Science* **234:** 364-368.

Rous P. (1911). A sarcoma of the fowl transmissible by an agent separable from the tumor cells. *J Exp Med* **13:** 397-411.

Rowley JD. (1977). Mapping of human chromosomal regions related to neoplasia: Evidence from chromosomes 1 and 17. *Proc Natl Acad Sci U S A* **74:** 5729-5733.

Rowley JD. (1975). Abnormalities of chromosome 1 in myeloproliferative disorders. *Cancer* **36:** 1748-1757.

Sakamaki JI, Daitoku H, Ueno K, Hagiwara A, Yamagata K, Fukamizu A. (2011). Arginine methylation of BCL-2 antagonist of cell death (BAD) counteracts its phosphorylation and inactivation by akt. *Proc Natl Acad Sci U S A* .

Schmitz R, Thomas RK, Harttrampf AC, Wickenhauser C, Schultze JL, Hansmann ML *et al*. (2006). The major subtypes of human B-cell lymphomas lack mutations in BCL-2 family member BAD. *Int J Cancer* **119:** 1738-1740.

Scott RB. (1970). Cancer chemotherapy--the first twenty-five years. *Br Med J* **4:** 259-265.

Sedlak TW, Oltvai ZN, Yang E, Wang K, Boise LH, Thompson CB *et al*. (1995). Multiple bcl-2 family members demonstrate selective dimerizations with bax. *Proc Natl Acad Sci U S A* **92:** 7834-7838.

Seo SY, Chen YB, Ivanovska I, Ranger AM, Hong SJ, Dawson VL *et al*. (2004). BAD is a pro-survival factor prior to activation of its pro-apoptotic function. *J Biol Chem* **279:** 42240-42249.

Skaff DA, Kim CS, Tsai HJ, Honzatko RB, Fromm HJ. (2005). Glucose 6-phosphate release of wild-type and mutant human brain hexokinases from mitochondria. *J Biol Chem* **280:** 38403-38409.

Smith AJ, Karpova Y, D'Agostino R,Jr, Willingham M, Kulik G. (2009). Expression of the bcl-2 protein BAD promotes prostate cancer growth. *PLoS One* **4:** e6224.

Subramanian RR, Masters SC, Zhang H, Fu H. (2001). Functional conservation of 14-3-3 isoforms in inhibiting bad-induced apoptosis. *Exp Cell Res* **271:** 142-151.

Suzuki M, Youle RJ, Tjandra N. (2000). Structure of bax: Coregulation of dimer formation and intracellular localization. *Cell* **103:** 645-654.

Swanstrom R, Parker RC, Varmus HE, Bishop JM. (1983). Transduction of a cellular oncogene: The genesis of rous sarcoma virus. *Proc Natl Acad Sci U S A* **80:** 2519-2523.

Tan Y, Demeter MR, Ruan H, Comb MJ. (2000). BAD ser-155 phosphorylation regulates BAD/Bcl-XL interaction and cell survival. *J Biol Chem* **275:** 25865-25869.

Taub R, Kirsch I, Morton C, Lenoir G, Swan D, Tronick S *et al*. (1982). Translocation of the c-myc gene into the immunoglobulin heavy chain locus in human burkitt lymphoma and murine plasmacytoma cells. *Proc Natl Acad Sci U S A* **79:** 7837-7841.

Teo K, Gemmell L, Mukherjee R, Traynor P, Edwards J. (2007). Bad expression influences time to androgen escape in prostate cancer. *BJU Int* **100:** 691-696.

Todorov TG, Yakimov M. (1967). Changes in the cultures of chicken bone marrow cells infected with the virus of chicken myelocytomatosis (strains mc-29 and mc-31). *Neoplasma* **14:** 613-617.

Tombal B, Weeraratna AT, Denmeade SR, Isaacs JT. (2000). Thapsigargin induces a calmodulin/calcineurin-dependent apoptotic cascade responsible for the death of prostatic cancer cells. *Prostate* **43:** 303-317.

Tsujimoto Y, Croce CM. (1986). Analysis of the structure, transcripts, and protein products of bcl-2, the gene involved in human follicular lymphoma. *Proc Natl Acad Sci U S A* **83:** 5214-5218.

Tsujimoto Y, Finger LR, Yunis J, Nowell PC, Croce CM. (1984). Cloning of the chromosome breakpoint of neoplastic B cells with the t(14;18) chromosome translocation. *Science* **226:** 1097-1099.

Vaux DL, Cory S, Adams JM. (1988). Bcl-2 gene promotes haemopoietic cell survival and cooperates with c-myc to immortalize pre-B cells. *Nature* **335:** 440-442.

Vennstrom B, Sheiness D, Zabielski J, Bishop JM. (1982). Isolation and characterization of c-myc, a cellular homolog of the oncogene (v-myc) of avian myelocytomatosis virus strain 29. *J Virol* **42:** 773-779.

Virdee K, Parone PA, Tolkovsky AM. (2000). Phosphorylation of the pro-apoptotic protein BAD on serine 155, a novel site, contributes to cell survival. *Curr Biol* **10:** R883.

Vogler M. (2011). BCL2A1: The underdog in the BCL2 family. *Cell Death Differ* .

Wang HG, Pathan N, Ethell IM, Krajewski S, Yamaguchi Y, Shibasaki F *et al*. (1999). Ca2+-induced apoptosis through calcineurin dephosphorylation of BAD. *Science* **284:** 339-343.

Wang K, Yin XM, Chao DT, Milliman CL, Korsmeyer SJ. (1996). BID: A novel BH3 domain-only death agonist. *Genes Dev* **10:** 2859-2869.

Wang XT, Pei DS, Xu J, Guan QH, Sun YF, Liu XM *et al*. (2007). Opposing effects of bad phosphorylation at two distinct sites by Akt1 and JNK1/2 on ischemic brain injury. *Cell Signal* **19:** 1844-1856.

Wei MC, Zong WX, Cheng EH, Lindsten T, Panoutsakopoulou V, Ross AJ *et al*. (2001). Proapoptotic BAX and BAK: A requisite gateway to mitochondrial dysfunction and death. *Science* **292:** 727-730.

Wilson-Annan J, O'Reilly LA, Crawford SA, Hausmann G, Beaumont JG, Parma LP *et al*. (2003). Proapoptotic BH3-only proteins trigger membrane integration of prosurvival bcl-w and neutralize its activity. *J Cell Biol* **162:** 877-887.

Wolter KG, Hsu YT, Smith CL, Nechushtan A, Xi XG, Youle RJ. (1997). Movement of bax from the cytosol to mitochondria during apoptosis. *J Cell Biol* **139:** 1281-1292.

Wooderchak WL, Zang T, Zhou ZS, Acuna M, Tahara SM, Hevel JM. (2008). Substrate profiling of PRMT1 reveals amino acid sequences that extend beyond the "RGG" paradigm. *Biochemistry* **47:** 9456-9466.

Yaffe MB, Rittinger K, Volinia S, Caron PR, Aitken A, Leffers H *et al*. (1997). The structural basis for 14-3-3:Phosphopeptide binding specificity. *Cell* **91:** 961-971.

Yan Y, Park SS, Janz S, Eckhardt LA. (2007). In a model of immunoglobulin heavy-chain (IGH)/MYC translocation, the igh 3' regulatory region induces MYC expression at the immature stage of B cell development. *Genes Chromosomes Cancer* **46:** 950-959.

Yang E, Zha J, Jockel J, Boise LH, Thompson CB, Korsmeyer SJ. (1995). Bad, a heterodimeric partner for bcl-XL and bcl-2, displaces bax and promotes cell death. *Cell* **80:** 285-291.

Yang H, Masters SC, Wang H, Fu H. (2001). The proapoptotic protein bad binds the amphipathic groove of 14-3-3zeta. *Biochim Biophys Acta* **1547:** 313-319.

Yang L, Omori K, Suzukawa J, Inagaki C. (2004). Calcineurin-mediated BAD Ser155 dephosphorylation in ammonia-induced apoptosis of cultured rat hippocampal neurons. *Neurosci Lett* **357:** 73-75.

Yang T, Buchan HL, Townsend KJ, Craig RW. (1996). MCL-1, a member of the BLC-2 family, is induced rapidly in response to signals for cell differentiation or death, but not to signals for cell proliferation. *J Cell Physiol* **166:** 523-536.

Yang T, Kozopas KM, Craig RW. (1995). The intracellular distribution and pattern of expression of mcl-1 overlap with, but are not identical to, those of bcl-2. *J Cell Biol* **128:** 1173-1184.

Yin XM, Oltvai ZN, Korsmeyer SJ. (1994). BH1 and BH2 domains of bcl-2 are required for inhibition of apoptosis and heterodimerization with bax. *Nature* **369:** 321-323.

Yoo NJ, Lee JW, Jeong EG, Soung YH, Nam SW, Lee JY *et al*. (2006). Expressional analysis of anti-apoptotic phospho-BAD protein and mutational analysis of pro-apoptotic BAD gene in hepatocellular carcinomas. *Dig Liver Dis* **38:** 683-687.

Yunis JJ, Oken MM, Kaplan ME, Ensrud KM, Howe RR, Theologides A. (1982). Distinctive chromosomal abnormalities in histologic subtypes of non-hodgkin's lymphoma. *N Engl J Med* **307:** 1231-1236.

Zech L, Haglund U, Nilsson K, Klein G. (1976). Characteristic chromosomal abnormalities in biopsies and lymphoid-cell lines from patients with burkitt and non-burkitt lymphomas. *Int J Cancer* **17:** 47-56.

Zha J, Harada H, Osipov K, Jockel J, Waksman G, Korsmeyer SJ. (1997). BH3 domain of BAD is required for heterodimerization with BCL-XL and pro-apoptotic activity. *J Biol Chem* **272:** 24101-24104.

Zha J, Harada H, Yang E, Jockel J, Korsmeyer SJ. (1996). Serine phosphorylation of death agonist BAD in response to survival factor results in binding to 14-3-3 not BCL-X(L). *Cell* **87:** 619-628.

Zhou P, Qian L, Kozopas KM, Craig RW. (1997). Mcl-1, a bcl-2 family member, delays the death of hematopoietic cells under a variety of apoptosis-inducing conditions. *Blood* **89:** 630-643.

Zhou X, Wang JL, Lu J, Song Y, Kwak KS, Jiao Q *et al*. (2010). Reversal of cancer cachexia and muscle wasting by ActRIIB antagonism leads to prolonged survival. *Cell* **142:** 531-543.

Zhou XM, Liu Y, Payne G, Lutz RJ, Chittenden T. (2000). Growth factors inactivate the cell death promoter BAD by phosphorylation of its BH3 domain on Ser155. *J Biol Chem* **275:** 25046-25051.

Chapter 2: Materials and Methods

2.1 Reagents

Antibodies raised against BAD (B0684), phosphospecific BAD serine 155 (SAB4300343), Bcl-xL (B9429) (used for western blotting) and α-Tubulin (T1568) were purchased from Sigma-Aldrich (St. Louis, MO). The antibody raised against Bcl-xL (#2762) used for co-immunoprecipitation was purchased from Cell Signaling Technologies. Cytochrome c antibody used for immunofluorescence (556432) was purchased from BD Pharmingen. 14-3-3ζ (c-16) antibody was purchased from Santa Cruz. Pan-14-3-3 antibody (sc-629) was a gift from Dr. Shairaz Baksh (originally purchased from Santa Cruz). Anti-mouse BrdU antibody was a gift from Dr. Chris Bleackley. Alexa Fluor® 488 goat anti rabbit IgG (A-11008) and Alexa Fluor® 555 goat anti mouse IgG (A-21422) were purchased from Invitrogen. siRNA duplexes HS_3 BAD(#SI00299348) and Allstars Negative Control siRNA (#SI03650318) were purchased from Qiagen. TMRE (Tetramethylrhodamine ester) (T669), annexin V-PE (51-65875x), DAPI, Lipofectamine™ 2000 (11668-027) and propidium iodide (P-3566) were purchased from Invitrogen. Sal I (NEB R0138S) and Xho I (NEB R0146S) restriction endonucleases as well as λ phosphatase (NEB, P0753) were purchased from New England Biolabs (NEB). Paclitaxel (T1912-5MG), Cisplatin (P4394-250MG) and staurosporine (G4400) were purchased from Sigma-Aldrich. Complete EDTA-free Protease Inhibitor Cocktail Tablets (11 873 580 001) and PhoSTOP phosphatase inhibitor tablets (04 906 837 001) were purchased from Roche.

2.2 Cell Culture

MDA-MB-231 breast cancer cells were obtained from Dr. Gordon Mills (MD Anderson Cancer Center, University of Texas). Cells were cultured in RPMI 1640 (Invitrogen/Gibco, 11875-093) supplemented with 10% fetal bovine serum (FBS) (Sigma-Aldrich Life Sciences, F1051-500mL) under normal growth conditions (37°C in the presence of 5% CO_2). Stable cell lines were carried in RPMI 1640 supplemented with 10% FBS and 1mg/mL Geneticin® (Gibco, 11811-031) made up in Dulbecco's Phosphate Buffered Saline (dPBS) (Gibco, 14190-144). All experiments were conducted in the absence of Geneticin® in RPMI 1640 supplemented with 10% FBS (complete media).

2.3 Stable Cell Line Creation

Stable lines were generated by transfecting cells with 3 µL Lipofectamine™ 2000 reagent and 800 ng of the appropriate DNA construct. $1x10^5$ MDA-MB-231 cells were transfected in a 24 well plate with either empty pcDNA3.1 vector or pcDNA3.2 vectors (Invitrogen) containing BAD constructs (see Figure 3 and Figure 4 for empty vector constructs). Cells were incubated for 48 hours prior to harvesting and transferred to a 10 cm^2 dish. Harvesting for stable lines consisted of washing 1x with 1mL trypsin-EDTA followed by incubation with 1 mL of trypsin-EDTA till cells were no longer adherent. Stable cells lines were selected using 1 mg/mL Geneticin (Invitrogen/Gibco) for approximately 14 days. Colonies were then marked (on bottom of plate), media was aspirated and plate was washed 2x with sterile dPBS. 0.5 µL of trypsin-EDTA was added to each marked colony, pipetted up and down slowly for 30

seconds and placed in a pre-filled 96 well flat bottom plate. Wells were filled with RPMI 1640+10% FBS and 1 mg/mL Geneticin®. Colonies were transferred individually into separate wells. After all marked colonies were transferred, plate was washed 2x with dPBS and complete media was replaced. Prior to reaching confluency, remaining cells were harvested and frozen in RPMI 1640 supplemented with 10% FBS and 10% dimethylsulfoxide (DMSO) as bulk stocks.

2.4 Transient Transfection

$8x10^4$ MDA-MB-231 breast cancer cells were seeded in a 24 well dish and incubated for 16-18 hours to adhere prior to transfection. Transfection complex was formed from using 3 µL of Lipofectamine™ 2000 (Invitrogen, 11668-027) diluted in 50 µL of Opti-MEM (Invitrogen, 11058-021). DNA constructs were simultaneously diluted in 50 µL of Opti-MEM and were incubated for 5 minutes. Lipofectamine™ 2000 solution was then mixed with diluted DNA and incubated for 15 minutes at room temperature. Media was removed from cells and replaced with 400 µL of warm complete media. After incubation, the transfection complex was added to cells as per manufacturer's instructions. Cells were incubated for 48 hours in transfection complex prior to harvesting or imaging.

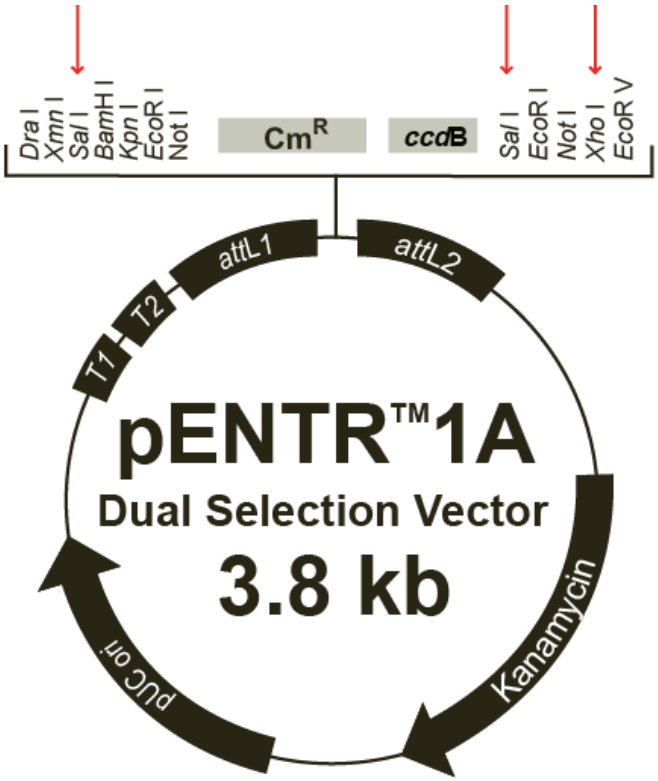

Comments for pENTR™1A
3754 nucleotides

*rrn*B T1 transcription termination sequence: bases 106-149
*rrn*B T2 transcription termination sequence: bases 281-308
*att*L1: bases 358-457 (complementary strand)
Chloramphenicol resistance gene (Cm^R): bases 608-1266
*ccd*B gene: bases 1608-1913
*att*L2: bases 1983-2082
Kanamycin resistance gene: bases 2205-3014
pUC origin: bases 3078-3751

invitrogen™

Figure 3: Vector map of pENTR1A

Red arrows indicate restriction sites used for cloning BAD into pENTR1A.

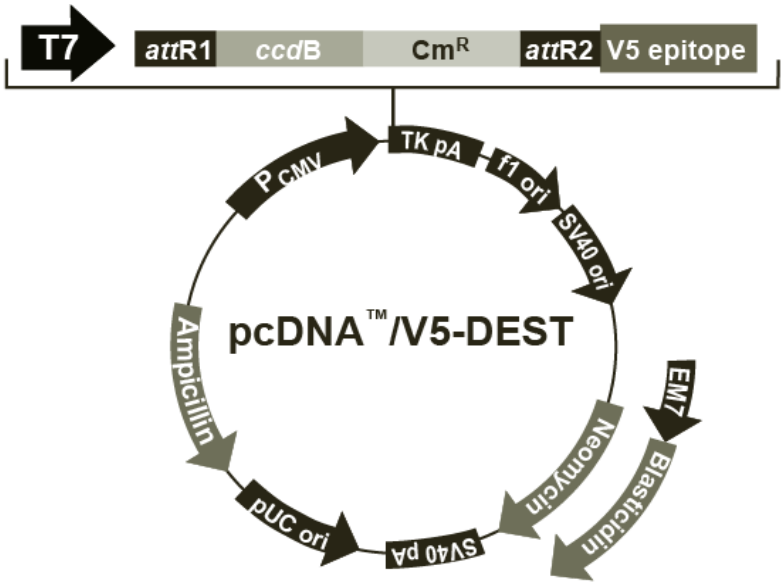

Comments for:	pcDNA™3.2/V5-DEST 7711 nucleotides	pcDNA™6.2/V5-DEST 7341 nucleotides
CMV promoter:	232-819	232-819
T7 promoter/priming site:	863-882	863-882
*att*R1 site:	911-1035	911-1035
*ccd*B gene (c):	1464-1769	1464-1769
Chloramphenicol resistance gene (c):	2111-2770	2111-2770
*att*R2 site:	3051-3175	3051-3175
V5 epitope:	3201-3242	3201-3242
V5 reverse priming site:	3210-3230	3210-3230
TK polyadenylation signal:	3269-3540	3269-3540
f1 origin:	3576-4004	3576-4004
SV40 early promoter and origin:	4031-4339	4031-4339
Neomycin resistance gene:	4414-5208	---
EM7 promoter:	---	4394-4460
Blasticidin resistance gene:	---	4461-4859
SV40 early polyadenylation signal:	5384-5514	5017-5147
pUC origin (c):	5897-6570	5530-6200
Ampicillin (*bla*) resistance gene (c):	6715-7575	6345-7205
bla promoter (c):	7576-7674	7206-7304

(c) = complementary strand

Invitrogen™
life technologies

Figure 4: Vector map of pcDNA3.2/V5-DEST

Expression vector map of pcDNA3.2/V5-DEST which was used to express BAD constructs.

2.5 RNA isolation from MCF7 cells

RNA from $6x10^6$ MCF7 breast cancer cells was extracted using Trizol RNA preparation (Invitrogen, 15596-026) of, as per manufacturer's instructions (by Richard Veldhoen). Briefly, cells were harvested and centrifuged at 500xg for 5 minutes. One mL of Trizol reagent was added and cells were incubated for 5 minutes. Two hundred µL of choloroform was then added to the 1mL solution and samples were shaken vigorously for 15 seconds, incubated for 3 minutes and centrifuged at 12 000xg for 15 minutes at 4°C. The colorless aqueous phase was removed and 500 µL of isopropanol was added, inverted three times and incubated for 10 minutes prior to centrifugation at 12 000xg for 10 minutes at 4°C. The supernatant was then removed and the sample was allowed to air dry prior to resuspension in 20µL of sterile water.

2.6 RT PCR of human BAD

The initial BAD construct was generated in our lab (by Graeme Quest) using Superscript III Reverse Transcriptase Polymerase Chain Reaction (RT-PCR) kit (Invitrogen). Reaction was performed as per manufacturer's instructions except that we used 1 µg of RNA (from above extraction), 10 µM forward and reverse BAD primers (Primer 1 and 2 in Table 1) and 1.25 Units of Platinum Pfx Polymerase (Invitrogen, 11708-013).

Primer	Primer Name	Sequence
1	hBAD (human BAD) forward	CAC CAT GTT CCA GAT CCC AGA GTT TG
2	hBAD reverse	AAG CTT CAC TGG GAG GGG GCG GAG CTT
3	WT BAD 5' for Gateway w/ Sal I	ACT ATG GTC GAC ATG TTC CAG ATC CCA GAG
4	WT BAD 3' for Gateway w/ Xho I	AAA AAT CTC GAG TCA CTG GGA GGG GGC GGA
5	hBAD S118A Mutagenesis 5'	CGA GCT CCG GAG GAT GGC TGA CGA GTT TGT GGA C
6	hBAD S118A Mutagenesis 3'	GTC CAC AAA CTC GTC AGC CAT CCT CCG GAG CTC G
7	hBAD S118D Mutagenesis 5'	CGA GCT CCG GAG GAT GGA TGA CGA GTT TGT GGA C
8	hBAD S118D Mutagenesis 3'	GTC CC AAA CTC GTC ATC CAT CCT CCG GAG CTC G

Table 1: Primer sequences

2.7 TA Cloning of hBAD

Cloning of BAD into pcDNA3.1D/V5/His was performed (by Graeme Quest) as per manufacturer's instructions (Invitrogen, K4800-01) with the following changes:

PCR product was diluted 1:30 due to high efficiency of prior PCR reaction. One µL of diluted PCR product was added to the reaction.

Transformation was carried out using 2µL from TOPO® Cloning reaction was added to transform 50µL One Shot® TOP10 Chemically Competent *E. coli* (see below for transformation protocol).

Upon completion, pcDNA3.1D/V5/His/hBAD was used as template DNA for Gateway® insertion.

2.8 Creation of SalI and XhoI restriction sites for Gateway® insertion

Generation of the wild-type BAD entry plasmid was done using TopTaq PCR protocol (Qiagen, 200203) as per manufacturer's instructions with the following manipulations. 10 ng of template DNA (pcDNA3.1D/V5/His/hBAD), 10 mM forward and reverse primers (primer number 3 and 4 in Table 1, respectively), 0.25 µL (1.25 Units) Top Taq Polymerase (200203 Qiagen), 5 µL of 10x TopTaq PCR Buffer, 1 µL of dNTPs (10 mM, 201900). Primers included 5' Sal I endonuclease recognition site (GTCGAC) upstream of ATG and a 3' Xho I recognition site (CTCGAG) downstream of stop codon. The PCR cycling protocol was as described in Table 2.

Segment	Cycles	Temperature (°C)	Time
Denaturation Step	1	94	3 minutes
	18	94	30 seconds
Annealing Step		57	30 seconds
Elongation Step		72	45 seconds
Final Elongation	1	72	5 minutes

Table 2: PCR protocol for amplification of hBAD DNA including Sal I and Xho I restriction sites

PCR reaction was performed using an Eppendorf Mastercycler Gradient PCR machine (Mullis *et al.*, 1986). PCR protocol was created based on primers being used and length of product DNA being created. (For sequence of primers see Table 1).

2.9 Gel Purification of PCR products

PCR products were then gel purified using the QIAquick Gel Extraction Kit (Qiagen, 28704) after samples were run on a 1% agarose gel as per manufacturer's instructions using the following method:

Agarose gel slice containing DNA was dissolved in 3:1 volumes QG buffer (Qiagen, 19063) to gel weight and heated at 50°C for 15 minutes. Next, 1 volume of isopropanol was added and the samples were placed into QIAquick spin columns and centrifuged at 14 000xg for 1 minute. Tubes were attached to vacuum manifold until flow through was removed and 500 µL QG buffer (Qiagen,19063) was added. Again, tubes were centrifuged and attached to vacuum manifold to remove flow through. The column was then washed with 750 µL PE buffer (Qiagen, 19065), centrifuged and attached to vacuum manifold. Prior to eluting, columns were centrifuged again and flow through was removed. Finally, 30 µL of sterile water was added, incubated for 5 minutes and centrifuged for 1 minute at 14 000xg, eluting samples into clean 1.5 mL tubes.

2.10 Creation of hBAD cDNA in Gateway® system

Gel purified products were cleaved using Sal I and Xho I endonucleases using the following procedure in Table 3. Reactions were incubated at 37^{o}C for 60 minutes and were screened for cleavage efficiency by agarose gel electrophoresis.

Component	Volume
BSA	0.5µL
10x NEB Buffer 3	5µL
Sal I	1µL
Xho I	1µL
hBAD PCR product or	28µL
pENTR1A (Figure 3)	1uL
Water	14.5µL
	41.5µL

Table 3: Restriction enzyme digestion of products designed for entrance into Gateway® system

Restriction enzyme digestion was carried out on PCR products to allow entrance of hBAD DNA into Gateway cloning system. Red lettering represents the differences in component parts involved in the pENTR1A restriction compared to hBAD PCR template.

Samples were run on a 0.8% agarose gel to ensure endonuclease products were properly cleaved. Cleaved template was then added to cleaved pENTR1A and a ligation reaction was performed using the T4 DNA Ligase kit (Invitrogen, 15224-017) as follows:

4 µL of 5x T4 DNA Ligase Buffer (10mM Tris-Hcl (pH 7.5), 50 mM KCl, 1 mM DTT and 50% (v/v) glycerol), 2.5 µL of pENTR1A (30 fmol), 10.2 µL of hBAD insert (90 fmol), 0.2 Units of T4 DNA Ligase and 3.1 µL water (20 µL total volume). The reaction was carried out at room temperature for 1 hr. After ligation, constructs were transformed into DH5α E.*coli.*

2.11 Transformation method

Transformation protocol modified from (Avery *et al.*, 1944). Briefly, transformation was done by adding 2 µL of ligated DNA to 50 µL of DH5α bacterial cells in a 13 mL bacterial tube (BD Falcon 352059) and incubating on ice for 5 minutes. Mixture was incubated in a water bath at 42°C for 30 seconds. The reaction was terminated by prompt placement on ice for a 5 minute incubation. Transformed cells were then resuspended in 250 µL of SOC media (prepared as per instructions in Molecular Cloning: A Laboratory Manual, Third Edition, Volume 3, Appendix A2.3) and incubated for 8 hours at 37°C in a bacterial shaker. One hundred µL of this mixture was then plated on LB (Lysogeny broth) - agar containing 100 µg/mL Kanamycin (Kan) and spread using a "hockey stick" style bacterial spreader. Single colonies were then isolated for continuation of Gateway® cloning protocol (LR Clonase reaction).

2.12 LR Clonase reaction

For placement of hBAD entry vector insert into pcDNA3.2 destination vector, an LR clonase reaction was performed. This reaction was performed as per instructions listed in Table 4. LR Clonase enzyme was added last after a brief vortex to mix. PCR tube containing reaction was incubated at 25°C for 60 minutes in PCR machine. Next, 2 µL of Proteinase K was added which was incubated for 10 minutes in a 37°C bacterial incubator. 1 µL of DNA was transformed into 50 µL of DH5α E.*coli* (see materials and methods for transformation protocol). Transformed bacteria were plated on LB-agar bacterial plates for 16 hours which contained 100 µg/mL Ampicillin (Amp).

Colonies were picked from Amp containing bacterial plates, grown overnight in 5 mL of LB containing Amp and DNA was extracted using GeneJet™ Plasmid Miniprep Kit (Fermentas, K0502) (see below).

2.13 Mini-prep DNA

GeneJet™ Plasmid Miniprep Kit was performed as per manufacturer's instructions. Briefly, bacterial cells were centrifuged at 6800xg for 2 min in a 1.5 mL centrifuge tube and excess media is decanted. Cells were then resuspended in 250 µL of resuspension buffer and vortexed to ensure full suspension. Cells were then lysed in 250 µL of lysis buffer and inverted 5 times. 350 µL of neutralization solution was added after a 5 minute incubation and inverted 5 times. Neutralized mixture is then

Component	Volume (µL) or amount
LR Reaction Buffer	2 µL
Entry Clone (hBAD/pENTR1A)	50 ng of DNA
Destination Vector (pcDNA3.2)	75 ng of DNA
Tris-EDTA (TE Buffer)	Bring solution up to 4 µL
LR Clonase Enzyme Mix	2 µL
Total Volume	8 µL

Table 4: LR Clonase reaction of hBAD/pENTR1A into pcDNA3.2

LR Clonase reaction which created hBAD/pcDNA3.2/V5-DEST. This construct was used as an expression vector for all experiments.

centrifuged at 14 000xg for 5 minutes and supernatant is moved to GeneJet™ spin column. Column is centrifuged for 1 minute at 14 000xg; flow through is discarded. Column is then washed 2 times with 500 µL of wash solution and centrifuged at 14 000xg for 45 seconds; flow through is discarded. After second centrifugation, column is centrifuged without adding wash solution to ensure column is fully dry. DNA is eluted from column in 40 µL of sterile water by adding water to top of column, incubating for 2 minutes and centrifuging for 2 minutes at 14 000xg. DNA is then analyzed using a standard spectrophotometer or Nanovue™ (GE Healthcare) spectrophotometer.

2.14 Site Directed Mutagenesis

Mutagenesis was performed using Quikchange® Lightning Site-Directed Mutagenesis Kit (Stratagene) as per manufacturer's instructions. Briefly, primers were designed to overlap the mutation site with a minimum of 10 base pairs on either side of the mutation site. Primers were designed using a web-based software program available at: http://www.stratagene.com/qcprimerdesign

Primers for the reactions were purchased from IDT (Coralville, Iowa) for both serine 118 Alanine and Aspartic Acid mutations (See primers 5-8, Table 1).

See site directed mutagenesis reaction mixture in Table 5. Solution was mixed prior to addition of Quikchange™ Lightning Enzyme. After addition of enzyme, solution was mixed gently and placed directly in PCR machine (see protocol, Table 6).

Component	Volume of supplied components or quantity of added components
10x Reaction Buffer	5 µL
Forward and Reverse Primer (see table 1)	(125 ng)
dNTP mixture	1 µL
Quik Solution Reagent	1.5 µL
Template DNA (pENTR1A/hBAD)	(100 ng)
Water	Up to 50 µL
Quikchange Lightning Enzyme	1 µL

Table 5: Site Directed Mutagenesis PCR Solution Mixture (Quikchange® Lightning Site Directed Mutagenesis Kit)

Segment	Cycles	Temperature (°C)	Time
Denaturation Step	1	95	2 minutes
Denaturation Step	18	95	20 seconds
Annealing Step		60	10 seconds
Elongation Step		68	1 min. 33 secs (30 seconds/kb)
Final Elongation	1	68	5 minutes

Table 6: Site Directed Mutagenesis PCR Protocol

After PCR reaction had taken place, 2 µL of DpnI endonuclease was added to cleave methylated DNA (template). Sequence of pENTR1A/hBAD S118A and pENTR1A/hBAD S118D were confirmed after PCR reaction.

2.15 Proliferation Assays

Protocol modified from (Craik *et al.*, 2010). Briefly, cells were plated at $1.0x10^5$ cells in multiple $60mm^2$ dishes corresponding to individual time points. Cells were allowed 16-18 hours to adhere to the plates before harvesting and counting with a haemocytometer. Following this initial time point, cells were harvested every 24 hours thereafter. Cell harvesting consisted of aspirating the growth media, washing with 1 mL dPBS (Dulbeccos Phosphate Buffered Saline, Invitrogen, 14040-133), followed by addition of 0.5 mL of 0.05% trypsin-EDTA (Invitrogen, 25300-062). Cells immersed in trypsin were subjected to a 5 minute incubation at 37°C (bacterial incubator) followed by addition of 2 mL of non-sterile growth media containing FBS to inactivate trypsin. Plates were counted in duplicate and values were averaged from three separate experiments.

2.16 Western Blotting Technique

Original technique developed by (Burnette, 1981; Davies and Stark, 1970). SDS-PAGE was performed on harvested cells and immunoprecipitated lysates in a similar fashion. Lysates were mixed with 2x loading buffer (100 mM Tris pH6.8, 16% glycerol, 3.2% SDS, 8% 2-β mercaptoethanol and 1% bromophenol blue) and equivalent cell number or fraction volume was added to each lane. 12% acrylamide

gels were used for all experiments. Electrophoresis of the acrylamide gels was accomplished using 180V for approximately 1 hour. Gels were then removed from running apparatus and equilibrated in methanol based transfer buffer (14.425 g/L glycine, 3 g/L Tris and 200 mL/L methanol). PVDF membrane (Biorad, 162-0177) was charged using pure methanol for 15 seconds prior to 5 minute incubation with western transfer buffer. Filter paper and transfer sponges were also incubated for 5 minutes prior to transfer assembly. Western transfers were electrophoresed for 1 hour at room temperature using 400 mA of current. After transfer completion, membranes were incubated at room temperature in 5% skim milk (made in Tris Buffered Saline-Tween20 (TBS-T)) for 1 hour. Primary antibodies were then added (see Table 7 for dilutions) overnight and incubated on shaking table in a 4°C walk-in refrigerator. Approximately 18 hours later, membranes were washed 3 times in TBS-T for 10 minutes each. Membranes were then incubated in HRP conjugated secondary antibodies (1:3000) for 1 hour. Following this incubation, membranes are washed with TBS-T 3 times for 10 minutes. Membranes are then developed using ECL systems (GE Healthcare) for western blot detection.

2.17 In Vivo Mouse Xenograft

As previously performed in (El-Kalla *et al.*, 2010). Briefly, cells were harvested from three 10 cm^2 dishes at approximately 95% confluency. An aliquot was removed for cellular quantification using a haemocytometer (Assistent, 0.100mm, Neubauer Improved). Cells were then pelleted by centrifugation at 500xg for 5 minutes. Media was aspirated and 900 µL of RPMI 1640 supplemented with 10% FBS was used to

resuspend cell pellet. Three hundred µL of Matrigel (BD #354234) was then added to each tube and the cells were immediately placed on ice. After thorough mixing, Dr. Shairaz Baksh or I injected 150 µL into each rear flank of an athymic nude mouse (Taconic Laboratories #NCRNU-M, CrTac:NCr-FoxN1Nu) using a 1 mL syringe (BD, 309602) attached to a 30G x ½" needle (BD, 305106). Palpable tumors were measured weekly using a ruler and charted for growth. Tumor volume was determined from the radius assuming spherical proportions ($\frac{4}{3}\pi r^3$). At the end of 38 days, mice were euthanized using high concentration CO_2 and pronounced dead prior to tumor excision. All procedures were in concordance with protocol #461 and were subject to ethics approval from University of Alberta Review Board.

2.18 Thymidine Block Cell Cycle Analysis

Protocol modified from (Czernick *et al.*, 2009) [originally discovered by (FIRKET, 1964)]. Cells were plated at low confluency ($5x10^4$ per well) and high confluency ($4x10^5$ per well) in a six well dish for each time point. Thymidine was added (2mM) for 16 hours. Cells were washed 3x with sterile dPBS warmed to 37°C. Two mL of 37°C RPMI 1640+10% FBS was added to each well and allowed to sit for 8 hours, releasing cells from cell cycle block. Cells were then subjected to a second thymidine block in which thymidine was added for 16 hours. After the second block, cells were again released and allowed to proliferate through the cell cycle for the indicated times. Cells were then harvested as mentioned above except media and wash were saved. Cells were then centrifuged at 500xg and fixed in 70% ethanol for a minimum of 24 hours. After ethanol fixation, cells were then washed with PBS and resuspended in propidium

iodide stain (0.1% Triton X-100, 2 mg/mL RNase, 20 µg/mL propidium iodide) for 15 minutes at 37°C. Flow cytometry was done using the FL-2 PMT of a FACSCalibur (BD).

2.19 BrdU Propidium Iodide Cell Cycle Analysis

Assay initially developed by (Darzynkiewicz *et al.*, 1983). $1x10^5$ cells are plated in a 24 well dish. Next day, media is removed and replaced with media containing 10 µM BrdU. Cells are grown in this media for 1 hour before washing three times with 1xPBS (37°C). Cells are then harvested at representative times and fixed in 70% ice cold ethanol. Fixed cells are left overnight prior to washing with 1xPBS. Supernatant is removed and 65 µL 2N HCl is added to cells at room temperature for 20 minutes. One hundred thirty five µL of 0.1 M sodium borate is added to neutralize solution. Fixed cells are then centrifuged at 1500xg for 5 minutes. Cells are washed with 1xPBS supplemented with 0.5% Tween-20 and 0.5% bovine serum albumin. Twenty µL of 2° anti-mouse FITC (1:100 in PBS-tween 20) is added and cells are incubated for 1 hour at room temperature in the dark. Cells are washed with 1xPBS supplemented with 0.5% Tween-20 and 0.5% bovine serum albumin three times. Two hundred fifty µL of propidium iodide stain (see above) is added to cells and incubated at 30 minutes at room temperature. Flow cytometry was done gating both FL-1 and FL-2 PMT of a FACSCalibur (BD). BrdU analysis was performed by Shanna Banman in Dr. Ing Swie Goping's laboratory.

2.20 Phosphatase Treatment for Two Dimensional Protein Analysis

A confluent 10 cm^2 dish was harvested (see above) for each Two Dimensional Western Blot. Cells were lysed in 200 µL of RIPA buffer (50 mM Tris pH 7.4, 150 mM NaCl, 1% NP-40, 0.5% NaDOC and 0.1% SDS) containing protease inhibitor and incubated on ice for 15 minutes. Lysates were then homogenized using a tephlon homogenizer (Cafcam, RZR1) (setting 6 for 30 seconds) and centrifugated at 10 000xg for 30 min at 4°C. Supernatant was removed and aliquoted into two equal halves. 2000 U (approximately, 100 U per µg of protein) of λ phosphatase (NEB, P0753) was added to half the lysate along with 1 mM $MnCl_2$ and 1x PMP (Protein MetalloPhosphatases) buffer and was incubated at 30°C for 30 minutes. Phosphatase inhibitor (Roche) was added to the other half of lysate and placed on ice during 30 minute incubation. Lysates were then frozen (-20°C) and transported to Dr. Li for completion of the protocol. Prior to isoelectric focusing, lysate was precipitated by mixing with five volumes of pre-chilled acetone and incubated at -20 °C overnight. The precipitates were collected by centrifugation (15,000 g for 15 min at 4°C) and washed twice with pre-chilled acetone. The precipitated proteins were then resuspended in 2D lysis buffer (7 M urea, 2 M thiourea, 4% CHAPS and 30 mM Tris-HCl pH 8.7) and quantified using the 2D Quant Kit from GE Healthcare (80-6483-56). One hundred fifty micrograms of protein was loaded for 2D analysis using rehydration method as described below.

2.21 Two Dimensional Protein Analysis

Cells from a 10-cm dish of 90% confluency were harvested and centrifuged at 500xg for 5 minutes. Dr. Li received this pellet, generated the lysate using 2D lysis buffer (7M Urea, 2M Thiourea, 4% CHAPS and 30 mM Tris-HCl pH 8.7) and performed the remainder of the protocol. Quantification was done using the 2D Quant Kit from GE Healthcare (80-6483-56) to equilibrate protein concentrations. One hundred fifty micrograms of protein (in a total volume of 125 µL, supplemented with rehydration buffer (7M urea, 2M thiourea, 2% CHAPS and 0.002% Bromophenol Blue) was incubated with a Immobiline™ DryStrip pH 4-7, 7cm (GE Healthcare) at room temperature for 20 hrs. The first dimensional electrophoresis was carried out on the IPGphor isoelectic focusing system (GE Healthcare) using the following protocol with a total of 8 kVh: (1) Step and hold: 300V, 2 hr 30 min; (2) Gradient 1000 V, 30 min; (3) Gradient: 5000 V, 1 hr 30 min; and (4) Step and hold: 5000 V, 30 minutes. Strips were then equilibrated using a two step buffer system. First they were incubated in Buffer 1 (6 M urea, 30% Glycerol, 2% SDS, 75 mM Tris-HCl pH 8.8 and 1% DTT) for 15 minutes, rinsed with MilliQ water and placed in Buffer 2 (6M Urea, 30% glycerol, 2% SDS, 50mM Tris-HCl pH 8.8 and 2.5% Iodoacetamide) for an additional 15 minutes. The second dimensional electrophoresis was performed on the Mini-PROTEAN II system (Bio-Rad). After equilibration, strips were placed on top of 12% SDS-PAGE gels, and were sealed using melted agar containing SDS-PAGE loading dye. Gels were run on constant power of 1W/gel, transferred to nitrocellulose membranes, followed by immunobloting with rabbit anti-BAD antibody (Sigma) at 1:1000 dilution. The ECL system (GE Healthcare) was used for western blot signal detection.

2.22 Killing Assay

As previously performed in (Czernick *et al.*, 2009). Briefly, $8x10^4$ cells were plated in a 24 well plate and were incubated for 16 hours prior to addition of treatment. 25 nM paclitaxel, 100 µM cisplatin, 20 µM sorafenib and 0.1% serum were added for 48 hours while 2.5 µM staurosporine was added for 4 hours. After treatments were completed, cells were harvested and incubated with TMRE or Annexin V-PE as per manufacturer's instructions (Invitrogen, 51-65875x). Cells were then analyzed for apoptotic induction by the use of FL-2 PMT of a FACSCalibur (BD) and compared to untreated controls.

2.23 Subcellular Fractionation

Cells were fractionated using HIM buffer (200 mM mannitol, 70 mM sucrose, 1 mM EGTA, 10 mM HEPES) lysis and differential centrifugation as previously described (Goping *et al.*, 1998). Briefly, cells were homogenized in HIM buffer in the presence of protease and phosphatase inhibitors. Nuclei and unlysed cells were removed via 700xg centrifugation for 10 minutes. The cleared lysate was then fractionated into supernatant (cytosol and light membranes, S fraction) and pellet (heavy membranes, P fraction). Equal volumes of either fraction were run on SDS PAGE and analyzed using standard western blotting techniques (see above).

2.24 Coimmunoprecipitation

Protocol modified from (Craik *et al.*, 2010). Cell lines were plated at $3x10^6$ in a 150 mm^2 dish and cultured for 72 hours prior to lysing. Cells were lysed using 650 µL of 1% CHAPS (50 mM Tris-HCl pH 7.4, 150 mM NaCl, 2 mM EDTA, 1% CHAPS). Lysates were spun at 700xg for 10 minutes at 4°C to remove unlysed and cellular debris. Twenty µL of supernatant was taken and frozen for input control. One µL of representative antibody was added to 200 µL of lysate and incubated overnight shaking at 4°C. Forty µL of 50% Protein A bead slurry (20 µL of packed beads) was then added to each lysate and incubated while shaking for 1 hour at 4°C. Beads were then centrifuged at 450 xg for 5 min prior to removing supernatant and washing with 3 times with 800 µL of 1% CHAPS buffer. Eighty µL of 2xSSB was added to input control and 100 µL of 2xSSB was added to beads prior to boiling. Equal quantities of lysate were run on SDS PAGE and analyzed using standard western blotting techniques (see above).

2.25 Immunofluorescence

Protocol modified from (Goping *et al.*, 2008). Briefly, 12 mm circular coverslips (Electron Microscopy Sciences, #1½, #72230-01) were immersed in 95% ethanol, ignited and individually placed in separate 24- wells. Cells were then seeded in this 24-well plate (Fisherbrand). $1x10^5$ cells were plated into each well and allowed to grow under normal conditions for 48 hours. Cells were washed with PBS prior to being fixed with 4% paraformaldehyde for 15 minutes. Cells were then washed 2x with PBS and permeabilized with 0.1% triton x-100 in PBS for 5 minutes at room temperature. Cells

were washed 2x with PBS before blocking with 4% normal donkey serum (NDS) diluted in PBS + $MgCl_2$ (1mM) for 60 minutes. Cells were washed 2x with PBS + $MgCl_2$ before adding primary antibodies at 1:100 in 4% NDS. Cytochrome c antibody (556432) was purchased from BD Pharmingen and BAD antibody was purchased from Sigma-Aldrich (B0684). Wells were washed with PBS + $MgCl_2$ 3x prior to addition of fluorescent secondary antibodies [donkey α rabbit 488 (A21206 Invitrogen) and donkey α mouse 555 (A31570 Invitrogen)] at 1:200 in 4% NDS. Coverslips were washed 3x with PBS + $MgCl_2$ prior to air drying and adding 10 uL of Mounting media (Dako, S3023) containing 1:5000 DAPI (Invitrogen). Slides were left overnight in dark prior to imaging.

2.26 Immunofluorescence Imaging

Images were taken with a 100x Oil Immersion lens using the Leica SP5 Scanning Confocal Microscope. Z-stacks were generated and compressed for all images. All images were taken under similar gain values although some manipulation was necessary to prevent saturation of images. PMT (Photomultiplier tube) settings were equivalent across all images. Images were obtained using Leica LAS software and were processed using the Lite version of this software. Images were exported from LAS Lite and final figure assembly was done using Adobe Illustrator.

2.27 siRNA knockdown proliferation assay

MDA-MB-231 stable cell lines were transfected with siRNA as previously described (Czernick et al. 2009). Briefly, $5x10^4$ cells were seeded in a 24 well plate allowing 16-18 hours for cells to adhere to plate. First, siRNA duplexes (either HS_3

BAD (Qiagen #SI00299348) or Allstars Negative Control siRNA (Qiagen #SI03650318)) were diluted in 100µL of Opti-MEM Serum Free Media (Invitrogen, 11058-021) to a final concentration of 10 nM. The siRNA was incubated for 5 minutes prior to addition of 3µL of Hiperfect (Qiagen, 301704) transfection reagent. The complete mixture was incubated for 10 minutes after a short vortex to ensure proper mixing. Media was removed from each well and replaced with 400 µL of complete media. siRNA/transfection complex was then added in a drop wise fashion ensuring complete coverage of single well. Transfection complexes were incubated for 12 hours and then harvested for western blot protein analysis. Alternatively in the KD proliferation assay, cells were incubated for 96 hours and were trypsinized and counted using a haemocytometer.

2.28 References - Methods and Materials

Avery OT, Macleod CM, McCarty M. (1944). Studies on the chemical nature of the substance inducing transformation of pneumococcal types : Induction of transformation by a desoxyribonucleic acid fraction isolated from pneumococcus type iii. *J Exp Med* **79:** 137-158.

Burnette WN. (1981). "Western blotting": Electrophoretic transfer of proteins from sodium dodecyl sulfate--polyacrylamide gels to unmodified nitrocellulose and radiographic detection with antibody and radioiodinated protein A. *Anal Biochem* **112:** 195-203.

Craik AC, Veldhoen RA, Czernick M, Buckland TW, Kyselytzia K, Ghosh S *et al*. (2010). The BH3-only protein bad confers breast cancer taxane sensitivity through a nonapoptotic mechanism. *Oncogene* .

Czernick M, Rieger A, Goping IS. (2009). Bim is reversibly phosphorylated but plays a limited role in paclitaxel cytotoxicity of breast cancer cell lines. *Biochem Biophys Res Commun* **379:** 145-150.

Darzynkiewicz Z, Traganos F, Melamed MR. (1983). Distinction between 5-bromodeoxyuridine labeled and unlabeled mitotic cells by flow cytometry. *Cytometry* **3:** 345-348.

Davies GE, Stark GR. (1970). Use of dimethyl suberimidate, a cross-linking reagent, in studying the subunit structure of oligomeric proteins. *Proc Natl Acad Sci U S A* **66:** 651-656.

El-Kalla M, Onyskiw C, Baksh S. (2010). Functional importance of RASSF1A microtubule localization and polymorphisms. *Oncogene* **29:** 5729-5740.

FIRKET H. (1964). Synchronization of hela cell cultures by an excess of thymidine. *C R Seances Soc Biol Fil* **158:** 1408-1410.

Goping IS, Gross A, Lavoie JN, Nguyen M, Jemmerson R, Roth K *et al*. (1998). Regulated targeting of BAX to mitochondria. *J Cell Biol* **143:** 207-215.

Goping IS, Sawchuk T, Rieger A, Shostak I, Bleackley RC. (2008). Cytotoxic T lymphocytes overcome bcl-2 inhibition: Target cells contribute to their own demise. *Blood* **111:** 2142-2151.

Mullis K, Faloona F, Scharf S, Saiki R, Horn G, Erlich H. (1986). Specific enzymatic amplification of DNA in vitro: The polymerase chain reaction. *Cold Spring Harb Symp Quant Biol* **51 Pt 1:** 263-273.

Chapter 3: The role of BAD in breast cancer cell proliferation and tumor growth

3.1 BAD over-expression stimulates cellular proliferation

While BAD is mostly known as a pro-apoptotic protein, emerging studies indicate that BAD has alternative activities. Our group had demonstrated that BAD increased the proliferative rate of breast cancer cells (Craik *et al.*, 2010). In order to understand this underexplored function of BAD, we generated breast cancer cell lines that stably over-expressed BAD. MDA-MB-231 cells, which express low levels of endogenous BAD protein (Craik *et al.*, 2010), were transfected with a BAD-expressing plasmid and individual clonal lines were expanded (Fig. 5A, inset). To measure proliferative rate, we recorded cell numbers over time. Since this assay measures increased cell cycle progression and/or decreased cell death, the term proliferation will be used to describe both parameters. Individual clonal cell lines were plated at equal density, and cell numbers were recorded every 24 h for a total of 96 h (Figure 5A). Six independent BAD over-expressing cell lines had greater total cell numbers by 96 h, compared to vector control cells (V2). To rule out that this effect was due to clonal variation, we used siRNA to deplete expression of exogenous BAD in one of the BAD over-expressing cell lines (Fig. 5B, inset). In this experiment, the BAD over-expressing cell line (BAD6) had elevated cell numbers relative to vector control (Figure 5B). Subsequent treatment with siRNA to BAD reduced overall cell numbers, indicating that cell number increases were dependent on BAD. Thus, BAD can specifically mediate increased proliferation of MDA-MB-231 cells over time.

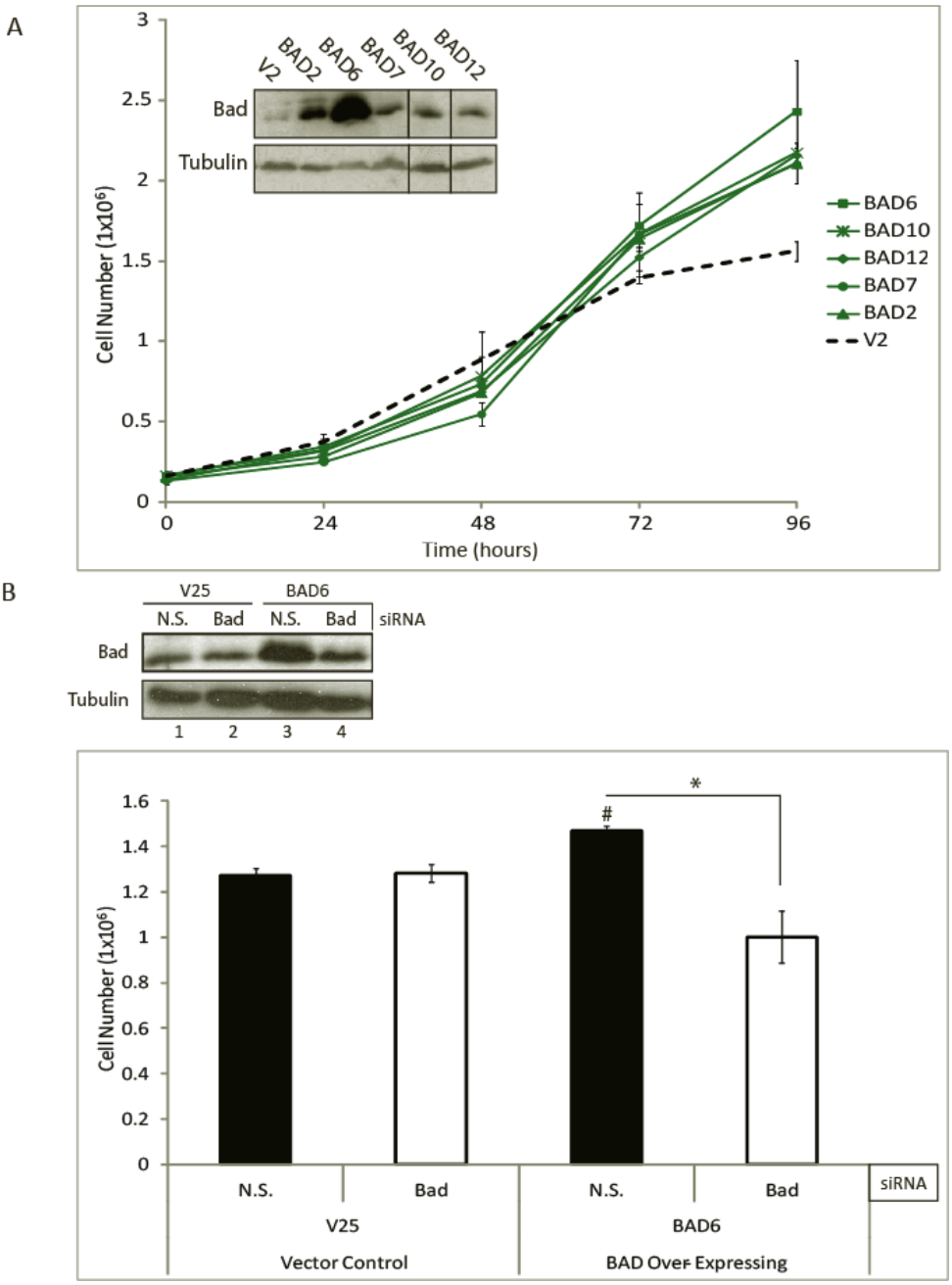

Figure 5: BAD over-expression promotes proliferation

(**A**) (Inset) Expression levels of MDA-MB-231 breast cancer cells stably transfected with either empty vector (V2) or human BAD (BAD 2, 6, 7, 10 and 12). (Graph) Proliferation assay as described in materials and methods, carried out for 96 hours, counting cells from individual 60mm dishes at the indicated time points. (**B**) (Inset) Detection of BAD knock-down efficiency was determined by western blot (*cont'd*)

analysis of BAD over-expressing clones treated with siRNA directed at BAD or negative siRNA control. Knock-down proliferation assay as described in material and methods was carried out on BAD over-expressing clones and vector controls. Black bars represent non-specific (N.S.) siRNA control while white bars represent BAD siRNA knock-down. Cells were counted at 96 hours post siRNA transfection. Graphs represent the average of three independent experiments. '*' indicates a P value of less than 0.05 in comparison. '#' represents a P value of less than 0.05 in comparison to V25 N.S. Graphs are represented as mean ± standard deviation.

3.2 BAD-mediated proliferation was not dependent on BCL-XL

We decided to investigate the mechanism of this BAD-directed growth advantage. A proliferative role for BAD had previously been demonstrated in non-transformed cells. In these reports, BAD stimulated cell cycle progression by antagonizing cell cycle arrest. This cell cycle arrest signal was mediated by BCL-XL (Chattopadhyay *et al.*, 2001; Janumyan *et al.*, 2008; Janumyan *et al.*, 2003). To assess whether BAD-dependent stimulation of breast carcinoma cell proliferation was dependent on BCL-XL, we generated mutants of BAD with increased or decreased affinity for BCL-XL. Serine 118 (S155 in mouse nomenclature) within the BH3 domain of BAD hinders binding to BCL-XL when phosphorylated (Tan *et al.*, 2000; Zhou *et al.*, 2000). Therefore, we generated a phospho-mimic (BADS118D) and a non-phosphorylatable (BADS118A) mutant to directly test the requirement for BCL-XL binding to BAD with respect to BAD-induced proliferation.

We generated MDA-MB-231 cell lines stably over-expressing the BADS118A/D mutants and verified that these mutations altered interactions with BCL-XL as expected. We demonstrated that immunoprecipitated BAD protein from vector control (V26) and wild-type BAD (BAD6) both interacted with BCL-XL (Figure 6A, upper panel). As predicted, the BAD S118A (S118A6) protein also strongly interacted with BCL-XL. Alternatively, BAD that had been immunoprecipitated from cell lines expressing the S118D mutant (S118D2) showed weak binding to BCL-XL. The reverse immunoprecipitation confirmed the above results as BCL-XL strongly associated with

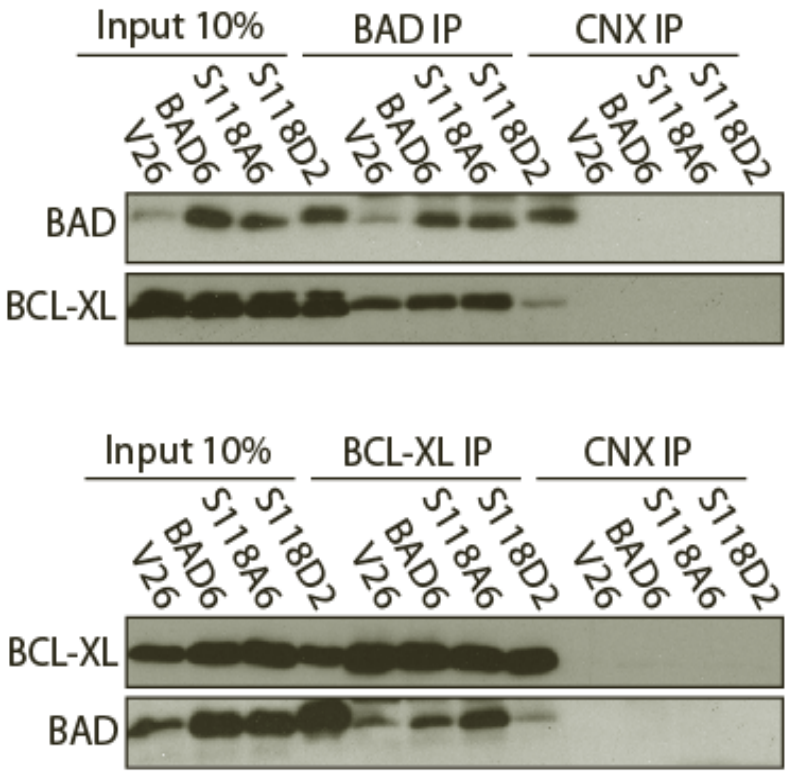

Figure 6: BAD serine 118 phospho-status determines binding affinity

Co-immunoprecipitation western blot analysis was conducted on stable cells lines under proteosomal and phosphatase inhibitor conditions. Lysates were immunoprecipitated with BAD, BCL-XL or negative binding control (calnexin, CNX) antibody and were immunoblotted with antibodies against BAD or BCL-XL. V26 cell line is over-expressing vector control, BAD6 is over-expressing wild-type BAD, S118A6 is over-expressing serine 118 to alanine mutation and S118D2 is over-expressing serine 118 to aspartic acid mutation.

wild-type BAD and BADS118A (Figure 6B), whereas BCL-XL interaction with BADS118D was reduced. Thus, we confirmed that within these cell lines, the mutation of BADS118 to aspartic acid inhibited interaction with BCL-XL, whereas mutation to alanine maintained or stimulated BAD interaction with BCL-XL.

We then used these mutant clones to assess whether BAD-mediated proliferation was dependent on BCL-XL. Using proliferation assays similar to those of Fig. 5, we observed that cells expressing BADS118D (S118D2) displayed an enhanced proliferative profile that was statistically similar to wild-type BAD clones (Figure 7; compare blue vs green lines). Since BADS118D bound BCL-XL more weakly than wild-type BAD, this data suggested that BAD-stimulated cell proliferation was not dependent on BCL-XL. Furthermore, the BADS118A expressing lines that had robust BAD:BCL-XL interactions, proliferated at a significantly lower rate than wild-type BAD or control cells (Figure 6; see red line). (Data from additional clonal cell lines are shown in Figure 8). These results indicated that BAD-mediated stimulation of cell proliferation in breast carcinoma MDA-MB-231 cells is independent of BCL-XL.

3.3 BAD does not alter cell cycle dynamics

Since, BAD potentially stimulated proliferation of MDA-MB-231 cells through a novel mechanism, we decided to characterize the effects of BAD over-expression on cell cycle. We synchronized cells at the G1/S boundary with double thymidine block

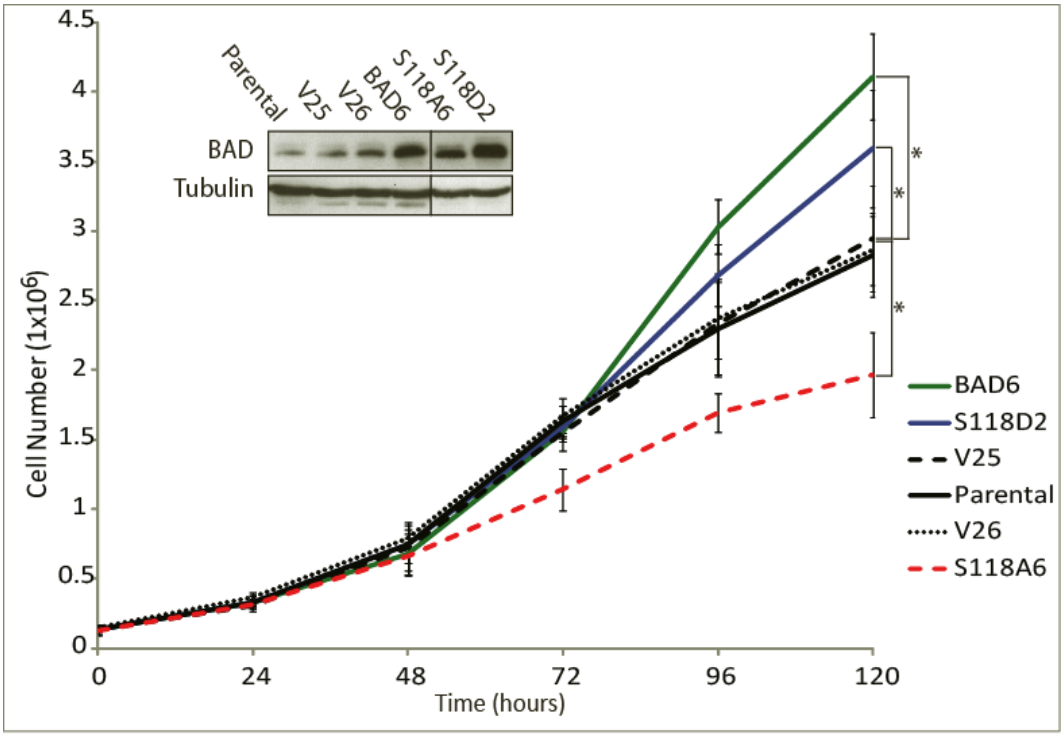

Figure 7: Breast cancer cell proliferation is BAD phosphorylation dependent

(Inset) Expression levels of MDA-MB-231 breast cancer cells stably transfected with either empty vector (V25, V26), human wild-type BAD (BAD6), serine 118 alanine mutant BAD (S118A6) or serine 118 aspartic acid mutant BAD (S118D2). (Graph) Proliferation assay as described in materials and methods, carried out for 120 hours, counting cells from individual 60 mm dishes at the indicated time point. Graphs represent the average of three independent experiments. '*' indicates a P value of less than 0.05 in comparison. Graphs are represented as mean ± standard deviation.

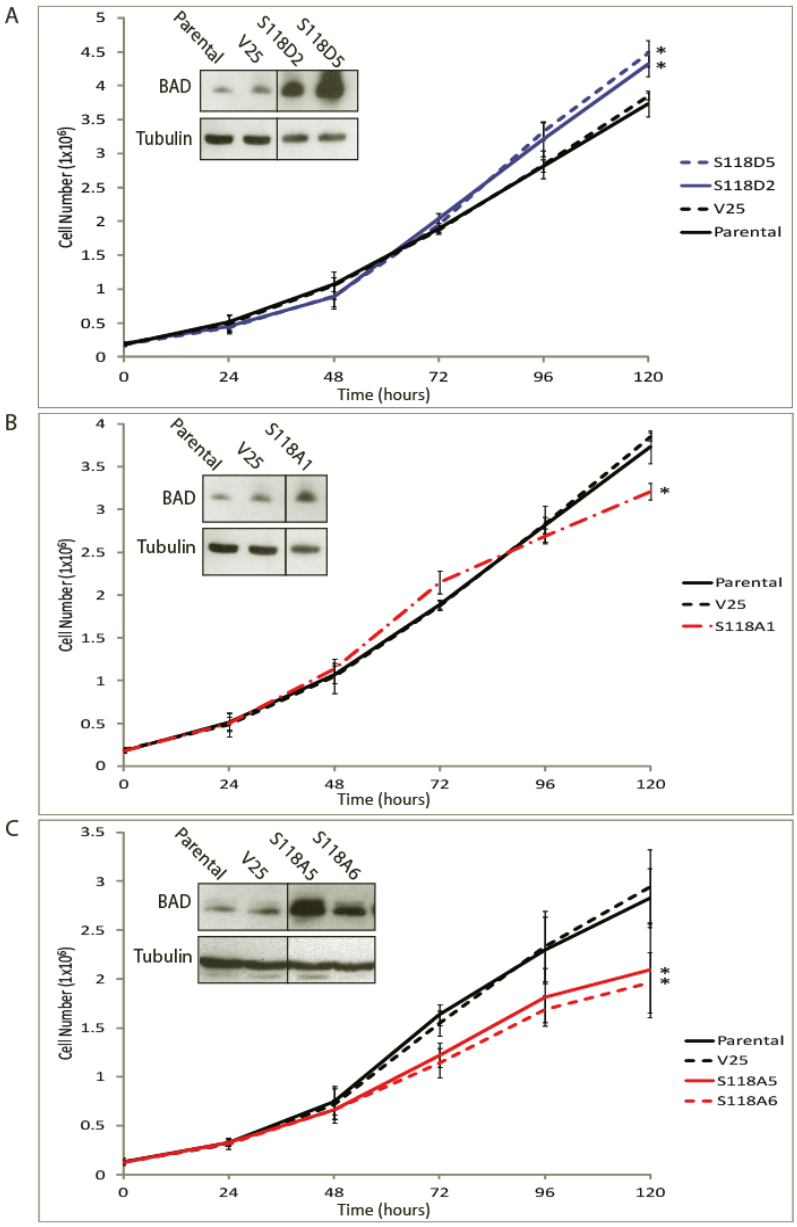

Figure 8: Confirmation of stable cell line proliferation

(A)(B)(C) Stable cell lines were immunoblotted for total BAD protein levels (inset) and graphed for cell proliferation over time. Red lines represent S118A clones, blue lines represent S118D clones and black lines represent vector control and parental cell lines. Graphs represent the average of three independent experiments. '*' indicates a P value of less than 0.05 in comparison to V25. Graphs are represented as mean ± standard deviation.

treatment (Czernick *et al.*, 2009; FIRKET, 1964). Cells were released from G1/S and harvested every 2 hours for a total of 30 h. Cell cycle stage was determined by propidium iodide DNA content analysis. As can be seen in Figure 9A, this methodology clearly demonstrated cell cycle transition (G1/S at 0h; S phase entry at 4h; G2/M progression at 8h and subsequent G1 entry at 10-12h). We reasoned that if BAD-mediated proliferative effects were due to a shortened cell cycle, then BAD over-expressing cells would show earlier transit through cell cycle stages compared to the vector control cells. This, however, was not the case, as there were no significant differences in cell cycle progression between vector control cells or cells over-expressing wild-type BAD, BADS118D or BADS118A (Figure 9B, upper panels).

Upon closer inspection of the cell growth assays (Figure 5 and 7), it appeared that the proliferative effect of BAD became significant at the later (96h-120h) time points. This suggested that as cell monolayers became confluent, the vector control cells delayed cell cycle progression, whereas wild-type BAD or BADS118D-expressing cells continued cycling. Therefore, we measured cell cycle transition of cells plated at both low and high confluency (Figure 9B). Under both low and high cell confluency conditions, we detected no consistent alteration in cell cycle progression of vector control cells relative to BAD over-expressing cells.

To confirm these results, we used another assay to verify that BAD over-expression did not affect cell cycle progression. We pulse labeled cells in S-phase with

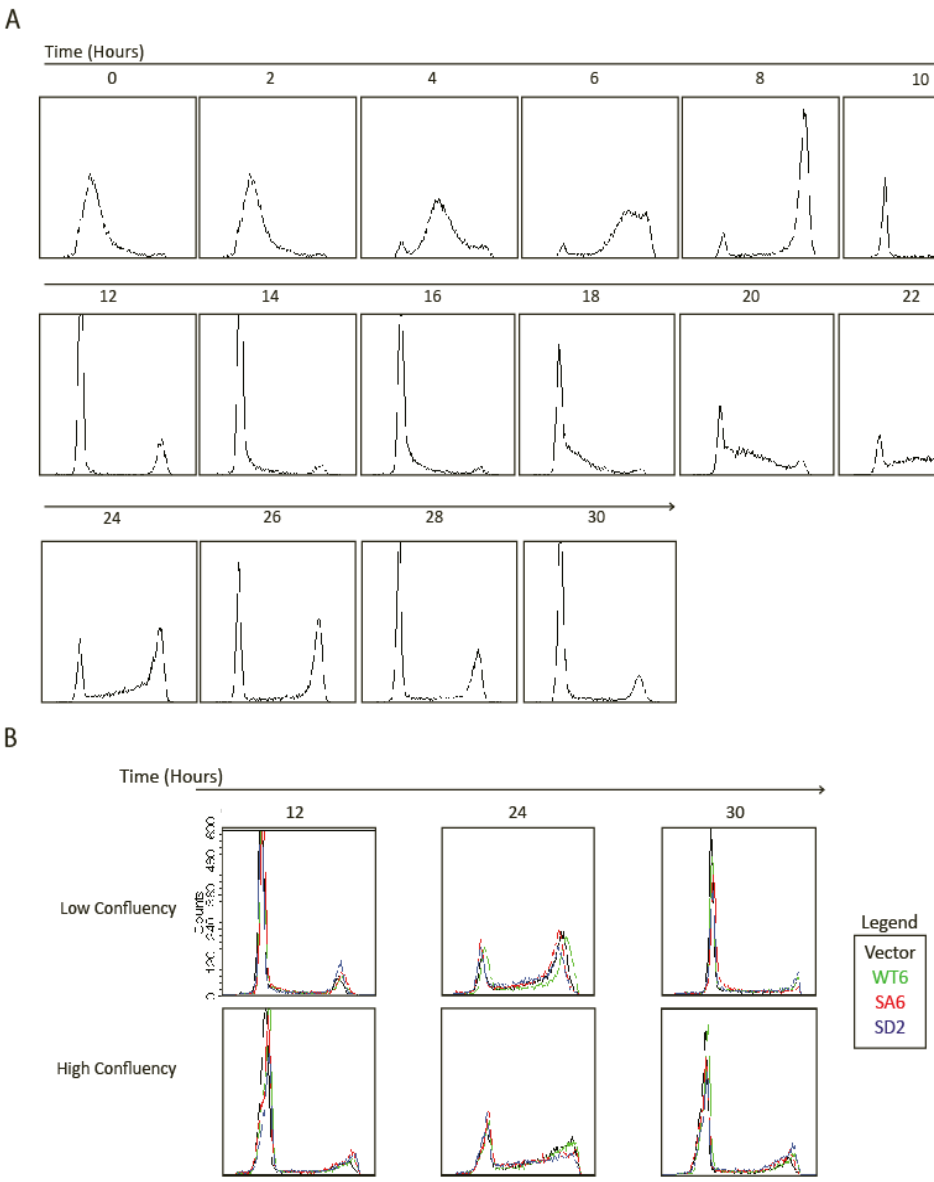

Figure 9: BAD over-expression does not affect cell cycle progression

(**A**) BAD6 cell cycle was synchronized by addition of 2 mM thymidine. Cells were released and stained with propidium iodide. Far left peak is indicative of Go/G1 phase cells, transition between peaks represents S-phase while far right peak represent G2/M phase cells. (**B**) Thymidine block propidium iodide analysis was done on stable cell lines at low or high confluency. Three time points were chosen based on transition status of cells (12 hours G1 phase, 24 hours S-phase and 30 hours return to G1 phase). Representative histogram profiles were overlapped for comparison. Plots are representative of three independent experiments. Overlapped histograms are representative of three independent experiments.

bromodeoxyuridine (BrdU) and analyzed the cell cycle progression of BrdU-positive cells over time. We measured cell cycle progression of vector control, wild-type BAD, BADS118D and BADS118A expressing cell lines (Figure 10). BrdU cell cycle analysis was performed by Shanna Banman of Dr. Ing Swie Goping's laboratory. We observed clear distinctions in cell cycle progression (S at 0h; G2/M at 6h; G1 at 12h). Similar to the thymidine block experiments, we detected no difference in cell cycle dynamics between the cell lines. Therefore, BAD over-expression did not alter cell cycle transit times.

3.4 BAD phosphorylation status alters sensitivity to apoptosis

Cell number proliferation over time can be a function of increased cell cycle dynamics or decreased apoptosis. Therefore, we tested whether BAD over-expressing cells had a diminished sensitivity to apoptotic stimuli. We treated cells with the apoptotic agents: staursporine, paclitaxel, cisplatin, sorafenib and serum starvation. We measured both loss of mitochondrial electrochemical potential (Figure 11A, TMRE negative cells) and phosphatidylserine externalization (Figure 11B, Annexin V positive cells). We found that vector control and wild-type BAD-expressing cell lines had similar sensitivities to paclitaxel, staurosporine and sorafenib treatments. Thus, it did not appear that a generalized anti-apoptotic phenotype was imparted by BAD over-expression. However, BAD over-expression in cisplatin and serum starved conditions provided a modest protective effect. Based on these results, apoptotic sensitivity may

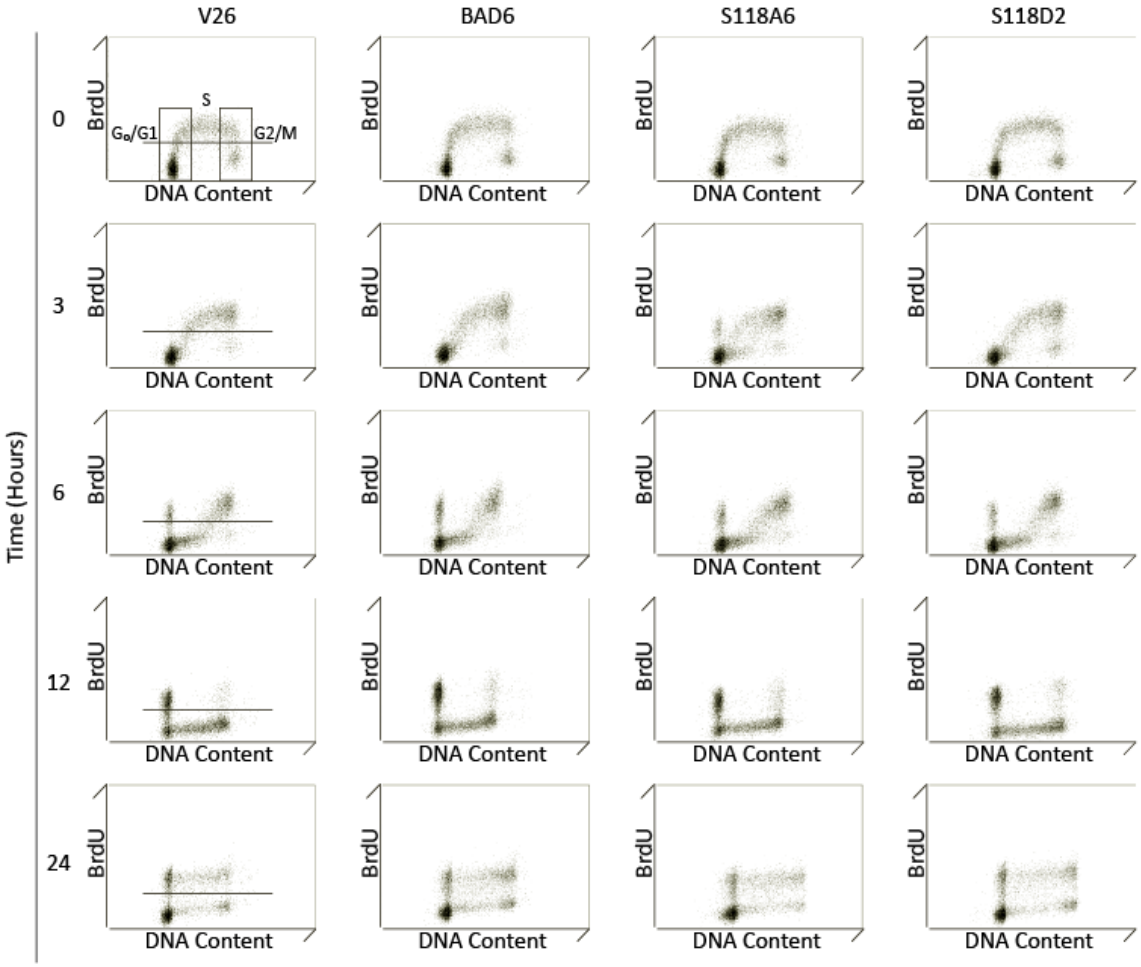

Figure 10: BAD over-expression does not affect cell cycle progression (BrdU method)

Cell cycle analysis using BrdU and propidium iodide stain. Y-axis of figure is increasing time points in hours. Y-axis of each dot plot is BrdU while X-axis is DNA content (propidium iodide). Cells were pulse labeled with BrdU for 1 hour prior to harvesting and analyzed using FL-1 and FL-2 PMT of FACSCalibur. Cells above horizontal line were considered BrdU positive and used for analysis.

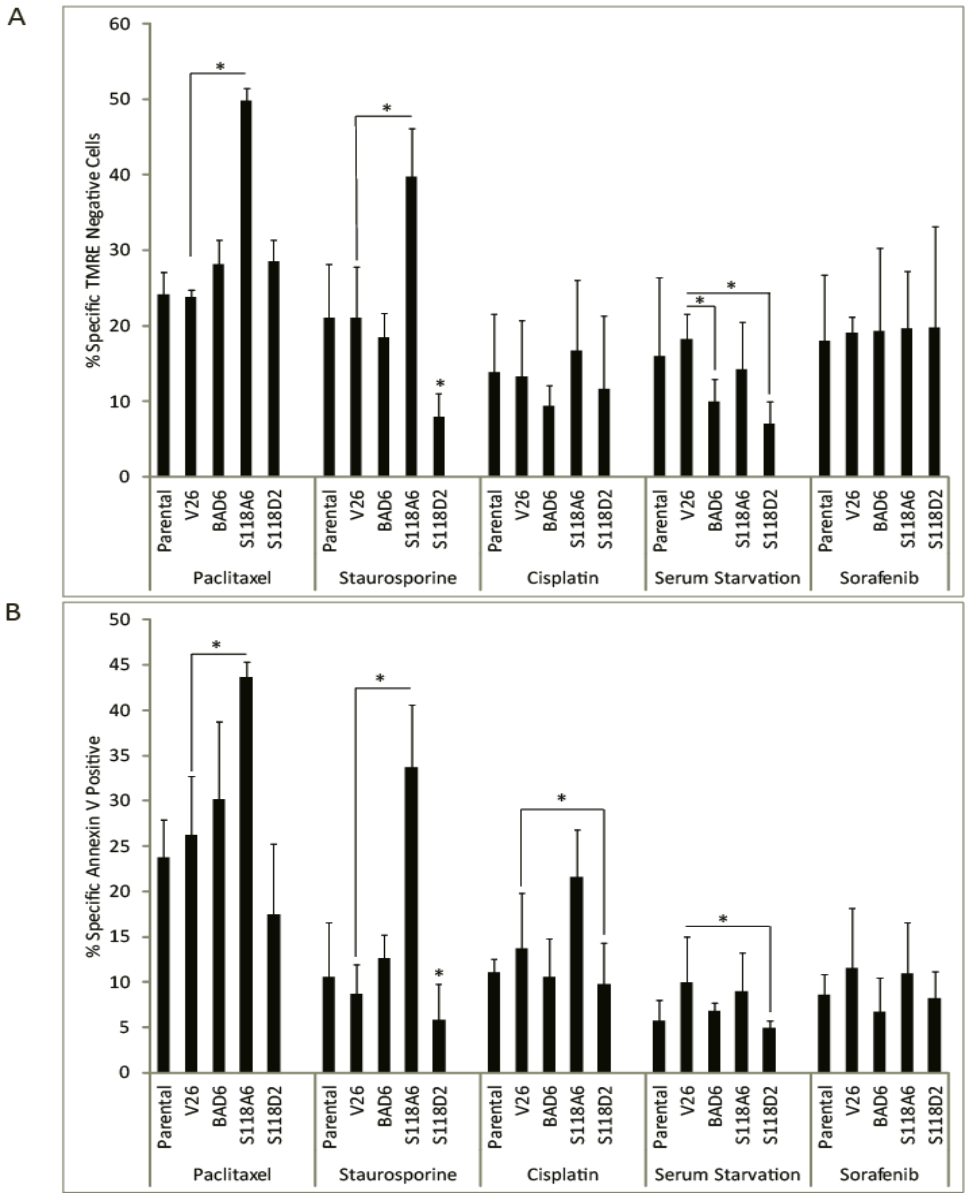

Figure 11: BAD serine 118 phosphorylation decreases apoptotic sensitivity

Stable cell lines were treated with 25 nM Paclitaxel (60 hours), 100 µM cisplatin (48 hours), 20 µM sorafenib (48 hours), 0.1% serum (48 hours) or 2.5 µM staurosporine (4 hours) prior to apoptotic analysis. Apoptotic induction was analyzed using either tetramethylrhodamine ester (TMRE) (**A**) or Annexin V (**B**). Graphs are represented as mean ± standard deviation of three independent experiments for paclitaxel, staurosporine, serum starvation and sorafenib. Cisplatin treatment was completed two independent times analyzed with TMRE and three independent times analyzed with Annexin V. '*' indicates a P value of less than 0.05 in comparison with indicated cell lines.

play a role in proliferative rate differences. Enforced phosphorylation of BAD at S118, as mimicked in the BAD S118D-expressing line, produced cells that were significantly more resistant to staurosporine and serum starvation-induced cell death. This resistance to apoptotic stimuli may partially explain the enhanced proliferative rate of the BADS118D-expressing cells. In contrast, the BADS118A-expressing cells were more sensitive to paclitaxel and staurosporine-induced cell death relative to the vector control, or other BAD-expressing cell lines. Contrary to this, BADS118A and V26 were equally sensitive to serum starvation and sorafenib treatment. As apoptotic sensitivity of BAD and BADS118A/D are stimulus dependent, this data demonstrated that the altered proliferation rates of the BADS118A/D mutants could be associated with differential apoptotic sensitivity.

3.5 The phosphorylation state of S118 determines BAD localization and interaction partners

Apoptotic sensitivity has been previously reported to be dependent on subcellular distribution of BAD (Wang *et al.*, 1999). Due to the different apoptotic thresholds mediated by BAD S118A or D mutation, we wanted to determine if this change in sensitivity was associated with changes in localization. First, we used biochemical fractionation to determine the intracellular localization of BAD and BAD mutants (Figure 12A). Vector control, wild-type BAD- and BADS118A-expressing cells had enrichment of BAD in the heavy membrane fraction associated with the mitochondrial marker Tom20 (Figure 12A, P fraction). In contrast, fractionation of the BADS118D-

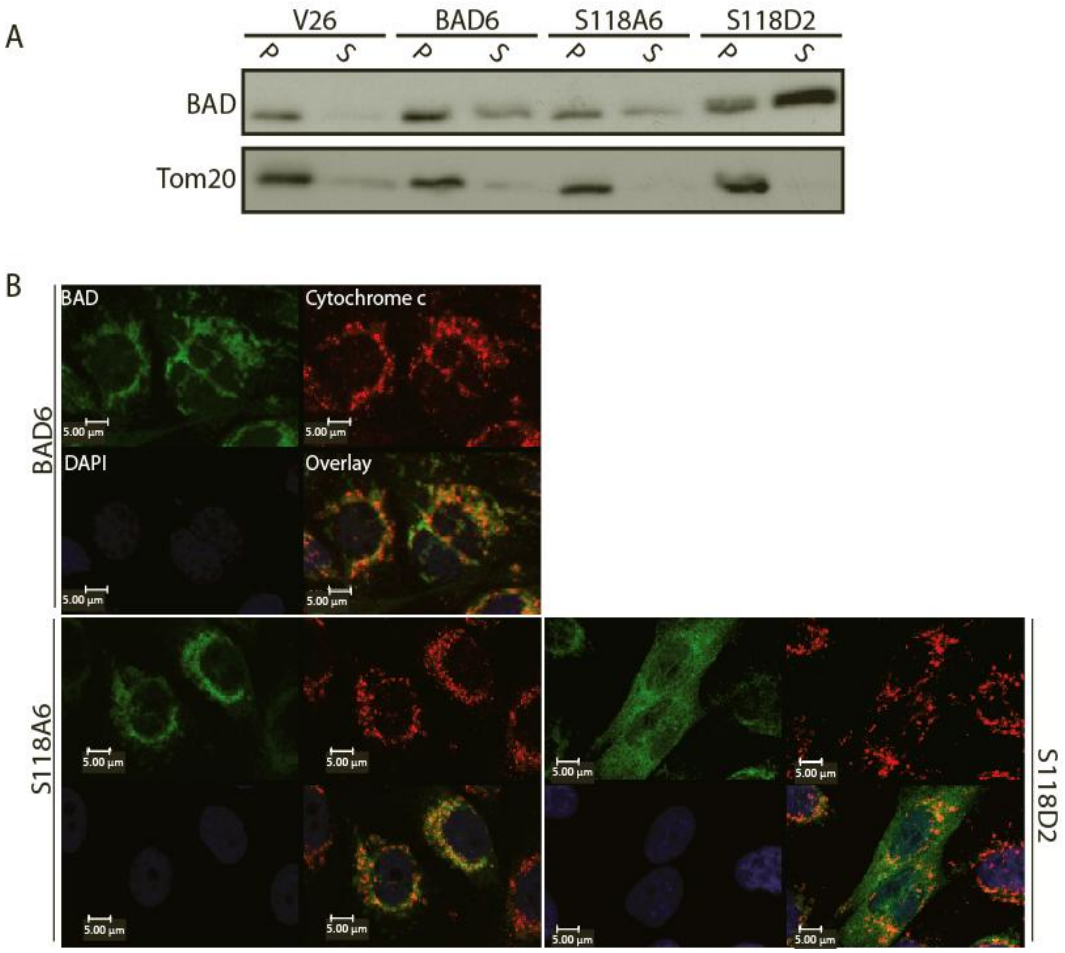

Figure 12: BAD serine 118 phosphorylation causes localization shift

(A) Subcellular fractionation of vector (V26), BAD over-expressing (BAD6), non-phosphorylatable serine 118 mutant of BAD (S118A6) and phospho-mimic of serine 118 BAD (S118D2). Equal volumes of lysate from each clone were loaded onto a 14% SDS-PAGE gel. Membrane was immunoblotted with indicated antibodies. Blot represents one of three replicates. (**B**) Indirect immunofluorescence was conducted on clones at approximately 50% confluency. Images are representative of three independent experiments. Green represents BAD, red represents cytochrome c, blue represents DAPI and the bottom right quadrant is the overlayed images.

expressing cells showed prominent BADS118D localization to the cytosolic (S) fraction (Figure 12A, S fraction).

We also used indirect immunofluorescence to confirm BAD localization. Wild-type BAD and BADS118A over-expressing cells showed a punctate staining pattern for BAD that overlapped with the mitochondrial marker, cytochrome c (Figure 12B). In contrast, BADS118D protein was enriched in the cytosol. Thus, increased sensitivity to apoptosis was coupled to BAD localization to mitochondria, whereas apoptotic resistance demonstrated by the S118D2 cell line was associated with cytosolic-localized BAD.

Intracellular distribution of BAD is mediated by protein associations. Specifically, cytosolic localization of BAD is mediated by interactions with the 14-3-3 family of proteins (Datta *et al.*, 2000; Zha *et al.*, 1996). Through co-immunoprecipitation we determined that both wild-type BAD and BADS118D were associated with 14-3-3 whereas the BADS118A mutant showed no detectable binding to 14-3-3 (Figure 13). Thus, our data is consistent with a model whereby BAD phosphorylation at S118 modulates its interactions with binding partners, which in turn regulates localization. Importantly, a phospho-mutant of BAD that is bound to 14-3-3 and enriched in the cytosol may act as an anti-apoptotic signal that facilitates cell proliferation.

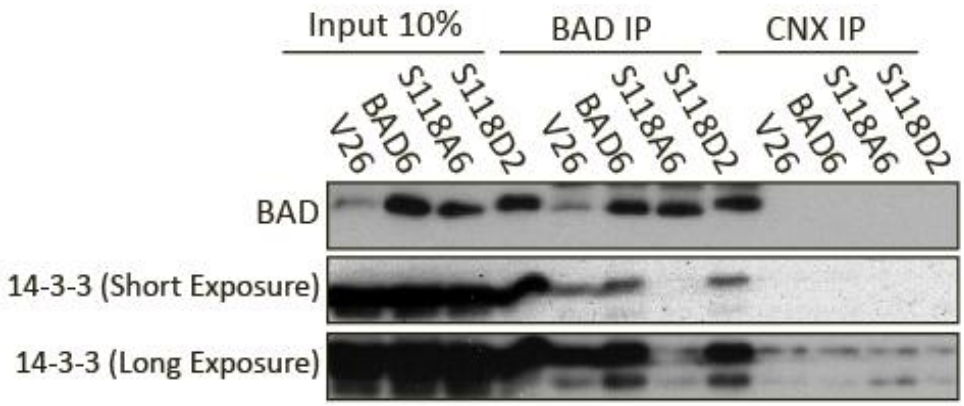

Figure 13: BAD 14-3-3 binding is dependent on serine 118 phosphorylation

Co-immunoprecipitation western blot analysis was conducted on stable cells lines under proteosomal and phosphatase inhibitor conditions. Lysates were immunoprecipitated with BAD or negative binding control (calnexin, CNX) antibody and were immunoblotted with antibodies against BAD, 14-3-3ζ.

Based on our results, we hypothesized that mimicking enforced phosphorylation of BAD at S118 stimulated survival pathways. Since BAD apoptotic activity is regulated by survival kinases (Datta *et al.*, 1997; del Peso *et al.*, 1997), we analyzed whether mutation of S118 altered BAD phosphorylation status. The PI3K survival pathway inhibits BAD pro-apoptotic activity through AKT-mediated phosphorylation of BAD at serine residue 99 (residue 136 in the mouse). Using phospho-specific antibodies, we determined that cells over-expressing BAD S118D had moderately enhanced phosphorylation of S75 and markedly enhanced phosphorylation of S99 (Figure 14A). These results suggest that over-expression of BAD S118D stimulated the PI3K pathway that may account for the anti-apoptotic phenotype of these cells. Alternatively, BADS118D may induce a conformational change that allows greater accessibility of active AKT.

To examine the phosphorylation status of BAD in an unbiased fashion, we analyzed the migration of BAD protein on two-dimensional/SDS-PAGE western blots (Figure 12B); these experiments were conducted by Dr. Lei Li of Dr. Roseline Godbout's laboratory. We detected 7 distinct isoelectric variants of BAD with migration properties consistent with increasing phosphorylation states (Figure 14B). Phosphatase treatment eliminated 6 of the 7 isoforms confirming that these isoforms represented phospho-proteins. To ensure serine 75, 99 and 118 were within the 7 isoforms detected, phospho-specific antibodies were used in the presence or absence of phosphatase (Figure 12 D). This result confirmed that BAD6 was phosphorylated at serine 118. By comparing the phosphorylation pattern of wild-type BAD to the serine

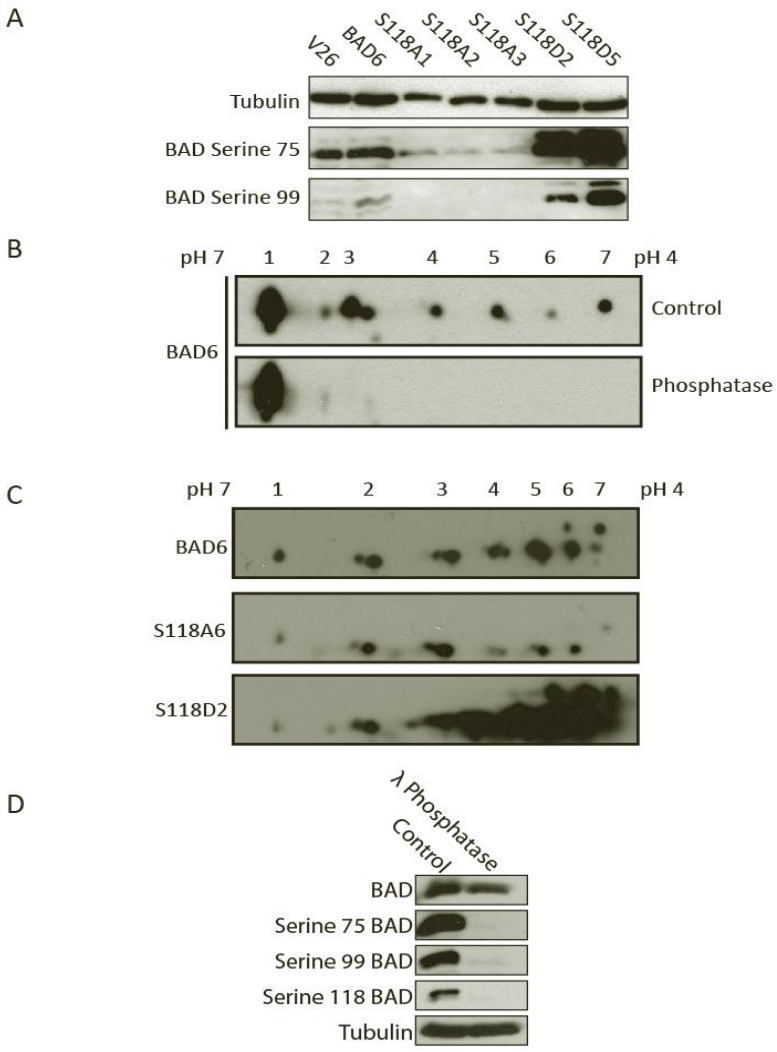

Figure 14: Wild-type BAD is phosphorylated at serine 75, 99 and 118

(A) Stable cell line lysates were loaded in each lane of a 14% SDS-PAGE gel. Lysates were equilibrated for equal cell number loaded in each lane. The gel was immunoblotted for the indicated proteins. (B) BAD6 cell lysates treated with λ-phosphatase or phosphatase inhibitor (control) and equal protein quantities (cont'd) were subjected to isoelectric focusing. 2-dimensional western blot was probed for BAD. **(C)** Stable cell lines were subjected to 2-dimensional western blot technique and were immunoblotted for BAD. Exposure lengths were equilibrated to isoform 2 for comparison purposes. Dr. Lei Li of Dr. Roseline Godbout's laboratory performed 2-dimensional western blot assays (B) and (C). (**D**) BAD6 cell line was lysed, aliquoted and either treated with phosphatase inhibitor (control) or λ phosphatase. An equal volume of lysate was loaded in each lane of an SDS-PAGE gel. The gel was immunoblotted for indicated proteins.

to alanine mutant (S118A), this mutant showed diminished intensities of multiple highly phosphorylated isoforms (Figure 14C, isoforms 4-7). These results indicated that S118 was indeed phosphorylated in wild-type BAD cells and importantly may also prime other phosphorylation sites. Consistent with this result, the migration of the BADS118D isoforms were strongly shifted towards the acidic isoelectric points. Specifically, the intensity of spot number two was equivalent between all cell lines demonstrating S118A had diminished intensities of acidic proteins and S118D had markedly more intense acidic proteins. These results indicated that BADS118A was hypophosphorylated and BADS118D was clearly hyperphosphorylated, relative to wild-type BAD. This suggested that enforced/stable phosphorylation of BAD at S118 stimulated subsequent phosphorylation of BAD at multiple sites. Thus cells over-expressing the S118D mutant of BAD have increased ability to phosphorylated BAD at alternative sites, reflecting a role for S118 as a priming site and suggest activation of survival signaling pathways.

3.6 BAD over-expression leads to enhanced tumor growth

Together, our data indicates that BAD over-expression causes a pro-growth phenotype that is phosphorylation-dependent. However, it was unclear to us why wild-type BAD and BADS118D had similar proliferative profiles in cell culture, yet showed such striking differences in intracellular localization, sensitivity to apoptosis, and phosphorylation patterns. We therefore decided to test whether the BADS118D mutant would demonstrate phenotypic differences under more physiological conditions, such as a mouse model of xenograft tumor growth (Figure 14A). Towards

this goal, vector control, wild-type BAD, BADS118A and BADS118D cells were injected subcutaneously into the rear flank of nude mice and tumor volume was measured every week for 5 weeks; these experiments were performed in part with Dr. Shairaz Baksh. Wild-type BAD over-expressing tumors grew at a significantly faster rate than the vector control lines, indicating that the BAD-induced proliferative phenotype was re-capitulated in this *in vivo* model (Figure 15A; compare green to black line). As well, tumors formed from BADS118A over-expressing cells grew at an equivalent rate as the control vector cells confirming a non-proliferative role for this mutant (Figure 15A, compare red to black line). On average, BADS118A formed smaller tumors than control cells. Interestingly, the tumors that arose from BADS118D over-expressing cells grew at a faster rate than wild-type BAD. Thus, *in vivo* tumor assays demonstrated an enhanced growth of BADS118D over wild-type BAD.

As a means of trying to explain this difference, tumor morphology and the tumor excision site were inspected. Vector control and BADS118A tumors had minimal vascularization (Figure 15B). Wild-type BAD and BADS118D tumors had enhanced vacularization accompanying their larger size. This suggests either a role for BAD in angiogenesis or due to enhanced tumor growth, subsequent vascularization occurs.

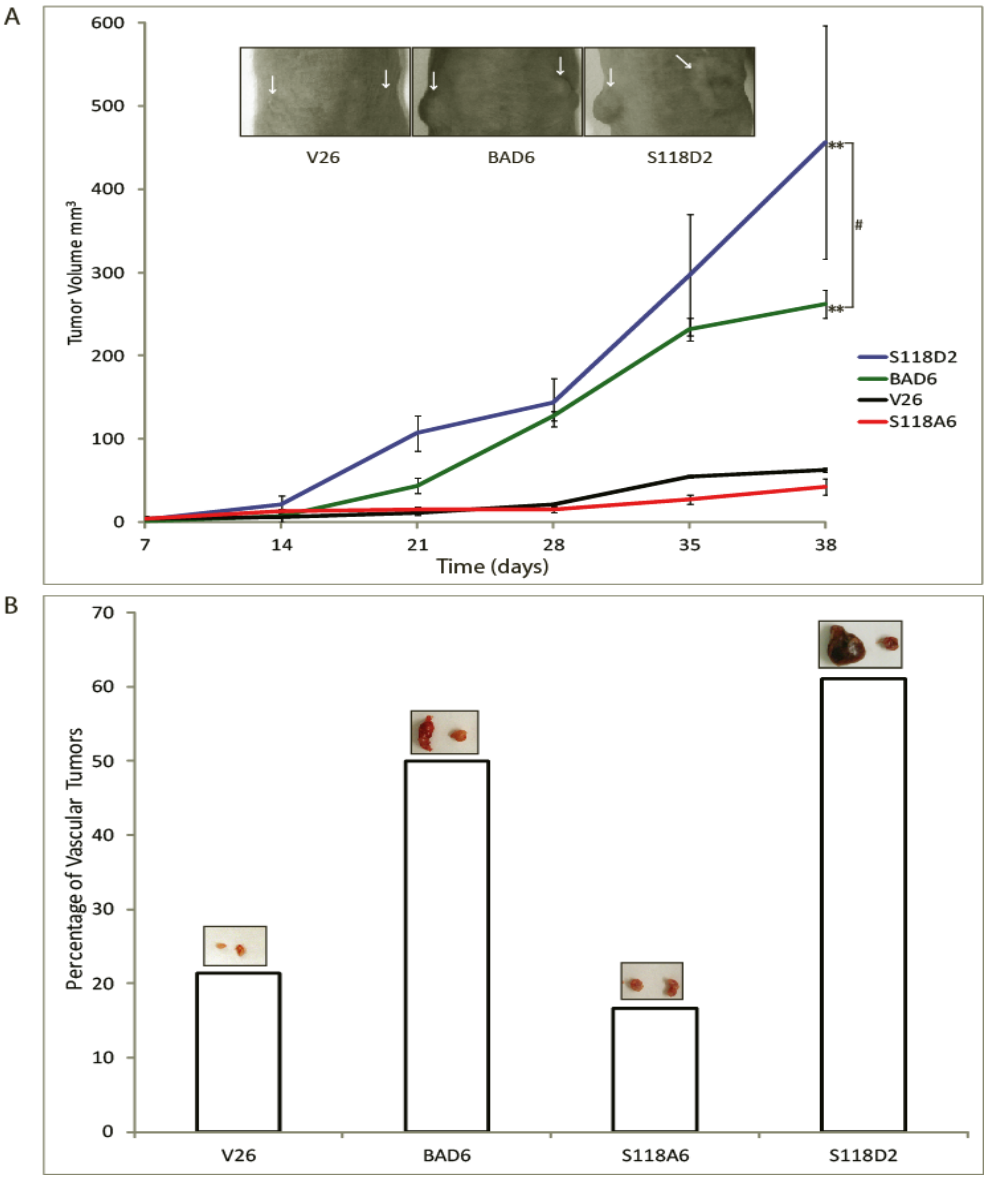

Figure 15: BAD over-expression and Ser-118 phosphorylation promote tumor growth

(**A**) Mice were injected in the rear flank with stably expressing cell lines. Graph indicates the growth of palpable tumors over the indicated time course. '#' indicates a P value of less than 0.05 in direct comparison. '**' indicates a P value of less than 0.01 in comparison to V26 vector control. Images (upper panel) are representative of three independent experiments. Tumor volumes were determined from the radius assuming spherical proportions ($\frac{4}{3}\pi r^3$).

(**B**) Vasculature of tumors was analyzed visually of both tumor and surrounding area. Tumors were then scored as either highly vascular or less vasuclar. Images (above bars) represent vasculature of representative tumors as a means of reference.

3.7 References - Results

Chattopadhyay A, Chiang CW, Yang E. (2001). BAD/BCL-[X(L)] heterodimerization leads to bypass of G0/G1 arrest. *Oncogene* **20:** 4507-4518.

Craik AC, Veldhoen RA, Czernick M, Buckland TW, Kyselytzia K, Ghosh S *et al*. (2010). The BH3-only protein bad confers breast cancer taxane sensitivity through a nonapoptotic mechanism. *Oncogene* .

Czernick M, Rieger A, Goping IS. (2009). Bim is reversibly phosphorylated but plays a limited role in paclitaxel cytotoxicity of breast cancer cell lines. *Biochem Biophys Res Commun* **379:** 145-150.

Datta SR, Dudek H, Tao X, Masters S, Fu H, Gotoh Y *et al*. (1997). Akt phosphorylation of BAD couples survival signals to the cell-intrinsic death machinery. *Cell* **91:** 231-241.

Datta SR, Katsov A, Hu L, Petros A, Fesik SW, Yaffe MB *et al*. (2000). 14-3-3 proteins and survival kinases cooperate to inactivate BAD by BH3 domain phosphorylation. *Mol Cell* **6:** 41-51.

del Peso L, Gonzalez-Garcia M, Page C, Herrera R, Nunez G. (1997). Interleukin-3-induced phosphorylation of BAD through the protein kinase akt. *Science* **278:** 687-689.

FIRKET H. (1964). Synchronization of hela cell cultures by an excess of thymidine. *C R Seances Soc Biol Fil* **158:** 1408-1410.

Janumyan Y, Cui Q, Yan L, Sansam CG, Valentin M, Yang E. (2008). G0 function of BCL2 and BCL-xL requires BAX, BAK, and p27 phosphorylation by mirk, revealing a novel role of BAX and BAK in quiescence regulation. *J Biol Chem* **283:** 34108-34120.

Janumyan YM, Sansam CG, Chattopadhyay A, Cheng N, Soucie EL, Penn LZ *et al*. (2003). Bcl-xL/Bcl-2 coordinately regulates apoptosis, cell cycle arrest and cell cycle entry. *EMBO J* **22:** 5459-5470.

Tan Y, Demeter MR, Ruan H, Comb MJ. (2000). BAD ser-155 phosphorylation regulates BAD/Bcl-XL interaction and cell survival. *J Biol Chem* **275:** 25865-25869.

Wang HG, Pathan N, Ethell IM, Krajewski S, Yamaguchi Y, Shibasaki F *et al*. (1999). Ca2+-induced apoptosis through calcineurin dephosphorylation of BAD. *Science* **284:** 339-343.

Zha J, Harada H, Yang E, Jockel J, Korsmeyer SJ. (1996). Serine phosphorylation of death agonist BAD in response to survival factor results in binding to 14-3-3 not BCL-X(L). *Cell* **87:** 619-628.

Zhou XM, Liu Y, Payne G, Lutz RJ, Chittenden T. (2000). Growth factors inactivate the cell death promoter BAD by phosphorylation of its BH3 domain on Ser155. *J Biol Chem* **275:** 25046-25051.

Chapter 4: Discussion

4.1 The role of BAD in cancer cell proliferation

BAD is well characterized as a pro-apoptotic protein; however novel roles such as proliferation are poorly understood. Furthermore, the regulatory switch between apoptosis and proliferation is unknown. One of our aims in this study was to characterize and understand the regulation of BAD induced proliferation in breast cancer cells. Toward this aim, we created stable BAD over-expressing MDA-MB-231 breast cancer clones. Initial proliferative characterization showed that vector control cells growing for 72 hours had a reduction in proliferative rate (Figure 3A). BAD over-expressing lines, however, continued accumulating at a significantly faster rate than vector control. Furthermore, serine 118 phospho-mimic (S118D2) had a similar proliferative rate to wild-type BAD while non-phosphorylatable BAD (S118A6) had a significant decrease (Figure 7). Due to the nature of this assay, a number of different stimuli could be causing this difference.

First, approximately after 72 hours of growth cells reached confluency. Thus contact inhibition signals may be ignored in BAD over-expressing cells. For this to occur, extracellular signaling pathways need to be inactivated by BAD over-expression. Furthermore, BADS118A (non-phosphorylatable BADS118) cells must be re-sensitized to this stimulus to inhibit proliferation. One possibility is that phosphorylated BAD binding 14-3-3 is promoting or inhibiting formation of a signaling complex. 14-3-3 proteins have been implicated in epithelial mesenchymal transition (EMT; a process that promotes contact inhibition insensitivity) (Hou *et al.*, 2010). A characteristic of EMT is the repression of E-cadherin by the repressor Snail and co-repressor, Ajuba. In HEK 293 (human embryonic kindney) cells, 14-3-3 γ, η and τ bound Snail and Ajuba.

These three proteins were necessary in forming a repressor complex which in non-transformed human mammary epithelia (MCF-10A) cells bound the E-cadherin repressor (Hou *et al.*, 2010). Potentially, BAD promotes this complex formation thus promoting EMT. However, in our cells (MDA-MB-231), E-cadherin is not expressed (Mbalaviele *et al.*, 1996). This could mean that either this complex binds a different EMT promoting repressor or BAD induces a novel signaling complex.

Second, due to continued growth of cells for 72 hours, depletion of growth factors may be limiting proliferation. BAD is known to respond to extracellular growth factors such as, epidermal growth factor (EGF) (Chao and Clement, 2006) and Insulin like growth factor -1 (IGF-1) (Gilmore *et al.*, 2002). Depletion of growth factors has been shown to induce dephosphorylation and the apoptotic role of BAD (Gilmore *et al.*, 2002). We are proposing a novel mechanism where BAD over-expression induces insensitivity to growth factor depletion. The basis of this mechanism is that BAD is unaffected by loss of growth factors and growth factor induced phosphorylation. We demonstrated using 2-dimensional western blot and phospho-specific antibodies that wild-type BAD is phosphorylated at serines 75, 99 and 118 (Figure 9A and D) under basal conditions. If under low growth factor conditions phosphorylation is unaffected, then this would inhibit apoptosis. As MDA-MB-231 breast cancer cells have multiple genomic mutations, a pro-survival kinase may be constitutively active. This activated kinase would promote survival independent of extracellular stimuli therefore allowing wild-type BAD to be phosphorylated in serum deprived conditions.

Consistent with this theory, BAD over-expressing and BADS118D clones, serum starvation did not induce mitochondrial depolymerization as effectively as in parental,

V26 and S118A6 (Figure 10A). However, for serum starvation to fully explain the proliferative difference, S118A6 sensitivity would need to be greater than that of V26. Based on these data, BADS118 phosphorylation-dependent serum starvation sensitivity is partially responsible for proliferative differences.

Third, glucose or glutamine depletion may also influence BAD induced proliferation. Although not directly tested, prolonged growth in media could deplete glucose or glutamine to a level where apoptosis occurred. The role of BAD in glucose homeostasis may underlie the observed proliferative effect. BAD has been shown to form a complex with glucokinase (hexokinase IV), PP1, PKA and WAVE-1 in mouse liver hepatocytes and pancreatic β-cells (Danial *et al.*, 2003; Danial *et al.*, 2008). This complex formation enables increased mitochondrial respiration which may provide a growth advantage for cancer cells. Although formation of this complex is phosphorylation independent, activation of glucokinase is serine 118 (mBAD 155) dependent (Danial *et al.*, 2003; Danial *et al.*, 2008). This was shown in pancreatic β cells using mBADS155A (hBADS118) and $BAD^{3SA/3SA}$ point mutants. They discovered that the inability of BAD to be phosphorylated at serine 118 prevented glucose induced insulin release from β cells.

If BADS118D enforced phosphorylation activated this complex, then increased glycolytic efficiency via mitochondrial respiration would correlate with increased proliferation. However, unlike hepatocytes and β-cells, breast cancer cells do not express glucokinase. Cancer cells express high levels of hexokinase II which has not been shown to form this complex (Rempel *et al.*, 1996). Preliminary data attempting to examine direct hexokinase binding to BAD has so far been unsuccessful. This may

mean that BAD does not form a complex with hexokinase II in MDA-MB-231 breast cancer cells or that this complex is not stable enough to detect. In order to conclusively determine if this complex exists, it may be necessary to carry out a 3-dimensional western blot similar to that described in (Danial *et al.*, 2003).

One or a combination of these factors may explain the observed differences in proliferation rate between S118A and S118D clones. Serum starvation showed a protective effect of BAD6 and S118D2 that correlated with the proliferation data. However, S118A6 was equally sensitive to serum starvation as V26 suggesting that serum starvation in combination with other factors is likely responsible. Proliferation assays manipulating each of these factors alone and in combination must be carried out to determine the cause of this difference.

4.2 BAD gene addiction

The increased proliferative rate of BAD over-expressing cells was specific to BAD as siRNA knock down inhibited this effect (Figure 5B). In comparison to vector, BAD over-expression led to increased cell numbers while siRNA to BAD caused decreased cell numbers. Intriguingly, siRNA to BAD inhibited cell proliferation of BAD6 below baseline (V26). Based on these data, one conclusion is that BAD over-expressing cells became "addicted" to BAD expression. Oncogene addiction has been shown previously in anti-apoptotic BCL-2 family members. In healthy cells, an exogenous death inducing signal is needed in order for apoptotic induction to occur (Certo *et al.*, 2006). For instance, in FL5.12-BCL-2 cells, addition of ABT-737 (BAD BH3 derived peptide) and IL-3 withdrawal induces cell death while ABT-737 alone does not.

However, in a leukemic model, addition of BH3 peptides known to bind BCL-2 directly induced cytochrome C release (Certo *et al.*, 2006). This suggests that unlike healthy cells, cancer cells are continuously being stimulated to die and increased BCL-2 levels are needed to compensate (Certo *et al.*, 2006). Due to pro-proliferative and pro-death roles of BAD, cancer cells may upregulate expression of anti-apoptotic BCL-2 members such as BCL-XL to prevent apoptosis. Once BAD expression is suppressed by siRNA, the increased expression of BCL-XL may prevent cell cycle progression and promote quiescence (Janumyan *et al.*, 2003). By using siRNA to BCL-XL as well as BAD, we would be able to determine if the addictive phenotype was due to increased BCL-XL expression.

Based on this analysis, BAD would have an intrinsically apoptotic function that was compensated for by BCL-XL. However in the BAD over-expressing stable clones, BAD does not increase apoptotic sensitivity to any of the agents or conditions (Figure 10A and B). An alternative explanation of BAD induced gene addiction is based on a pro-survival role. In this role, siRNA to BAD would induce increased apoptotic sensitivity. Although those experiments were not performed, over-expression of BAD is mildly protective to certain stimuli (Figure 10A, Cisplatin treatment). This result is consistent with data obtained from an endometrial cell line microarray which demonstrated that BAD expression correlated with cisplatin resistance. Furthermore, in the Ishikawa cell line, induced BAD phosphorylation via siRNA to PP2C promoted Cisplatin resistance. In conjunction with our study, these results suggest that BAD over-expression leads to a protective phenotype dependent on intracellular kinase activity and phosphorylation state of BAD.

4.3 BAD induced proliferation is cell cycle independent

As a means of determining the mechanism of BAD induced proliferation, we manipulated the ability of BAD to bind BCL-XL. BCL-XL has been shown to inhibit cell cycle progression by binding BAX and indirectly promoting p27 stability (Chattopadhyay *et al.*, 2001; Janumyan *et al.*, 2008; Janumyan *et al.*, 2003). BAD has been shown to overcome the anti-proliferative effects of BCL-XL and promote S phase progression (Chattopadhyay *et al.*, 2001; Janumyan *et al.*, 2003). When serine 118 is phosphorylated (as shown by phospho-mimic S118D2), BAD has a decreased binding affinity to Bcl-xL (Figure 6A) yet has an increased proliferative rate (Figure 7) (Tan *et al.*, 2000; Zhou *et al.*, 2000). To determine if BAD over-expression or BCL-XL binding influenced cell cycle dynamics under basal conditions, a low confluency time course was performed (Figure 6B and C). This study determined that although there were minor changes in individual experiments, overall no significant trend was observed. Due to proliferative differences occurring after confluency, this variable was also tested. Again, no consistent pattern emerged from high confluency experiments.

Based on these data, BAD may not play a role in cell cycle progression of MDA-MB-231 breast cancer cells. However, future experiments are needed to test whether stimuli such as serum starvation and glucose deprivation induce a cell cycle role for BAD in breast cancer.

4.4 Serine 118 is a priming site for other BAD phosphorylation sites

Although phosphorylation of serines 75, 99 and 118 all inhibit apoptosis, an activation hierarchy has been proposed. In mBAD over-expressing HEK 293 cells (human embryonic kidney), serine 136 (hBADS99) phosphorylation was necessary for serine 155 (hBADS118) phosphorylation (Datta *et al.*, 2000). *In vitro*, serine 136 was sufficient to induce binding to 14-3-3 which promoted PKA induced serine 155 phosphorylation. Based on this study, 14-3-3 binding to BAD may induce a conformational change or promote close localization of serine 155 kinases (Datta *et al.*, 2000). However, in HEK 293 cells transfected with a serine 112 and 136 non-phophorylatable mutant (mBADS112/136A), serine 155 was phosphorylated with PKA stimulation (forskolin) (Tan *et al.*, 2000). These cells were also resistant to Rous Sarcoma Virus infection in the presence of a serine 155 kinase (RSK1) therefore demonstrating a protective role for serine 155 independent of serine 112 and 136 (Tan *et al.*, 2000). As our study focused on hBAD serine 118, we wanted to specifically address whether this site can activate other phosphorylation sites.

Our 2-dimensional western blot analysis determined that wild-type BAD was phosphorylated at potentially six sites (Figure 9B). Enforced phosphorylation at serine 118 (S118D) promoted an increase in acidic species indicative of increased phosphorylation. Alternatively, non-phosphorylatable serine 118 (S118A) inhibited prevalence of acidic species. Based on these data, serine 118 phosphorylation enhances alternative phosphorylation sites including serine 75 and 99 (Figure 12A and 12C). Although serine 118 has never been shown to have this priming role, multiple scenarios can be used to explain this relationship.

First, serine 118 phosphorylation promotes a conformational change that allows increased kinase accessibility to other phosphorylation sites. Studies to directly test this theory have not been done; however, mutations to the BH3 domain have been shown to occlude phosphorylation *in vitro* (Adachi *et al.*, 2003). In COS-7 cells over-expressing hBADD119G, serine 75, 99 and 118 phosphorylation was inhibited. As a means of determining if D119G prevented S118 from being phosphorylated, BADD119G was incubated with the catalytic subunit of PKA. Both serine 75 and 118 could be phosphorylated *in vitro* (Adachi *et al.*, 2003). Based on these data and since BADD119G is a highly conserved residue of BH3 domains (Zha *et al.*, 1997), this mutation may promote a BH3 conformation that cannot be phosphorylated.

In our S118D2 cells, a preliminary study was conducted using λ phosphatase. The 2-dimensional western blot showed that unlike BAD6 which fully collapses under phosphatase treatment (Figure 12B) S118D2 did not. There were a number of phosphatase insensitive bands that remained after treatment. These data suggest that unlike wild-type BAD, BADS118D2 is unable to conform to a phosphatase receptive species. However, BADS118D2 is not actually phosphorylated which may prevent conformational changes based on amino acid composition rather than phospho-mimic properties.

In order to test this theory, structural studies would need to be conducted. However, BAD is an innately unstructured protein making analysis of a phosphorylation dependent conformational change difficult (Hinds *et al.*, 2007). Although the BH3 domain becomes structured upon protein interactions, most phosphorylation sites do not reside in this region (Hinds *et al.*, 2007). In order to conclusively determine if

serine 118 phosphorylation causes a conformational change, further analysis of the structure of human BAD needs to be done.

Second, serine 118 phosphorylation may induce phosphorylation of other sites through pathway activation. BAD has been shown to be critical for glucokinase activity at the mitochondria that is dependent on mBADS155 (hBADS118) phosphorylation. In our study, BADS118D bound strongly with 14-3-3 (Figure 4B) and localized to the cytosol (Figure 8A and B). Based on this binding affinity, BAD may induce formation of a signaling complex at 14-3-3 protein sites. Speculatively, BAD could induce a similar protein complex to its role in metabolism (Danial *et al.*, 2003). Furthermore, BAD binding 14-3-3 may induce subcellular localization changes that are sufficient to promote kinase accessibility. In MCF10A cells, 14-3-3ζ over-expression promotes plasma membrane localization of PI3K subunit p85 (Neal *et al.*, 2011). This localization induces activation of PI3K and downstream activation of Akt. As 14-3-3 proteins are dimeric and have the potential to bind two substrates simultaneously (Petosa *et al.*, 1998; Yaffe *et al.*, 1997), we propose that BAD is targeted to activated AKT. In S118D2 cells, the localization of BAD is diffuse although increased plasma membrane localization may also be observed (Figure 11B). When BAD binds 14-3-3ζ, this interaction could promote intracellular localization of BAD to active PI3K and Akt. Based on these data, we propose a model whereby cytosolic 14-3-3 bound localization promotes pro-survival complexes which then further phosphorylate BAD (Figure 14).

4.5 Is serine 118 directly causing proliferative promoting effects?

As we demonstrated using 2-dimensional western blot and phospho-specific antibodies (Figure 12A and C), serine 118 phosphorylation induces phosphorylation at other sites. Therefore, we can not conclusively state whether serine 118 is causing these effects directly or through other phosphorylation sites. Specifically, serine 118 is not within a 14-3-3 consensus binding site (Virdee *et al.*, 2000). Therefore, BAD:14-3-3 interactions are likely governed through alternative sites. In order to be confident about the role of serine 118, mutational studies of the other sites specifically serine 75 and 99, are needed.

4.6 Serine 118 phosphorylation is advantageous for tumor growth

Clinically, increased BAD expression has been shown to be prognostic for overall patient survival (Huang *et al.*, 2011b). Furthermore, BAD expression in breast cancer, positively correlates with response to tamoxifen (Cannings *et al.*, 2007) and Paclitaxel (Craik *et al.*, 2010). However, the role of BAD in tumor progression is poorly understood. In prostate cancer cells, BAD over-expression induces increased tumor growth in nude mice (Smith *et al.*, 2009). Alternatively, in A549 lung cancer cells, BAD over-expression inhibited xenograft tumor growth (Huang *et al.*, 2011a). Due to the conflicting nature of these studies, BAD expression is an unreliable predictive marker for tumor growth.

Cancer cell proliferation often correlates with tumor volume. For instance, C4-2 prostate cancer cells over-expressing BAD had increased proliferation rates and

increased xenograft tumor volume (Smith *et al.*, 2009). However in our study, there is discordance between proliferation (Figure 7) and tumor growth (Figure 13A) in wild-type BAD and BADS118D stable cell lines. One phenotypic difference between these two proteins is the strong cytosolic localization of S118D (Figure 8A and B) in comparison to wild-type BAD. This suggests that increased BAD concentrations in the cytosol promote tumor growth. However, due to the similar 14-3-3 binding interactions, it is difficult to know how S118D is promoting tumor growth. One potential explanation is that BADS118D is binding and forming a complex with a novel interacting partner. Preliminary studies using GST-BAD immunoprecipitations in MDA-MB-231 cells have provided no significant lead. However, if this interaction is transient then our screening methods so far may not have detected this interaction.

4.7 BAD induced angiogenesis?

In our xenograft model, the ability of BAD to bind 14-3-3 increased the size and vasculature of the tumors (Figure 13A and B). One potential explanation for this result is that BAD bound to 14-3-3 induces angiogenesis. A recent study using the angiogenic inhibitor sunitinib determined that BAD promoted vascular endothelial growth factor (VEGF) induced survival (Saito *et al.*, 2011). In this study, Sunitinib (VEGF receptor inhibitor) promoted mBADS136 dephosphorylation by inhibition of S6K1. However, BAD has never been shown to induce angiogenesis. Since BADS118D had increased vasculature, this suggests that 14-3-3 binding or simply cytosolic localization may induce this phenotype. One potential way in which BAD might induce angiogenesis is through complex formation at 14-3-3 binding sites. Similar to where BAD is necessary

for glucokinase activity, BAD may be part of other kinase complexes that promote angiogenesis.

Alternatively, the lipid binding domains of BAD may promote lipid interactions and therefore promote VEGFR signaling. In WEHI-231 cells, anti-IgM treatment promoted increased protein interaction between BAD and 14-3-3 (Malissein *et al.*, 2006). Furthermore, this treatment also promoted localization of BAD to lipid rafts. A major receptor for angiogenesis signaling VEGFR has also been shown to interact with lipid rafts (Saulle *et al.*, 2009). In this study, it was shown that GM-CSF and VEGFR2 together promote cell proliferation. It was shown using detergent solubility fractionation that VEGFR2 in the absence of GM-CSF did not strongly localize with lipid rafts. However, upon GM-CSF stimulation VEGFR2 localized strongly to lipid rafts.

As BAD is a sentinel of apoptotic signals, it is reasonable to speculate that BAD localizing to lipid rafts would prevent apoptosis (through GM-CSF stimulation) and potentially promote VEGFR2 stability. This novel localization of BAD may be crucial to determining its pro-proliferative and tumorigenic properties.

4.8 Summary

The role of BAD in proliferation and tumor progression is controversial. This study addressed these roles of BAD in a breast cancer tissue culture model and *in vivo* xenograft mouse model. We demonstrated that BAD over-expression induces increased proliferation in breast cancer cells that is independent of a cell cycle component. We also proposed a regulatory mechanism of BAD induced proliferation

and tumor progression through serine 118 phosphorylation (Figure 16). Serine 118 phosphorylation may induce these factors alone or through its priming of other phosphorylation sites. This study suggests that in order to use BAD as a prognostic or therapeutic target, the phospho-status of BAD must also be examined.

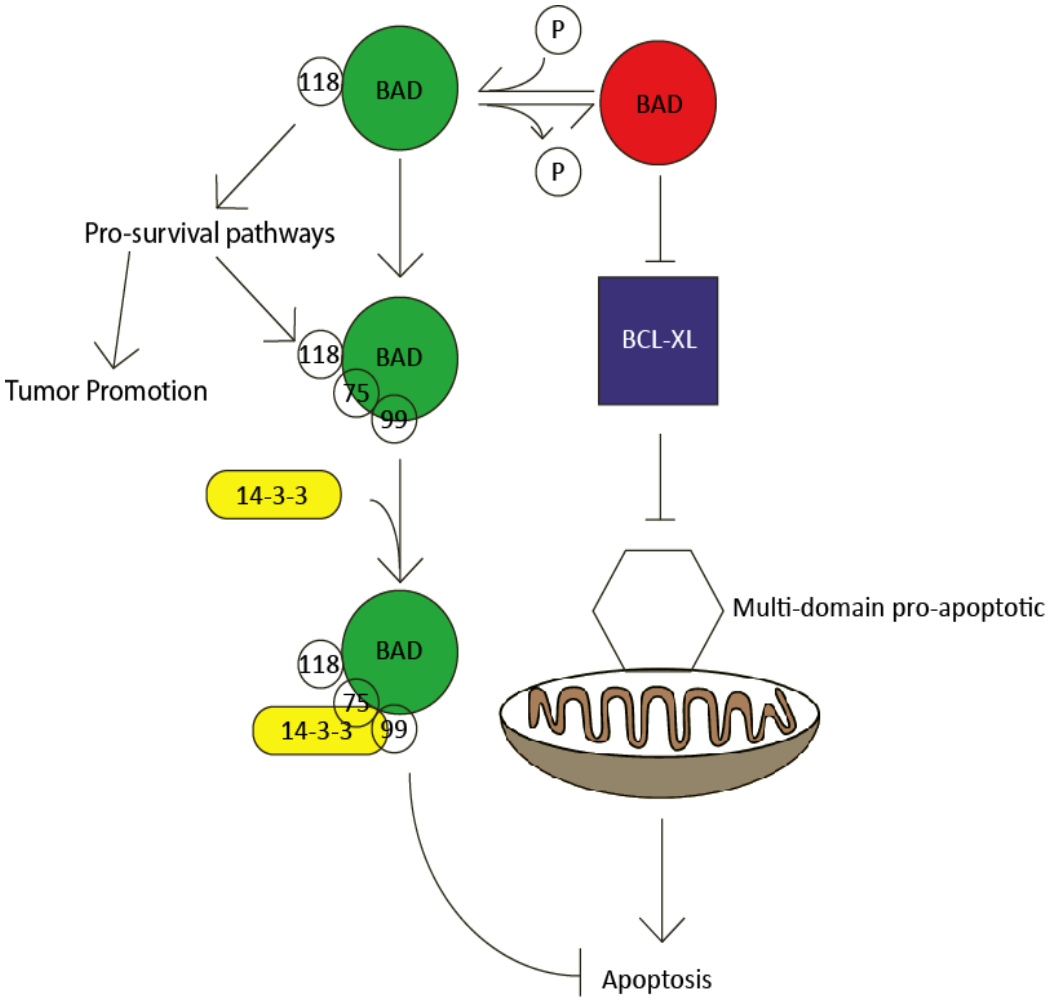

Figure 16: Model of serine 118 phosphorylation induced effects

Dephosphorylation of serine 118 induces interaction with BCL-XL. This interaction promotes an apoptotic sensitive phenotype. When BAD is phosphorylated at serine 118, alternative phosphorylation sites are activated. This may be through conformational changes to BAD or through pro-survival pathway activation which would lead to other site activation. These other phosphorylation sites, for instance serines 75 and 99, promote BAD binding to 14-3-3 proteins. This interaction with 14-3-3 proteins may lead to inhibition of apoptosis although BAD phosphorylated at serine 118 may prevent apoptosis without 14-3-3. Serine 118 phosphorylated BAD also promotes tumor growth potentially through pro-survival pathway activation.

4.9 References - Discussion

Adachi M, Zhang YB, Imai K. (2003). Mutation of BAD within the BH3 domain impairs its phosphorylation-mediated regulation. *FEBS Lett* **551:** 147-152.

Cannings E, Kirkegaard T, Tovey SM, Dunne B, Cooke TG, Bartlett JM. (2007). Bad expression predicts outcome in patients treated with tamoxifen. *Breast Cancer Res Treat* **102:** 173-179.

Certo M, Del Gaizo Moore V, Nishino M, Wei G, Korsmeyer S, Armstrong SA *et al*. (2006). Mitochondria primed by death signals determine cellular addiction to antiapoptotic BCL-2 family members. *Cancer Cell* **9:** 351-365.

Chao OS, Clement MV. (2006). Epidermal growth factor and serum activate distinct pathways to inhibit the BH3 only protein BAD in prostate carcinoma LNCaP cells. *Oncogene* **25:** 4458-4469.

Chattopadhyay A, Chiang CW, Yang E. (2001). BAD/BCL-[X(L)] heterodimerization leads to bypass of G0/G1 arrest. *Oncogene* **20:** 4507-4518.

Craik AC, Veldhoen RA, Czernick M, Buckland TW, Kyselytzia K, Ghosh S *et al*. (2010). The BH3-only protein bad confers breast cancer taxane sensitivity through a nonapoptotic mechanism. *Oncogene* .

Danial NN, Gramm CF, Scorrano L, Zhang CY, Krauss S, Ranger AM *et al*. (2003). BAD and glucokinase reside in a mitochondrial complex that integrates glycolysis and apoptosis. *Nature* **424:** 952-956.

Danial NN, Walensky LD, Zhang CY, Choi CS, Fisher JK, Molina AJ *et al*. (2008). Dual role of proapoptotic BAD in insulin secretion and beta cell survival. *Nat Med* **14:** 144-153.

Datta SR, Katsov A, Hu L, Petros A, Fesik SW, Yaffe MB *et al*. (2000). 14-3-3 proteins and survival kinases cooperate to inactivate BAD by BH3 domain phosphorylation. *Mol Cell* **6:** 41-51.

Gilmore AP, Valentijn AJ, Wang P, Ranger AM, Bundred N, O'Hare MJ *et al*. (2002). Activation of BAD by therapeutic inhibition of epidermal growth factor receptor and transactivation by insulin-like growth factor receptor. *J Biol Chem* **277:** 27643-27650.

Hinds MG, Smits C, Fredericks-Short R, Risk JM, Bailey M, Huang DC *et al*. (2007). Bim, bad and bmf: Intrinsically unstructured BH3-only proteins that undergo a localized conformational change upon binding to prosurvival bcl-2 targets. *Cell Death Differ* **14:** 128-136.

Hou Z, Peng H, White DE, Wang P, Lieberman PM, Halazonetis T *et al*. (2010). 14-3-3 binding sites in the snail protein are essential for snail-mediated transcriptional repression and epithelial-mesenchymal differentiation. *Cancer Res* **70:** 4385-4393.

Huang N, Zhu J, Liu D, Li YL, Chen BJ, He YQ *et al*. (2011a). Overexpression of bcl-2-associated death inhibits A549 cell growth in vitro and in vivo. *Cancer Biother Radiopharm* .

Huang Y, Liu D, Chen B, Zeng J, Wang L, Zhang S *et al*. (2011b). Loss of bad expression confers poor prognosis in non-small cell lung cancer. *Med Oncol* .

Janumyan Y, Cui Q, Yan L, Sansam CG, Valentin M, Yang E. (2008). G0 function of BCL2 and BCL-xL requires BAX, BAK, and p27 phosphorylation by mirk, revealing a novel role of BAX and BAK in quiescence regulation. *J Biol Chem* **283:** 34108-34120.

Janumyan YM, Sansam CG, Chattopadhyay A, Cheng N, Soucie EL, Penn LZ *et al*. (2003). Bcl-xL/Bcl-2 coordinately regulates apoptosis, cell cycle arrest and cell cycle entry. *EMBO J* **22:** 5459-5470.

Malissein E, Verdier M, Ratinaud MH, Troutaud D. (2006). Activation of bad trafficking is involved in the BCR-mediated apoptosis of immature B cells. *Apoptosis* **11:** 1003-1012.

Mbalaviele G, Dunstan CR, Sasaki A, Williams PJ, Mundy GR, Yoneda T. (1996). E-cadherin expression in human breast cancer cells suppresses the development of

osteolytic bone metastases in an experimental metastasis model. *Cancer Res* **56:** 4063-4070.

Neal CL, Xu J, Li P, Mori S, Yang J, Neal NN *et al*. (2011). Overexpression of 14-3-3zeta in cancer cells activates PI3K via binding the p85 regulatory subunit. *Oncogene* .

Petosa C, Masters SC, Bankston LA, Pohl J, Wang B, Fu H *et al*. (1998). 14-3-3zeta binds a phosphorylated raf peptide and an unphosphorylated peptide via its conserved amphipathic groove. *J Biol Chem* **273:** 16305-16310.

Rempel A, Mathupala SP, Griffin CA, Hawkins AL, Pedersen PL. (1996). Glucose catabolism in cancer cells: Amplification of the gene encoding type II hexokinase. *Cancer Res* **56:** 2468-2471.

Saito Y, Tanaka Y, Aita Y, Ishii KA, Ikeda T, Isobe K *et al*. (2011). Sunitinib induces apoptosis in pheochromocytoma tumor cells by inhibiting VEGFR2/AKT/mTOR/S6K1 pathways through modulation of bcl-2 and BAD. *Am J Physiol Endocrinol Metab* .

Saulle E, Riccioni R, Coppola S, Parolini I, Diverio D, Riti V *et al*. (2009). Colocalization of the VEGF-R2 and the common IL-3/GM-CSF receptor beta chain to lipid rafts leads to enhanced p38 activation. *Br J Haematol* **145:** 399-411.

Smith AJ, Karpova Y, D'Agostino R,Jr, Willingham M, Kulik G. (2009). Expression of the bcl-2 protein BAD promotes prostate cancer growth. *PLoS One* **4:** e6224.

Tan Y, Demeter MR, Ruan H, Comb MJ. (2000). BAD ser-155 phosphorylation regulates BAD/Bcl-XL interaction and cell survival. *J Biol Chem* **275:** 25865-25869.

Virdee K, Parone PA, Tolkovsky AM. (2000). Phosphorylation of the pro-apoptotic protein BAD on serine 155, a novel site, contributes to cell survival. *Curr Biol* **10:** R883.

Yaffe MB, Rittinger K, Volinia S, Caron PR, Aitken A, Leffers H *et al*. (1997). The structural basis for 14-3-3:Phosphopeptide binding specificity. *Cell* **91:** 961-971.

Zha J, Harada H, Osipov K, Jockel J, Waksman G, Korsmeyer SJ. (1997). BH3 domain of BAD is required for heterodimerization with BCL-XL and pro-apoptotic activity. *J Biol Chem* **272:** 24101-24104.

Zhou XM, Liu Y, Payne G, Lutz RJ, Chittenden T. (2000). Growth factors inactivate the cell death promoter BAD by phosphorylation of its BH3 domain on Ser155. *J Biol Chem* **275:** 25046-25051.